Lehigh University
Lehigh Preserve

Theses and Dissertations

1968

Ultimate strength of longitudinally stiffened plate panels (large and small b/t, general material properties)

Donald R. Rutledge
Lehigh University

Follow this and additional works at: https://preserve.lehigh.edu/etd

 Part of the Civil Engineering Commons

Recommended Citation
Rutledge, Donald R., "Ultimate strength of longitudinally stiffened plate panels (large and small b/t, general material properties)" (1968). *Theses and Dissertations*. 3670.
https://preserve.lehigh.edu/etd/3670

This Thesis is brought to you for free and open access by Lehigh Preserve. It has been accepted for inclusion in Theses and Dissertations by an authorized administrator of Lehigh Preserve. For more information, please contact preserve@lehigh.edu.

ULTIMATE STRENGTH
OF
LONGITUDINALLY STIFFENED PLATE PANELS

(LARGE AND SMALL b/t, GENERAL MATERIAL PROPERTIES)

by

Donald R. Rutledge

A Thesis
Presented to the Graduate Committee
of Lehigh University
in Partial Fulfillment of the Requirements
for the Degree of
Master of Science
in
Civil Engineering

Lehigh University
September 1968

CERTIFICATE OF APPROVAL

This thesis is accepted and approved in partial fulfillment of the requirements for the degree of Master of Science.

September 17, 1968
Date

Alexis Ostapenko
Dr. Alexis Ostapenko
Professor in Charge

David A. VanHorn
Dr. David A. VanHorn, Chairman
Department of Civil Engineering

ACKNOWLEDGEMENTS

This thesis describes part of the work done for a research project on Built-Up Members in Plastic Design in the Department of Civil Engineering, Fritz Engineering Laboratory, Bethlehem, Pennsylvania. Dr. David A. VanHorn is the Chairman of the Department and Dr. Lynn S. Beedle is the Director of the Laboratory.

The research has been sponsored by the Department of the Navy under the Naval Ship Engineering Center Contract No. N00024-67-C-5243. The support of the project by Mr. John Vasta of the Naval Ship Engineering Center is gratefully acknowledged.

The author wishes to acknowledge the advice and encouragement given to him by Dr. Alexis Ostapenko, the Project Director and thesis supervisor.

The figures were prepared by Mrs. Sharon Balogh and Miss Marilyn Courtright typed the flow diagrams. Their assistance is greatly appreciated.

TABLE OF CONTENTS

ABSTRACT

This thesis represents a phase in a study of the ultimate strength analysis of longitudinally stiffened plate panels. The panels are assumed to be wide enough so that lateral interaction between stiffeners is negligible, thereby allowing a beam-column approach. Axial and lateral loads are considered, ~~as~~ are residual stresses and plate components which buckle prior to the ultimate condition. Design nomographs based on the results of analysis have been previously reported.

A comprehensive computer program has been written to determine the ultimate strength of stiffened panels based on the fundamental principles previously developed and to extend the method to non-linear materials (not previously considered). Herein, this program is described.

In addition, an assumption which had been the cause for concern - the post-buckling behavior assumption for the plate - is investigated by using the computer program as a test simulator to determine bounds of possible error in the design nomographs resulting from the assumption. The results indicate that errors are negligible and that the nomographs may be used with confidence.

1. INTRODUCTION

The study of the ultimate strength of longitudinally stiffened plate panels subjected to lateral and axial loads may be simplified to the study of the instability of beam-columns if it is assumed that plate action in the transverse direction is negligible. The stiffened panels of particular interest in the current work are those used in ship bottom structures. Because their analysis is complicated by unsymmetrical cross sections, residual stresses due to welding, lateral loads, and also by the possibility of buckling of the plate components before the ultimate condition is reached, the numerous studies performed for ordinary structural sections are not directly applicable.

A theoretical elastic-plastic analysis for the beam-column instability of longitudinally stiffened plate panels subjected to an axial compressive load and uniformly distributed lateral loading was first developed by Kondo.[9]* Cross-sectional dimensions were restricted so that the stiffened plate panels would fail as a unit without premature local buckling of the plate components, and the stress-strain

*The numbers in parentheses refer to the list of references.

relationship of the materials was assumed to be elastic - perfectly plastic. Tables of moment - curvature - axial load relationships were utilized to overcome the difficulties resulting from the non-linear effects of inelastic action and large deformations. Panels with fixed and pinned ends were analyzed, and numerical results were incorporated in a design chart for stiffened panels with small plate slenderness ratios (small b/t).

Davidson presented evidence that the behavior of a plate loaded in compression in the plane of the plate could be described by several average stress - edge strain theories but particalarly well by the Koiter equation.(10) This equation was shown to adequately describe the elastic post-buckling behavior for plates of several materials. Accordingly, Tsuiji extended the general approach of Kondo to stiffened panels for which the ultimate load of the panel may be preceded by buckling of the plate component.(11) Here, too, the stress-strain relationship of the material was assumed elastic - perfectly plastic, and numerical work was limited to fixed-end and pinned-end panels. Tests on stiffened panels substantiated validity of the analysis, and design nomographs were developed for panels with large b/t to facilitate practical application.(11,12,13)

During the development of the method of analysis, a number of restrictive assumptions had to be made for the behavior of the plate component and for material properties which could not be checked out with the available experimental work. Of primary concern was an assumption for the inelastic post-buckling response of the plate.[10,11] Since a theoretical analysis to clarify the assumptions poses at present insurmountable difficulties and a planned experimental program seemed to lead to too meager results for the expense involved, it was decided to explore the importance of these assumptions to the ultimate strength of stiffened panels by arbitrarily modifying the assumed portion of the average stress - edge strain relationship. Furthermore, it was desirable to extend the method to non-linear materials. The comprehensive computer program developed for these purposes is described by Ref. 14; the techniques of analysis and the results obtained are reported here.

The computer program can determine the ultimate strength of longitudinally stiffened panels without restrictions on the material properties or the dimensions of the plate components. Although the fundamental principles of analysis are those established in the earlier work, the numerical approach was

made much more general and flexible. This numerical approach is the subject of Part I and should be considered a continuation of the reports of Refs. 9, 11, and 14.

In Part II the results obtained by using the computer program as a test simulator are presented. Specifically, the assumed portion of the average stress - edge strain relationship for the plate was allowed to vary between considered limits of behavior and the resulting effect on ultimate strength was studied. An attempt was also made to pinpoint those combinations of parameters governing ultimate strength for which the assumption may have no, moderate, or considerable influence. The results indicate that ultimate strength for the range of parameters studied previously and used in the development of the design nomographs of Refs. 9 and 12 should not be substantially affected by the plate behavior assumption.

PART I. NUMERICAL TECHNIQUES OF THE COMPUTER PROGRAM

By assuming that the behavior of the plate before and after buckling can be described by an average stress - edge strain relationship and that the lateral interaction between stiffeners due to the nearly cylindrical bending of wide panels is insignificant, the problem of determining the ultimate strength of longitudinally stiffened panels can be reduced to an ultimate strength analysis of a beam-column consisting of a plate and a stiffener with different material properties (Fig. 1). Steps involved in the determination of ultimate strength are the establishment of the average stress - edge strain relationship for the plate, the computation of a moment-curvature relationship for a given axial load, and a stepwise integration solution for the length of the column for which the given loads (axial and lateral) are ultimate loads.

The analysis by Kondo, though exhaustive, restricted the plate dimensions so that the ultimate strength of the beam-column could be attained prior to the occurrence of plate local buckling.[9] Variation in strain through the thickness of the plate due to flexure of the panel was taken into account and residual stresses in the plate and the stiffener flange were

considered. The materials were assumed to have the ideally elastic-plastic relationship.

Tsuiji extended the analysis to stiffened panels for which the failure of the panel is preceded by the buckling of plate components.[11] The description of the behavior of the plate was accomplished by the average stress - edge strain relationship of a long plate simply supported on the sides and loaded in the plane of the plate by loads on the two ends. The effects of residual stresses in the plate were considered. Residual stresses in the stiffener flange had previously been found to have negligible effect on ultimate strength and thus were omitted.[9,11] As suggested by the use of an average stress - edge strain relationship for the plate, variation of strain through the plate thickness was neglected. Again, materials were assumed to be elastic - perfectly plastic.

A computer program was developed to determine the ultimate strength of stiffened panels based on the fundamental principles described above and to extend the method to non-linear materials.[14] This program, unrestricted by plate dimensions or material properties, was made possible by the adoption of:

1) Approximate numerical solution techniques.

2) The assumptions made by Tsuiji exclusive of the restriction on material properties.

3) An extension of the description of plate behavior by an average stress - edge strain relationship to plates with small b/t.

In the succeeding Chapters the equations and numerical techniques of solution employed in the computer program are developed. A brief description of the features of the program and some recommendations for the most efficient use conclude Part I.

2. NONDIMENSIONAL STRESS-STRAIN RELATIONSHIPS FOR THE COMPONENTS OF THE STIFFENED PANEL

2.1 Average Stress vs. Edge Strain Relationship - Assumptions

The average stress - edge strain relationship for the plate, which may include the effects of plate buckling and residual stresses, shall be referred to as the effective stress-strain relationship. The following assumptions are fundamental to the establishment of this relationship:

1) Stresses in the plate are constant through the thickness.

2) The elastic post-buckling behavior of plates with large b/t can de described by the Koiter equation.

3) The inelastic post-buckling behavior of plates with small b/t can be described by a constant stress equal to the average stress which exists when the membrane edge stress has reached the critical buckling level. (The effect of residual stresses is described in Article 2.4)

4) The inelastic post-buckling behavior of plates with large b/t can be described by a constant stress

equal to the average stress which exists when the membrane edge stress has reached the yield level. (The effect of residual stresses is described in Article 2.5)

5) For materials which exhibit other than an ideally elastic-plastic stress-strain relationship, the yield stress shall be defined by the 0.2 per cent offset rule.

6) The plate may contain residual stresses in the pattern shown in Fig. 2(b).

7) The residual stress pattern does not vary along the panel length.

8) Lateral loads on the plate are small. Neither the buckling stress nor the post-buckling behavior of the plate is significantly influenced by lateral load.

9) Strain reversal does not take place. In other words, a strain defines a corresponding stress uniquely.

10) The effect of shear deformations is negligible.

2.2 The Koiter Equation and Non-linear Materials

The Koiter equation has been used with some confidence to describe the elastic post-buckling behavior of plates for which the stress-strain properties of the materials approach the elastic - perfectly plastic configuration.[10,11,12] The computer program implicitly allows the same use for any material.

Experiments for which the load-shortening behavior of plates has been recorded are in short supply, and the only distinctly non-linear material for which such test results are known to exist is aluminum. Ojalvo and Hull conducted tests on 24 S-T3 aluminum plates.[4] The plates had aspect ratios of 4 and 8, and b/t ratios of 71, 91, 138, and 232. Botman and Besseling tested plates of 24 S-T and 75 S-T aluminum.[2,3] The aspect ratio was 4.7 and the b/t ratio varied from 51 to 124. Stein conducted a single test on a 2024-T3 aluminum alloy plate.[5] The aspect ratio was 5.4 and the b/t ratio - 65.

Davidson found that the experimental results of Botman and Besseling agreed extremely well with the Koiter equation and that the equation conservatively predicted the ultimate load of the tests of Ojalvo and Hull for the plates in the lower b/t range.[10] The plate tested by Stein carried a load

greater than that which would be predicted by the Koiter equation. Davidson concluded that the Koiter equation can be used with confidence for long plates having a b/t ratio less than 120.

The Koiter equation is a product of elastic theory and is not valid when inelastic action occurs. For non-linear materials the demarcation is somewhat arbitrary. The 0.2 per cent offset rule has been adopted for this work to define the yield stress. Plate response is based on an assumption after the onset of inelastic action. That more experimental evidence shall prove useful to validate the inelastic post-buckling behavior of plates and the point at which inelastic behavior begins is self-evident.

2.3 Plate Buckling Stress

The behavior of the plate component is assumed to be that of a rectangular plate simply supported on all its edges and loaded in its middle plane by forces uniformly distributed along two opposite sides. The side edges are assumed to remain straight although they are free to move. When loaded in compression, the plate eventually arrives at an unstable condition and buckling occurs. This critical value of the compressive stress is

given by

$$\sigma_{cr} = K \frac{\pi^2 E_t}{12(1-\nu^2)(b/t)^2} \qquad (2.1)$$

where

K = buckling coefficient

E_t = tangent modulus of elasticity

ν = Poisson's ratio

b = plate width

t = plate thickness

The length of the plate is the length of the panel. Since the length to width ratio for longitudinally stiffened panels is usually greater than 3, the value of K is approximately equal to 4. Therefore

$$\sigma_{cr} = \frac{\pi^2 E_t}{3(1-\nu^2)(b/t)^2} \qquad (2.2)$$

A plate shall be said to have a small b/t ratio if

$$\sigma_{cr} \geq \sigma_y \qquad (2.3)$$

Numerical Determination of σ_{cr}. Let Fig. 3 depict an example stress-strain curve for the material of the plate. The curve is described by points with coordinates (σ,ϵ) spaced so that the curve is adequately described by linear segments connecting the points. A table of coordinates containing N_p

entries, the first of which represents the extreme positive point and the m^{th} of which is the (0,0) coordinate, shall represent the curve numerically.

The yield stress, b/t, and ν are known values. E_t is not known analytically, but can be determined segmentally from the table of coordinates. The numerical solution for σ_{cr} can be obtained as follows:

1) Starting with i=m, calculate E_t for the straight line segment connecting the i and i-1 points.

$$E_t = \frac{\sigma_{i-1} - \sigma_i}{\epsilon_{i-1} - \epsilon_i} \qquad (2.4)$$

2) Calculate σ_{cr} with Eq. 2.2 .

3) If σ_{cr} lies between σ_{i-1} and σ_i, then σ_{cr} is the buckling stress; if not, then i should be reduced by 1 and σ_{cr} recalculated.

Steps 1) through 3) are continued until the condition of step 3) is satisfied.

The flow diagram of Fig. 5 illustrates the programmed procedure. Notice the extra steps required because of the discontinuities in E_t at points. The flow diagram also includes

the comparison of σ_{cr} with σ_y which classifies the plate as one with either large or small b/t, where σ_y is the yield stress of the material of the plate. The nondimensionalizing parameters σ_o and ϵ_o, discussed in detail later, take on different values according to the classification.

2.4 Plates With Small b/t

When stresses are less than the buckling stress, the effective stress-strain curve for a plate with no residual stresses will coincide with the material stress-strain curve. This coincidence ceases after the plate buckles. Due to the lack of test results to establish the behavior of the plate after buckling (an inelastic phenomenon), the average stress is assumed to remain equal to the buckling stress.

The effect of residual stresses is two-fold. Equation 2.2 is applicable only to plates subjected to uniform compression. With residual stresses the stress distribution is not uniform. However, the tensile residual stress zones are narrow compared to the compressive zone and located at the plate edges. Thus, it is assumed that the effect of tensile residual stresses on the buckling stress is negligible and that the plate buckles when the sum of the compressive residual stress and the externally applied stress is equal to the buckling stress. The

second effect is in the deviation of the effective stress-strain curve from the material stress-strain curve for stresses less than the buckling stress.

Numerical Development of the Effective Stress-Strain Curve for Plates with Small b/t. Let the curve of Fig. 3 describe the stress-strain properties of the plate material. For the given b/t and ν, σ_{cr} has been found to be larger than σ_y. Residual stresses are as shown in Fig. 2(b).

For a zero externally applied force, the integral of residual stresses across the width of the plate will be zero. Figure 6(a) illustrates the location of residual stresses on the stress-strain curve. The vertical line 1 locates the compressive residual strain, line 2 the externally applied strain, and line 3 the tensile residual strain.

When an external compressive force is applied to the plate the location of the vertical lines shifts to the right as shown in Fig. 6(b). The dimensions $\Delta\epsilon_1$ and $\Delta\epsilon_2$ are constant. Therefore, the plate can be symbolically loaded by shifting the location of the three vertical lines as a unit across the original stress-strain curve. For each position of the line unit, the strain located by line 2 and the calculated effective

stress (the average externally applied stress) comprise coordinates of a point on the effective stress-strain curve.

It is desirable that the effective stress-strain curve retain as much information as is contained in the original stress-strain curve. This is accomplished by calculating the effective stress for each location of line 2 for which either line 1 or 3 intersects the stress-strain curve at a point. If N_p denotes the number of points in the stress-strain curve, then the effective stress-strain curve may contain as many as $2(N_p-1)$ points.

As the plate is loaded in compression, eventually σ_{max} (Figs. 6(a) and 6(b)) will equal σ_{cr} (Fig. 4) at which point the plate buckles. The post-buckling behavior is described by the effective stress which exists at this point. This assumption is illustrated in Fig. 4 .

The equations of equilibrium developed in succeeding sections contain stresses and strains in nondimensional form. The effective stress-strain curve will be most convenient if it is expressed in the same form. To this end, parameters σ_o and ϵ_o have been adopted for nondimensionalizing. In the interest of compatibility with past work, the following values

are assigned to σ_o and ϵ_o:

For plates with small b/t $\begin{cases} \sigma_o = \sigma_y \\ \epsilon_o = \epsilon_y \end{cases}$

For plates with large b/t $\begin{cases} \sigma_o = \sigma_{cr} \\ \epsilon_o = \epsilon_{cr} \end{cases}$

The flow diagrams of Figs. 7, 8, and 9 describe the manner in which the effective, nondimensional stress-strain curve for plates with small b/t is developed in the computer program.

2.5 Plates With Large b/t

The effective stress-strain curve for large b/t plates is developed in a manner identical to that for small b/t plates for stresses less than the buckling stress. However, since the buckling stress is less than the yield stress, the post-buckling behavior of the plate includes an elastic range.

An adequate, and suitably general, description of the behavior of the plate in the post-buckling range has not been complete because of the absence of either test results or theory for deformations beyond the ultimate loads. Thus, it

was assumed that for plate panels with large slengerness ratios the compression branch of the average stress - edge strain curve consists of three distinct parts as shown in Fig. 10: -

1) The pre-buckled part for which the plate average stress - edge strain curve may differ from the material stress-strain curve only to the extent of the residual stresses (curve OA or OA').

2) The elastic post-buckling region defined by the Koiter equation between the buckling stress and the ultimate stress (curve AB or A'B').

3) The post-yield region for which it is assumed that the plate will continue to carry the ultimate average stress (curve BC or B'C').

Experiments have shown that it is reasonable to assume that the ultimate average stress in a plate with no residual stresses is equal to the average stress which exists when the membrane edge stress has reached the yield level. However, if residual stresses exist in the pattern of Fig. 2(b), initial yielding will occur at points A. For this condition the ultimate average stress is influenced by both the reduction in buckling stress and the location of first yield.

The Koiter equation gives the nondimensional average stress in the plate as a function of the strain at the connection with the stiffener (edge strain).

$$\left(\frac{\sigma_p}{\sigma_{cr}}\right) = 1.2\left(\frac{\epsilon_p}{\epsilon_{cr}}\right)^{0.6} - 0.65\left(\frac{\epsilon_p}{\epsilon_{cr}}\right)^{0.2} + 0.45\left(\frac{\epsilon_p}{\epsilon_{cr}}\right)^{-0.2} \qquad (2.5)$$

where

σ_p = average stress

ϵ_p = edge strain

As the stress distribution in the plate is unknown, it has been assumed to be parabolic.[11] With this assumption a relationship between the strain at the stiffener and the ultimate average stress in the plate (determined by first yielding) can be written.

$$\left(\frac{\epsilon_p}{\epsilon_{cr}}\right)_u = \frac{2\left(\frac{\epsilon_y}{\epsilon_{cr}}\right) + 3\left[\left(1 - \frac{c}{b}\right)^2 - 1\right]\left(\frac{\sigma_p}{\sigma_{cr}}\right)_{ult}}{3\left(1 - \frac{c}{b}\right)^2 - 1} \qquad (2.6)$$

If Eq. 2.5 is rewritten

$$\left(\frac{\sigma_p}{\sigma_{cr}}\right)_{ult} = 1.2\left(\frac{\epsilon_p}{\epsilon_{cr}}\right)_u^{0.6} - 0.65\left(\frac{\epsilon_p}{\epsilon_{cr}}\right)_u^{0.2} + 0.45\left(\frac{\epsilon_p}{\epsilon_{cr}}\right)_u^{-0.2} \qquad (2.7)$$

then the ultimate average stress in the plate can be obtained by solving Eqs. 2.6 and 2.7 simultaneously.

Numerical Development of the Effective Stress-Strain Curve for Plates with Large b/t. From the given b/t, ν, and table of coordinates for points representing the stress-strain curve, σ_{cr} has been calculated and found to be less than σ_y. Residual stresses may exist.

When the maximum stress in the plate is less than the buckling stress, the calculation of the coordinates of the points representing the effective stress-strain curve is carried out as described in Article 2.4. At some point in the development of the compression branch, the maximum stress will be equal to the buckling stress (Fig. 11) and the plate will buckle.

The elastic post-buckling region is described by the Koiter equation. The upper limit of validity for this equation is given by the $(\sigma_p)_{ult}$ and $(\epsilon_p)_u$ obtained from Eqs. 2.6 and 2.7. For compatibility with equations developed for solution by numerical techniques, the Koiter equation is not retained in analytical form. Instead, the elastic post-buckling region is described by several coordinates calculated using Eq. 2.5 .

The inelastic post-buckling region consists of constant stress equal to $(\sigma_p)_{ult}$.

The flow diagram of Fig. 12 illustrates the programmed version of the above described procedure. The final result is a table of coordinates representing points of the nondimensional, effective stress-strain curve for the plate with large b/t.

2.6 The Stiffener

The stiffener has a symmetrical cross section about its web. In addition, the dimensions are restricted so that the stiffener components will not buckle before the ultimate load of the stiffened panel is reached, and the effect of residual stresses is neglected. Therefore, the "effective" stress-strain table for the stiffener is the stress-strain table for the material of the stiffener. For convenience, the table is nondimensionalized by σ_o and ϵ_o, where these parameters take on the values as discussed previously.

3. MOMENT - CURVATURE - AXIAL LOAD RELATIONSHIP

3.1 Assumptions

The following assumptions influence the development of the moment - curvature - axial load relationship:

1) The cross section is idealized as shown in Fig. 2(a).
2) The plate remains flat and its load-deformation characteristics are described by the effective stress-strain relationship.
3) The cross section remains plane and normal to the centroidal axis after deformations.
4) The axial load is applied at the centroid of the cross section.

The sign convention used is:

1) Bending moment M and curvature $\emptyset$ are positive if they tend to cause compression in the plate.
2) Stress and strain are positive in compression.
3) Compressive axial loads are positive.

3.2 Basic Equations

Assumption 2) above states that the strain distribution in the cross section is always linear. Figure 13 illustrates such a distribution, where

$\epsilon_{p\ell}$ = effective (edge) strain in the plate

$\epsilon_{f\ell}$ = strain in the stiffener flange

d = stiffener depth

αd = distance from the plate to the centroid of the cross section

The moment M and the axial load N are shown in the positive directions. They are obtained by integrating stresses over the cross section.

$$N = \int_A \sigma \, dA \tag{3.1}$$

$$M = \int_A \sigma z \, dA - N\alpha d \tag{3.2}$$

From Eq. 3.1

$$N = \sigma_{p\ell} A_p + \sigma_{f\ell} A_f + \int_0^d \sigma_z t_w dz \tag{3.3}$$

and from Eq. 3.2

$$M = \sigma_{f\ell} A_f d + \int_0^d \sigma_z t_w z dz - N\alpha d \tag{3.4}$$

where

$\sigma_{p\ell}$ = effective (average) stress in the plate

$\sigma_{f\ell}$ = stress in the stiffener flange

A_p = area of the plate

A_f = area of the stiffener flange

t_w = stiffener web thickness

z = parameter specifying distance from the plate

σ_z = stiffener stress at location z

The curvature ϕ is given by

$$\phi = \frac{\epsilon_{p\ell} - \epsilon_{f\ell}}{d} \tag{3.5}$$

Equations 3.3, 3.4, and 3.5 can be nondimensionalized in the following form:

$$\bar{N} = \frac{N}{N_o} = \frac{\sigma_{p\ell}}{\sigma_o}\left(\frac{A_p}{A_o}\right) + \frac{\sigma_{f\ell}}{\sigma_o}\left(\frac{A_f}{A_o}\right) + \int_0^1 \frac{\sigma_z}{\sigma_o}\left(\frac{A_w}{A_o}\right) d\bar{z} \tag{3.6}$$

$$\bar{M} = \frac{M}{M_o} = \frac{\sigma_{f\ell}}{\sigma_o}\left(\frac{A_f}{A_o}\right)\frac{d}{d_o} + \int_0^1 \frac{\sigma_z}{\sigma_o}\frac{t_w d}{A_o}\left(\frac{d}{d_o}\right)\bar{z}d\bar{z} - \frac{N}{N_o}\alpha\left(\frac{d}{d_o}\right) \tag{3.7}$$

and

$$\bar{\phi} = \frac{\phi}{\phi_o} = \left(\frac{\epsilon_{p\ell}}{\epsilon_o} - \frac{\epsilon_{f\ell}}{\epsilon_o}\right)\left(\frac{d}{d_o}\right) \tag{3.8}$$

where

$$A_w = t_w d \tag{3.9a}$$

$$\bar{z} = \frac{z}{d_o} \tag{3.9b}$$

and N_o, M_o, σ_o, ϵ_o, ϕ_o, and d_o are, for the moment, arbitrary nondimensionalizing parameters.

Selection of the values for the nondimensionalizing parameters was done to produce greatest consistency with previous work and/or to produce parameters which have been shown to have an effect on the ultimate strength of the

stiffened panel. The result of this selection is

$$N_o = \sigma_o A_o \tag{3.10a}$$

$$M_o = \sigma_o A_o d_o \tag{3.10b}$$

$$A_o = A \tag{3.10c}$$

$$\phi_o = \epsilon_o / d_o \tag{3.10d}$$

$$d_o = d \tag{3.10e}$$

$$\sigma_o = \sigma_{cr} \text{ or } \sigma_y \text{ (see Article 2.4)} \tag{3.10f}$$

$$\epsilon_o = \epsilon_{cr} \text{ or } \epsilon_y \text{ (see Article 2.4)} \tag{3.10g}$$

Kondo has concluded that the cross-sectional parameters $\frac{A_{st}}{A_p}$ and $\frac{A_f}{A_{st}}$ have an effect on the ultimate strength [9], where

$$A_{st} = A_f + A_w \tag{3.11}$$

With Eqs. 3.10, Eqs. 3.6, 3.7, and 3.8 can be rewritten

$$\bar{N} = k_1 \bar{\sigma}_{p\ell} + k_2 \bar{\sigma}_{f\ell} + k_3 \int_0^1 \bar{\sigma} d\bar{z} \tag{3.12}$$

$$\bar{M} = k_2 \bar{\sigma}_{f\ell} + k_3 \int_0^1 \bar{\sigma}\, \bar{z} d\bar{z} - \alpha \bar{N} \tag{3.13}$$

$$\bar{\phi} = \bar{\epsilon}_{p\ell} - \bar{\epsilon}_{f\ell} \tag{3.14}$$

where

$$k_1 = \frac{1}{1 + A_{st}/A_p} \tag{3.15a}$$

$$k_2 = \frac{A_{st}}{A_p}\left(\frac{A_f}{A_{st}}\right)k_1 \qquad (3.15b)$$

$$k_3 = \left(1 - \frac{A_f}{A_{st}}\right)\left(\frac{A_{st}}{A_p}\right)k_1 \qquad (3.15c)$$

$$\bar{\sigma} = \frac{\sigma_z}{\sigma_o} \qquad (3.15d)$$

The nondimensional distance from the plate to the centroidal axis of the cross section can also be expressed in terms of these parameters.

$$\alpha = \tfrac{1}{2}\frac{A_{st}}{A_p}\left(1 + \frac{A_f}{A_{st}}\right)k_1 \qquad (3.16)$$

Notice that now stresses and strains for both the plate and the stiffener are in the nondimensional, "effective" forms that were developed in Articles 2.4, 2.5, and 2.6.

Equations 3.12 through 3.16 and the functions

$$\bar{\sigma}_{p\ell} = f(\bar{\epsilon}_{p\ell}) \qquad (3.17a)$$

$$\bar{\sigma}_{f\ell} = f(\bar{\epsilon}_{f\ell}) \qquad (3.17b)$$

represented by the tables of stress-strain coordinates from Chapter 2 are sufficient to calculate a moment-curvature relationship for a given axial load $\bar{N}$.

3.3 Development of the Moment - Curvature - Axial Load Relationship

All of the methods which have been used for the determination of the moment - curvature - axial load relationship may be classified as analytical (restricted to extremely simple cross sections), graphical or semi-graphical, or semi-numerical (cross section is divided into sub-areas so that in each sub-area the analytical integration can be easily done). In all cases the application has been restricted to the elastic - perfectly plastic relationship between stress and strain.

The method developed here for the computer program is totally numerical and is believed to be original. It was developed assuming that the program would be used in high speed computers because the effort of compiling tables of analytical equations for all possible equilibrium configurations (required by the above methods) has been transferred to the computer to carry out simple, but time consuming, numerical procedures. The method allows the use of any stress-strain relationship and only minor modifications would be required to extend its use to cross sections and residual stress patterns different from those illustrated by Figs. 2(a) and 2(b).

The problem is to determine M and $\emptyset$ for a given value of N and some specified strain (hereafter, this reference strain shall always be the edge strain in the plate, ϵ_{pl}). If the moment-curvature relationship developed is to be useful then N should be the axial load in the stiffened panel. Due to lateral loading, however, N varies along the length of the panel, and it would seem that an infinite number of moment-curvature relationships is required. Fortunately, numerical results have shown that for the magnitudes of lateral load encountered on ship hulls the axial load N at any point in the stiffened panel differs only negligibly (less than 0.05 per cent) from the load P applied to the panel ends. Therefore, the moment-curvature relationship for N, where

$$N = P \tag{3.18}$$

is used for the entire structure.

3.3.1 Limits on the Nondimensional, Effective Stress-Strain Curves

The algorithm developed for calculating the $\overline{M}$-$\overline{\emptyset}$-$\overline{N}$ relationship can be relatively free from complications if it is assumed that the tables of coordinates representing the behavior of plate and stiffener are always delivered in some standard form. That standard form includes the requirement

that all coordinates be usable. Let us see how some coordinates of the effective stress-strain tables (as developed in Chapter 2) may not be usable.

The computer program user prepares input tables of coordinates which adequately describe the material properties. The extent of a table (from the largest strain to the smallest strain) is arbitrary; however, the computer can make no assumptions about the behavior of the material outside the limits of the tables. These limits are retained in the nondimensional, effective stress-strain tables.

Let Fig. 14 illustrate the nondimensional, effective stress-strain curves which result from the procedures advanced in Chapter 2, where $(\bar{\sigma}_f, \bar{\epsilon}_f)$ denote the nondimensional coordinates for the stiffener. N_p and N_s are the current number of points describing the curves for the plate and stiffener. Assume for a given $\bar{N}$ and $\bar{\epsilon}_{p\ell}$, say

$$\bar{\epsilon}_{p\ell} = \frac{(\epsilon_p)_a}{\epsilon_o} = (\bar{\epsilon}_p)_a \qquad \text{(see point a in Fig. 14)}$$

that the Eq. 3.12 is satisfied when

$$\bar{\epsilon}_{f\ell} = \frac{(\epsilon_f)_b}{\epsilon_o} = (\bar{\epsilon}_f)_b$$

Then that portion of the plate stress-strain curve for strains

greater than $(\bar{\epsilon}_p)_a$ is useless as long as $\bar{N}$ remains constant because stiffener flange strains smaller than $(\bar{\epsilon}_f)_b$ would be required to satisfy Eq. 3.12. Those strains are not available. Similarly, for the same $\bar{N}$, some strain $(\bar{\epsilon}_p)_c$ can be found so that Eq. 3.12 is satisfied when $\bar{\epsilon}_{f\ell}$ is equal to $(\bar{\epsilon}_f)_d$. Then that portion of the plate stress-strain curve for strains less than $(\bar{\epsilon}_p)_c$ is of no use. Situations could just as easily arise where portions of the stiffener stress-strain curve would be found useless.

These limits are automatically located by the computer program, and the nondimensional, effective stress-strain curves are reduced to the useful regions. For the remainder of this Chapter it will be assumed that all coordinates are useful, and that the coordinates have been re-indexed starting with 1 at the largest permissible strain and ending with N_p or N_f at the smallest permissible strain.

Notice that the limits on strains result in limits on curvature. These limits are denoted by $\bar{\phi}_{max}$ and $\bar{\phi}_{min}$.

3.3.2 Numerical Techniques

The cross-sectional dimensions $\frac{A_{st}}{A_p}$ and $\frac{A_f}{A_{st}}$ are known, and the tables of coordinates, $(\bar{\sigma}_p, \bar{\epsilon}_p)$ and $(\bar{\sigma}_f, \bar{\epsilon}_f)$, for the components of the stiffened panel have been developed. $\bar{P}$ is given and it is desired that

$$\bar{N} = \bar{P} \tag{3.19}$$

The moment-curvature relationship for the given axial load is developed by assigning values to $\bar{\epsilon}_{p\ell}$ over the full range of allowable values, $(\bar{\epsilon}_p)_1$ to $(\bar{\epsilon}_p)_{N_p}$, and for each solving Eqs. 3.12, 3.13, and 3.14. The user of the computer program inputs a number $N_{M\emptyset}$ which determines the number of coordinates $(\bar{M}, \bar{\emptyset})$ to be calculated. The computer program automatically distributes the coordinates in equal increments of curvature over the full range between $\bar{\emptyset}_{max}$ and $\bar{\emptyset}_{min}$.

A single coordinate is calculated by:

1) Assigning a value to $\bar{\epsilon}_{p\ell}$.
2) Determining $\bar{\epsilon}_{f\ell}$ by trial and error so that $\bar{N}$ is sufficiently close to $\bar{P}$, in other words, so that

$$|\bar{N} - \bar{P}| \leq \tau \bar{P} \tag{3.20}$$

where $\bar{N}$ is calculated from Eq. 3.12 and τ is a tolerance factor.

3) Solving Eqs. 3.13 and 3.14 for $\overline{M}$ and $\overline{\emptyset}$.

The algorithm developed to carry out these three steps shall be introduced by an example. Let $\overline{\epsilon}_{p\ell}$ be some arbitrary plate strain between $(\overline{\epsilon}_p)_1$ and $(\overline{\epsilon}_p)_{N_p}$ and let $\overline{\epsilon}_e$ (see Fig. 14) be the required stiffener flange strain so that $\overline{N} = \overline{P}$. Since $\overline{\epsilon}_e$ is unknown, assumption of uniform strain over the entire cross section is as reasonable a first estimate as any other, so that

$$\overline{\epsilon}_{f\ell} = \overline{\epsilon}_{p\ell} \tag{3.21}$$

This strain condition is illustrated in Fig. 15(a). From Eq. 3.12

$$\overline{N} = k_1 \overline{\sigma}_{p\ell} + (k_2 + k_3) \overline{\sigma}_{f\ell} \tag{3.22}$$

A check would disclose that the condition of Eq. 3.20 fails for this example, and that

$$(\overline{N} - \overline{P}) > 0 \tag{3.23}$$

Thus, the desired $\overline{\epsilon}_{f\ell}$ is less than $\overline{\epsilon}_{p\ell}$ and the search shall be concentrated in the strain range $\overline{\epsilon}_{p\ell}$ to $(\overline{\epsilon}_f)_{N_s}$.

The stiffener stress-strain coordinates are temporarily re-indexed starting with 1' and ending with N_s' as shown by the primed numbers in Fig. 14. If $\overline{N}$ had been less than $\overline{P}$, then the re-indexing would have begun at $\overline{\epsilon}_f = \overline{\epsilon}_{p\ell}$ and proceeded in

the positive direction.

The next logical assumption for $\bar{\epsilon}_{f\ell}$ is

$$\bar{\epsilon}_{f\ell} = (\bar{\epsilon}_f)_{2'} \tag{3.24}$$

The strain distribution is shown in Fig. 15(b). From Eq. 3.12

$$\bar{N} = k_1\bar{\sigma}_{p\ell} + k_2(\bar{\sigma}_f)_{2'} + \tfrac{1}{2}k_3[(\bar{\sigma}_f)_{1'} + (\bar{\sigma}_f)_{2'}]\left[\frac{(\bar{\epsilon}_f)_{2'} - (\bar{\epsilon}_f)_{1'}}{(\bar{\epsilon}_f)_{2'} - (\bar{\epsilon}_f)_{1'}}\right] \tag{3.25}$$

For simplicity, let Eq. 3.25 be rewritten

$$\bar{N} = k_1\bar{\sigma}_{p\ell} + k_2\bar{\sigma}_2 + \tfrac{1}{2}k_3(\bar{\sigma}_1 + \bar{\sigma}_2)\left(\frac{\bar{\epsilon}_2 - \bar{\epsilon}_1}{\bar{\epsilon}_2 - \bar{\epsilon}_1}\right) \tag{3.26}$$

where it is understood that $\bar{\sigma}_i$ and $\bar{\epsilon}_i$ refer to the re-indexed (primed) stiffener stress-strain coordinates (the same simplification has been made in Fig. 15).

To deduce the general form of Eq. 3.26 let $\bar{\epsilon}_{f\ell}$ undergo several reductions. For $\bar{\epsilon}_{f\ell} = \bar{\epsilon}_3$ (see Fig. 15(c))

$$\bar{N} = k_1\bar{\sigma}_{p\ell} + k_2\bar{\sigma}_3 + \tfrac{1}{2}k_3\left[(\bar{\sigma}_1 + \bar{\sigma}_2)\left(\frac{\bar{\epsilon}_2 - \bar{\epsilon}_1}{\bar{\epsilon}_3 - \bar{\epsilon}_1}\right) + (\bar{\sigma}_2 + \bar{\sigma}_3)\left(\frac{\bar{\epsilon}_3 - \bar{\epsilon}_2}{\bar{\epsilon}_3 - \bar{\epsilon}_1}\right)\right] \tag{3.27}$$

For $\bar{\epsilon}_{f\ell} = \bar{\epsilon}_4$ (see Fig. 15(d))

the positive direction.

The next logical assumption for $\bar{\epsilon}_{f\ell}$ is

$$\bar{\epsilon}_{f\ell} = (\bar{\epsilon}_f)_{2'} \tag{3.24}$$

The strain distribution is shown in Fig. 15(b). From Eq. 3.12

$$\bar{N} = k_1\bar{\sigma}_{p\ell} + k_2(\bar{\sigma}_f)_{2'} + \tfrac{1}{2}k_3[(\bar{\sigma}_f)_{1'} + (\bar{\sigma}_f)_{2'}][\frac{(\bar{\epsilon}_f)_{2'} - (\bar{\epsilon}_f)_{1'}}{(\bar{\epsilon}_f)_{2'} - (\bar{\epsilon}_f)_{1'}}] \tag{3.25}$$

For simplicity, let Eq. 3.25 be rewritten

$$\bar{N} = k_1\bar{\sigma}_{p\ell} + k_2\bar{\sigma}_2 + \tfrac{1}{2}k_3(\bar{\sigma}_1 + \bar{\sigma}_2)(\frac{\bar{\epsilon}_2 - \bar{\epsilon}_1}{\bar{\epsilon}_2 - \bar{\epsilon}_1}) \tag{3.26}$$

where it is understood that $\bar{\sigma}_i$ and $\bar{\epsilon}_i$ refer to the re-indexed (primed) stiffener stress-strain coordinates (the same simplification has been made in Fig. 15).

To deduce the general form of Eq. 3.26 let $\bar{\epsilon}_{f\ell}$ undergo several reductions. For $\bar{\epsilon}_{f\ell} = \bar{\epsilon}_3$ (see Fig. 15(c))

$$\bar{N} = k_1\bar{\sigma}_{p\ell} + k_2\bar{\sigma}_3 + \tfrac{1}{2}k_3[(\bar{\sigma}_1 + \bar{\sigma}_2)(\frac{\bar{\epsilon}_2 - \bar{\epsilon}_1}{\bar{\epsilon}_3 - \bar{\epsilon}_1}) + (\bar{\sigma}_2 + \bar{\sigma}_3)(\frac{\bar{\epsilon}_3 - \bar{\epsilon}_2}{\bar{\epsilon}_3 - \bar{\epsilon}_1})] \tag{3.27}$$

For $\bar{\epsilon}_{f\ell} = \bar{\epsilon}_4$ (see Fig. 15(d))

$$\bar{N} = k_1\bar{\sigma}_{p\ell} + k_2\bar{\sigma}_4 + \tfrac{1}{2}k_3\left[(\bar{\sigma}_1+\bar{\sigma}_2)\left(\frac{\bar{\epsilon}_2-\bar{\epsilon}_1}{\bar{\epsilon}_4-\bar{\epsilon}_1}\right)+(\bar{\sigma}_2+\bar{\sigma}_3)\left(\frac{\bar{\epsilon}_3-\bar{\epsilon}_2}{\bar{\epsilon}_4-\bar{\epsilon}_1}\right)\right.$$

$$\left.+(\bar{\sigma}_3+\bar{\sigma}_4)\left(\frac{\bar{\epsilon}_4-\bar{\epsilon}_3}{\bar{\epsilon}_4-\bar{\epsilon}_1}\right)\right] \qquad (3.28)$$

The general equation for $\bar{N}$ for the i^{th} reduction in $\bar{\epsilon}_{f\ell}$ is clearly

$$\bar{N} = k_1\bar{\sigma}_{p\ell} + k_2\bar{\sigma}_{i+1} + \tfrac{1}{2}k_3\,\frac{\sum_{n=1}^{i}(\bar{\sigma}_n+\bar{\sigma}_{n+1})(\bar{\epsilon}_{n+1}-\bar{\epsilon}_n)}{\bar{\epsilon}_{i+1}-\bar{\epsilon}_1} \qquad (3.29)$$

Equation 3.29 with the condition of Eq. 3.20 constitutes the numerical equivalent of Eqs. 3.12 and 3.19. As Eq. 3.29 is repeatedly used for increasing i, eventually either the condition of Eq. 3.20 shall be satisfied (an unlikely occurrence) or

$$(\bar{N} - \bar{P}) < 0 \qquad (3.30)$$

The second event would occur for the example when the index i reached n' (see Fig. 14), in which case

$$\bar{\epsilon}_{i+1} < \bar{\epsilon}_e < \bar{\epsilon}_i \qquad (3.31)$$

By making use of $(\bar{N} - \bar{P})$ vs. $\bar{\epsilon}_{f\ell}$ relationships, the trial and error process is continued by adjusting $\bar{\epsilon}_{f\ell}$ within the interval given by Eq. 3.31 until $\bar{N} - \bar{P}$ is as small as desired.

When $\bar{\epsilon}_{f\ell}$ has been determined to satisfaction (the axial load is balanced), then the strain range in the cross section

is known. Figure 16(a) illustrates that range isolated from the stiffener stress-strain curve. The coordinate indexing is identical to the primed indexing of Fig. 14 with one exception; a new coordinate has been created at $\bar{\epsilon}_e$ and indexed n+1. Figure 16(c) shows the strains and stresses in the cross section.

The contribution to $\bar{M}$ made by the typical stress block of Fig. 16(b) is

$$\bar{M}_i = k_3\bar{\sigma}_i\left[\frac{\bar{\epsilon}_{i+1}-\bar{\epsilon}_i}{\bar{\epsilon}_{n+1}-\bar{\epsilon}_1}\right]\left[\frac{\bar{\epsilon}_i-\bar{\epsilon}_1}{\bar{\epsilon}_{n+1}-\bar{\epsilon}_1} + \tfrac{1}{2}\frac{\bar{\epsilon}_{i+1}-\bar{\epsilon}_i}{\bar{\epsilon}_{n+1}-\bar{\epsilon}_1}\right]$$

$$-\tfrac{1}{2}(\bar{\sigma}_i-\bar{\sigma}_{i+1})\left[\frac{\bar{\epsilon}_{i+1}-\bar{\epsilon}_i}{\bar{\epsilon}_{n+1}-\bar{\epsilon}_1}\right]\left[\frac{\bar{\epsilon}_i-\bar{\epsilon}_1}{\bar{\epsilon}_{n+1}-\bar{\epsilon}_1} + \frac{2}{3}\frac{\bar{\epsilon}_{i+1}-\bar{\epsilon}_i}{\bar{\epsilon}_{n+1}-\bar{\epsilon}_1}\right] \qquad (3.32)$$

The total contribution of the stiffener web is obtained by summing all stress block contributions. With some rearrangement

$$\bar{M}_{web} = \tfrac{1}{2}\frac{k_3}{(\bar{\epsilon}_{n+1}-\bar{\epsilon}_1)^2}\sum_{i=1}^{n}[\bar{\sigma}_i(\bar{\epsilon}_{i+1}-\bar{\epsilon}_i)(\bar{\epsilon}_{i+1}+\bar{\epsilon}_i-2\bar{\epsilon}_1)$$

$$+\frac{1}{3}(\bar{\sigma}_{i+1}-\bar{\sigma}_i)(\bar{\epsilon}_{i+1}-\bar{\epsilon}_i)(2\bar{\epsilon}_{i+1}+\bar{\epsilon}_i-3\bar{\epsilon}_1)] \qquad (3.33)$$

Finally

$$\bar{M} = \alpha\bar{N} - k_2\bar{\sigma}_{f\ell} - \bar{M}_{web} \qquad (3.34)$$

where

$$\bar{\sigma}_{f\ell} = \bar{\sigma}_{n+1} \tag{3.35}$$

The curvature is obtained from Eq. 3.14.

The detailed flow diagram of Fig. 17 illustrates the general algorithm of the computer program for developing the moment-curvature relationship.

4. ULTIMATE STRENGTH OF THE STIFFENED PANEL

4.1 Introduction

With the moment-curvature relationship for a given axial load known, the length of the stiffened panel for which the combination of axial and lateral loading is ultimate can be determined. The moment-curvature relationship depended on the shape of the cross section, the axial load, the residual stresses, and the material properties; the panel length for which the given loads are ultimate loads depends on the moment-curvature relationship, the lateral loading, and the boundary conditions. The problem is to determine this ultimate panel length.

For a given loading system, the length-deformation characteristic of a structure becomes a curve on a length-deformation plot, which rises to a maximum point and then falls off with the weakening of the section due to yielding. A typical length-deformation curve which conforms to the general configuration encountered for stiffened panels is shown is Fig. 21, where L is the column length and ϕ^o is the maximum curvature (the curvature at the panel mid-point when boundary conditions are identical at both ends). The curve represents equilibrium points which may be stable or unstable. A unique curve would be obtained

for a given combination of axial and lateral loads and for a given boundary condition.

The criterion to define the column length for which the given loads are ultimate loads was explained by Kondo in terms of the length-deformation characteristic. It can be expressed by

$$\left(\frac{dL}{d\phi_o}\right)_{\substack{P=\text{constant}\\ q=\text{constant}}} = 0 \qquad (4.1)$$

where P is the axial load applied to the ends of the column and q is the uniformly distributed lateral loading. In Fig. 21, the point of zero gradient is designated by Eq. 4.1 as the transition point from stable to unstable equilibrium and L_{max} is the ultimate column length (the column length for which the given loads are ultimate). Determination of L_{max} is accomplished by calculating the length-deformation curve and locating the point of zero gradient.

Numerically, the length-deformation curve is constructed by repetively determining the panel length as the mid-point curvature is assigned different values. In the following Articles the equations involved in determining the panel length and the techniques of solution are presented.

4.2 Basic Equations

Shown in Fig. 22 is a stiffened panel subjected to the axial load P and a line load of magnitude qb, where q is the uniformly distributed lateral loading on the plate and b is the plate width. A typical panel segment of infinitesimal length ds appears in Fig. 23. The equilibrium equations for the segment are

$$dH = qb\ ds_p \sin\theta \tag{4.2}$$

$$dV = qb\ ds_p \cos\theta \tag{4.3}$$

$$dM = -H\sin\theta ds - V\cos\theta ds - \tfrac{1}{2}qb\ ds_p\ ds \tag{4.4}$$

Since αd is the distance from the centroidal axis to the plate

$$ds_p = (1 - \emptyset\alpha d)ds \tag{4.5}$$

Neglecting terms of higher order, Eqs. 4.2, 4.3, and 4.4 become

$$\frac{dH}{ds} = (1 - \emptyset\alpha d)qb\sin\theta \tag{4.6}$$

$$\frac{dV}{ds} = (1 - \emptyset\alpha d)qb\cos\theta \tag{4.7}$$

$$\frac{dM}{ds} = -H\sin\theta - V\cos\theta \tag{4.8}$$

where

$$\sin\theta = \frac{dy}{ds} \tag{4.9}$$

$$\cos\theta = \frac{dx}{ds} \tag{4.10}$$

The curvature ϕ is given by

$$\phi = \frac{d\theta}{ds} \tag{4.11}$$

After rearranging and nondimensionalizing, Eqs. 4.6 through 4.11 become

$$\frac{d\bar{H}}{ds} = \frac{qb\ell_o}{N_o}\left[1 - \left(\frac{\alpha d}{\ell_o}\right)\frac{d\theta}{ds}\right]\frac{d\bar{y}}{ds} \tag{4.12}$$

$$\frac{d\bar{V}}{ds} = \frac{qb\ell_o}{N_o}\left[1 - \left(\frac{\alpha d}{\ell_o}\right)\frac{d\theta}{ds}\right]\frac{d\bar{x}}{ds} \tag{4.13}$$

$$\frac{d\bar{M}}{ds} = -\frac{N_o\ell_o}{M_o}\left(\bar{H}\frac{d\bar{y}}{ds} + \bar{V}\frac{d\bar{x}}{ds}\right) \tag{4.14}$$

$$\frac{d\bar{y}}{ds} = \sin\theta \tag{4.15}$$

$$\frac{d\bar{x}}{ds} = \cos\theta \tag{4.16}$$

$$\frac{d\theta}{ds} = (\ell_o\phi_o)\bar{\phi} \tag{4.17}$$

where

$$\bar{H} = H/N_o \tag{4.18a}$$

$$\bar{V} = V/N_o \tag{4.18b}$$

$$\bar{M} = M/M_o \tag{4.18c}$$

$$\bar{\phi} = \phi/\phi_o \tag{4.18d}$$

$$\bar{s} = s/\ell_o \tag{4.18e}$$

$$\bar{x} = x/\ell_o \tag{4.18f}$$

$$\bar{y} = y/\ell_o \tag{4.18g}$$

All of the nondimensionalizing parameters (denoted by the subscript o) except ℓ_o are given by Eqs. 3.10. If

$$\ell_o = r \tag{4.19}$$

where r is the radius of gyration of the cross section, and if

$$k_5 = \frac{r}{d}\,\epsilon_o \tag{4.20a}$$

$$k_6 = \frac{qbr}{\sigma_o A} \tag{4.20b}$$

$$k_7 = \frac{\alpha}{r/d} \tag{4.20c}$$

$$k_8 = -\frac{r}{d} \tag{4.20d}$$

then

$$\frac{d\bar{H}}{d\bar{s}} = k_6\left(1 - k_7 \frac{d\theta}{d\bar{s}}\right) \frac{d\bar{y}}{d\bar{s}} \tag{4.21}$$

$$\frac{d\bar{V}}{d\bar{s}} = k_6\left(1 - k_7 \frac{d\theta}{d\bar{s}}\right) \frac{d\bar{x}}{d\bar{s}} \tag{4.22}$$

$$\frac{d\bar{M}}{d\bar{s}} = k_8\left(\bar{H} \frac{d\bar{y}}{d\bar{s}} + \bar{V} \frac{d\bar{x}}{d\bar{s}}\right) \tag{4.23}$$

$$\frac{d\theta}{d\bar{s}} = k_5 \bar{\emptyset} \tag{4.24}$$

4.3 Numerical Integration

Figure 24 shows the i^{th} panel segment of finite length $\Delta\bar{s}$. Forces and dimensions are in the nondimensional form developed above. The variation of the curvature within the segment is not known. Assuming that it is constant, at the location $\bar{z}$ in the

segment the curvature is

$$\bar{\phi}(\bar{z}) = \bar{\phi}_i + \frac{\bar{\phi}_{i+1} - \bar{\phi}_i}{\Delta\bar{s}}\bar{z} \tag{4.25}$$

Then, from Eq. 4.24

$$\theta(\bar{z}) = \theta_i + k_5(\bar{\phi}_i\bar{z} + \tfrac{1}{2}\frac{\bar{\phi}_{i+1}-\bar{\phi}_i}{\Delta\bar{s}}\bar{z}^2) \tag{4.26}$$

From Eqs. 4.21, 4.22, and 4.23 the stress resultants at location $\bar{z}$ are

$$\bar{H}(\bar{z}) = \bar{H}_i + k_6[(\bar{y}-\bar{y}_i) + k_7(\cos\theta - \cos\theta_i)] \tag{4.27}$$

$$\bar{V}(\bar{z}) = \bar{V}_i + k_6[(\bar{x}-\bar{x}_i) - k_7(\sin\theta - \sin\theta_i)] \tag{4.28}$$

$$\bar{M}(\bar{z}) = \bar{M}_i + k_8\Big\{(\bar{H}_i - k_6k_7\cos\theta_i)(\bar{y}-\bar{y}_i) + (\bar{V}_i + k_6k_7\sin\theta_i)(\bar{x}-\bar{x}_i) + \tfrac{1}{2}k_6[(\bar{y}-\bar{y}_i)^2 + (\bar{x}-\bar{x}_i)^2]\Big\} \tag{4.29}$$

From Eq. 4.15

$$\bar{y}-\bar{y}_i = \int_{\bar{s}_i}^{\bar{s}_i+\bar{z}} \sin\theta\, d\bar{s} \tag{4.30}$$

where

$$\sin\theta = \sin(\theta_i+\Delta\theta) = \sin\theta_i\cos\Delta\theta + \cos\theta_i\sin\Delta\theta \tag{4.31}$$

Since $\Delta\theta$ is small, let

$$\cos\Delta\theta = 1 \tag{4.32}$$

$$\sin\Delta\theta = \Delta\theta = k_5(\bar{\phi}_i\bar{z} + \tfrac{1}{2}\frac{\bar{\phi}_{i+1}-\bar{\phi}_i}{\Delta\bar{s}}\bar{z}^2) \tag{4.33}$$

Then

$$\bar{y}-\bar{y}_i = \sin\theta_i\int_0^{\bar{z}} d\bar{z} + k_5\cos\theta_i\int_0^{\bar{z}}(\bar{\phi}_i\bar{z} + \tfrac{1}{2}\frac{\bar{\phi}_{i+1}-\bar{\phi}_i}{\Delta\bar{s}}\bar{z}^2)\,d\bar{z}$$

or

$$\bar{y}-\bar{y}_i = \bar{z}\sin\theta_i + k_5\cos\theta_i(\bar{\phi}_i\frac{\bar{z}^2}{2} + \frac{1}{6}\frac{\bar{\phi}_{i+1}-\bar{\phi}_i}{\Delta\bar{s}}\bar{z}^3) \tag{4.34}$$

Similarly

$$\bar{x}-\bar{x}_i = \bar{z}\cos\theta_i - k_5\sin\theta_i\left(\bar{\phi}_i \frac{\bar{z}^2}{2} + \frac{1}{6}\frac{\bar{\phi}_{i+1}-\bar{\phi}_i}{\Delta\bar{s}}\bar{z}^3\right) \quad (4.35)$$

4.3.1 The Numerical Technique for Determining Ultimate Strength

Let the stress resultants $\bar{H}_i$ and $\bar{V}_i$ and also the geometric parameters $\bar{\phi}_i$, θ_i, $\bar{x}_i$, $\bar{y}_i$, and $\bar{s}_i$ be known quantities. $\bar{M}_i$ is also known because the moment-curvature relationship is equivalent to

$$\bar{M}_i = f(\bar{\phi}_i, \bar{N}_i) \quad (4.36)$$

where $\bar{N}_i$ is the axial load at point i

$$\bar{N}_i = \bar{H}_i\cos\theta_i - \bar{V}_i\sin\theta_i \quad (4.37)$$

It is desired to calculate these parameters at the panel location $\bar{s}_{i+1}$.

Let the segment length $\Delta\bar{s}$ be small so that the assumptions of Eqs. 4.25, 4.32, and 4.33 create no problems, and let $\bar{z}$ be equal to $\Delta\bar{s}$. The curvature $\bar{\phi}_{i+1}$ is unknown and must be obtained by trial and error. Try

$$\bar{\phi}_{i+1} = \bar{\phi}_a \quad (4.38)$$

where $\bar{\phi}_a$ is an assumed value. From Eq. 4.26

$$\theta_{i+1} = \theta_i + k_5\left(\frac{\bar{\phi}_a+\bar{\phi}_i}{2}\right)\Delta\bar{s} \quad (4.39)$$

From Eqs. 4.34 and 4.35

$$\Delta\bar{y} = \bar{y}_{i+1} - \bar{y}_i = \Delta\bar{s}\sin\theta_i + k_5\left(\frac{\bar{\phi}_i}{3} + \frac{\bar{\phi}_a}{6}\right)\cos\theta_i(\Delta\bar{s})^2 \qquad (4.40)$$

$$\Delta\bar{x} = \bar{x}_{i+1} - \bar{x}_i = \Delta\bar{s}\cos\theta_i - k_5\left(\frac{\bar{\phi}_i}{3} + \frac{\bar{\phi}_a}{6}\right)\sin\theta_i(\Delta\bar{s})^2 \qquad (4.41)$$

and from Eq. 4.29

$$\bar{M}_{i+1} = \bar{M}_i + k_8\Big\{(\bar{H}_i - k_6k_7\cos\theta_i)\Delta\bar{y} + (\bar{V}_i + k_6k_7\cos\theta_i)\Delta\bar{x} + \tfrac{1}{2}k_6(\Delta\bar{y}^2 + \Delta\bar{x}^2)\Big\} \qquad (4.42)$$

The curvature corresponding to $\bar{M}_{i+1}$ can be located in the moment-curvature table, in other words

$$\bar{\phi}_c = f(\bar{M}_{i+1}, \bar{N}) \qquad (4.43)$$

where $\bar{\phi}_c$ denotes a calculated $\bar{\phi}_{i+1}$. It is desired that

$$\bar{\phi}_c = \bar{\phi}_a \qquad (4.44)$$

If a discrepancy exists, then the iterative solution for $\bar{\phi}_{i+1}$ is accomplished by setting $\bar{\phi}_a$ equal to $\bar{\phi}_c$, recalculating Eqs. 4.39 through 4.43, and readjusting $\bar{\phi}_a$ if necessary until Eq. 4.44 is satisfied (or nearly so). Then

$$\bar{\phi}_{i+1} = \bar{\phi}_c \qquad (4.45)$$

and

$$\bar{H}_{i+1} = \bar{H}_i + k_6[\Delta\bar{y} + k_7(\cos\theta_{i+1} - \cos\theta_i)] \qquad (4.46)$$

$$\bar{V}_{i+1} = \bar{V}_i + k_6[\Delta\bar{x} - k_7(\sin\theta_{i+1} - \sin\theta_i)] \qquad (4.47)$$

The panel length and deflections at $\bar{s} = \bar{s}_{i+1}$ are

$$\bar{s}_{i+1} = \bar{s}_i + \Delta\bar{s} \tag{4.48}$$

$$\bar{y}_{i+1} = \bar{y}_i + \Delta\bar{y} \tag{4.49}$$

$$\bar{x}_{i+1} = \bar{x}_i + \Delta\bar{x} \tag{4.50}$$

In preparation for solving the equilibrium equations for the succeeding panel segment, the initial values are updated.

$$\bar{s}_i = \bar{s}_{i+1} \tag{4.51a}$$

$$\bar{x}_i = \bar{x}_{i+1} \tag{4.51b}$$

$$\bar{y}_i = \bar{y}_{i+1} \tag{4.51c}$$

$$\bar{H}_i = \bar{H}_{i+1} \tag{4.51d}$$

$$\bar{V}_i = \bar{V}_{i+1} \tag{4.51e}$$

$$\bar{M}_i = \bar{M}_{i+1} \tag{4.51f}$$

$$\theta_i = \theta_{i+1} \tag{4.51g}$$

$$\bar{\phi}_i = \bar{\phi}_{i+1} \tag{4.51h}$$

4.3.2 Initial Values

The stepwise integration procedure can be commenced only after the values for the stress resultants and geometric parameters at the panel mid-point have been specified. Designating mid-point values by the superscript o

$$\bar{H}^o = \bar{P} \tag{4.52a}$$

$$\bar{y}^o = 0 \qquad (4.52b)$$

$$\bar{x}^o = 0 \qquad (4.52c)$$

$$\bar{s}^o = 0 \qquad (4.52d)$$

For a structure whose loading edges have identical boundary conditions

$$\bar{V}^o = 0 \qquad (4.53)$$

The curvature $\bar{\phi}^o$ is arbitrary. The calculated $\bar{L}$ for any $\bar{\phi}^o$ constitutes a single coordinate of the panel length-deformation curve.

4.3.3 Boundary Conditions

Numerical work has been done for only two boundary conditions - pinned ends and fixed ends. The pinned end condition is defined by zero moment

$$\bar{M} = 0 \qquad (4.54)$$

and the fixed end condition by zero slope

$$\theta = 0 \qquad (4.55)$$

4.3.4 Ultimate Condition

The instability criterion is given by Eq. 4.1. In nondimensional form the equation is

$$\left(\frac{d\bar{L}}{d\bar{\phi}^o}\right)_{\substack{\bar{P}=\text{constant} \\ k_6=\text{constant}}} = 0 \qquad (4.56)$$

The stepwise integration procedure is carried out for each assumed $\bar{\phi}^o_k$, producing an $\bar{L}_k$. If each $\bar{\phi}^o_{k+1}$ is larger than $\bar{\phi}^o_k$, then eventually

$$\bar{L}_{k-2} < \bar{L}_{k-1} > \bar{L}_k \qquad (4.57)$$

The value of $\bar{\phi}^o$ for which Eq. 4.56 is satisfied lies between $\bar{\phi}^o_{k-2}$ and $\bar{\phi}^o_k$. A quadratic function relating $\bar{L}$ and $\bar{\phi}^o$ can then be used to more closely approximate $\bar{L}_{max}$.

The stepwise integration procedure is time consuming even in very high speed computers. To reduce the number of $\bar{\phi}^o$'s that must be assumed before the condition of Eq. 4.57 occurs, the numerical results of all past work have been studied. The result noted is that a small range of curvatures encompassing the desired $\bar{\phi}^o$ can almost always be determined by

$$\bar{\phi}^o = f(\beta \bar{M}_{max}, \bar{N})$$

where the function f refers to the moment-curvature-axial load relationship, $\bar{M}_{max}$ is the maximum moment in the moment-curvature relationship, and β is a value which varies between 0.90 and 0.95. When the materials of the stiffened panel exhibit non-linear stress-strain relationships, $\bar{M}_{max}$ usually does not correspond to the maximum curvature in the moment-curvature

table.

The flow diagram of Fig. 25 illustrates the programmed version of the procedure for determining ultimate strength.

4.3.5 Errors in Stepwise Integration

The error arising from the assumption that the axial load $\overline{N}$ is everywhere equal to the load $\overline{P}$ applied to the panel ends has been discussed in Article 3.3. Other error sources will be considered here.

Integration errors which are a function of the segment length have been investigated in some detail by Kondo.[9] The computer program automatically adjusts the segment length so that the total error in $\overline{L}$ arising from the segment length is less than 0.05 per cent.

As $\overline{\emptyset}^{o}$ approaches the ultimate condition of Eq. 4.56, the initial stages of the stepwise integration procedure involves utilizing the moment-curvature relationship in that region for which

$$\frac{d\overline{M}}{d\overline{\emptyset}} \ll 1$$

Therefore, small errors in $\overline{M}$ are amplified in the corresponding $\overline{\emptyset}$. Figure 28(a) illustrates the moment-curvature relationship

which was calculated for a sample problem (only approximately 10 per cent of the calculated coordinates are shown). The broken lines represent possible true curves which would have resulted without the inevitable errors in the approximate numerical development of the moment-curvature relationship.

The length-deformation curves of Fig. 28(b) show the effects of the modifications. Large differences occur only in the unstable branch. Errors from this source are negligible if the band of $\bar{\emptyset}^o$'s corresponding to the condition of Eq. 4.57 is small. The computer program continually narrows this band until the difference between $\bar{L}_{max}$ as determined by quadratic approximation and the $\bar{L}_{max}$ resulting from re-integration starting with the corresponding $\bar{\emptyset}^o$ is less than 0.005 per cent.

5. THE COMPUTER PROGRAM

5.1 Purpose

Making use of the equations and techniques described in the preceding Chapters, the computer program described by Ref. 14 can, for a beam-column with given cross-sectional dimensions, material properties, loads, and boundary conditions, produce the column length for which the applied loads are ultimate. The program was specifically designed for efficient mass production of computed data from which design charts may be constructed. Also foreseen is the possibility that the program may be incorporated into a comprehensive computer system for design of ship structures.

5.2 Error Detection System

The program contains an automatic error detection system which can discern the severity of the error and make decisions accordingly. Error messages inform the user of the location of the error and the probable cause.

Most errors originate in the input data, and usually the source is an inadequate extent of a table of coordinates of

points describing material stress-strain properties. To assure that the tables contain enough information to calculate a column length, the following rules are suggested:

1) For the material of the plate, supply stress-strain coordinates over the strain range from $+6\epsilon_y$ (compression) to $-3\epsilon_y$ (tension).
2) For the material of the stiffener, supply stress-strain coordinates over the strain range from $+15\epsilon_y$ (compression) to $-6\epsilon_y$ (tension).

5.3 Controllable Errors Arising from the Numerical Techniques

In calculating a single column length by the numerical techniques presented, several iterative loops must be negotiated by the computer. The general scheme for acceptance of a solution produced by trial and error is that a calculated parameter must be very nearly equal to the initially assumed value. This can be expressed by

$$|F_a - F_c| \leq \tau\mu F_c$$

where F_a is the assumed value of some parameter F, F_c is the calculated value, and the product $\tau\mu$ determines how equal "very nearly equal" means. Values for μ, which were assigned according to the calculation being made, are a permanent part

of the computer program. The user inputs γ. Increased accuracy obtained by reducing γ is accompanied by increased running times. As a suggestion, when γ is equal to 0.002 the total error in panel length arising from all sources of error in the numerical technique shall be less than approximately 1.0 per cent.

5.4 Recommendations for Efficient Use

The program is most efficient when used in the manner for which it was designed, in other words, for mass data production. The input parameters which describe geometry and loads are the parameters which have been found to have an effect on ultimate strength. For mass data production, parameters such as $\frac{r}{d}$, $\frac{d}{t}$, $\frac{A_f}{A_{st}}$, $\frac{A_{st}}{A_p}$, $\frac{qbr}{\sigma_y A}$, and $\frac{b}{t}$ need not be calculated individually for specific values of d, A, σ_y, b, t, etc. Instead, realistic ranges for the parameters should be determined and the parameters allowed to take on several specific values within the range.

For the best efficiency the user should be familiar with the order in which computations are carried out. The following information may prove useful for both estimating and reducing computer time:

1) Every change in plate dimension $(\frac{b}{t})$, residual stresses $(\frac{\sigma_{rc}}{\sigma_y}, \frac{\sigma_{rt}}{\sigma_y})$, yield stress for the plate material (σ_y), Poisson's ratio (γ), or material properties (σ, ϵ tables) requires that the program start at the beginning. At the beginning means at the point where the nondimensional, effective stress-strain tables are developed. Typically, 2-3 seconds are required to develop these tables.*

2) Every change in cross section $(\frac{A_f}{A_{st}}, \frac{A_{st}}{A_p})$ and axial load $(\frac{P}{\sigma_y A})$ requires that a new moment-curvature table be developed. However, the program can loop through as many combinations of these three parameters as the user desires without computing again the effective stress-strain tables. Typically, 5-6 seconds are required to build a moment-curvature table.*

3) Changes only in lateral load $(\frac{qbr}{\sigma_y A})$ do not affect the tables described above. Specification of lateral load completes a problem definition and 2-3 seconds are required to produce the pair of column lengths corresponding to pinned ends and fixed ends.*

---

* Note: All running times are given for the IBM 360/65 machine.

PART II. TEST SIMULATION AND CONCLUSIONS

The method of analysis presented in Part I is based on several assumptions. Most of these assumptions either restrict the type of structure that can be analyzed or require the acceptance of small computational errors which arise from numerical techniques. However, one assumption was required due to the lack of test results and demands special attention because its effect on the results of analysis is uncertain. That assumption, referred to in the remainder of this report as "the assumption", is:

> The behavior of the plate component in a longitudinally stiffened panel shall be represented by an average stress - edge strain relationship. For plates with large b/t, the inelastic post-buckling portion of this relationship is described by a constant stress equal to the average stress which exists at the time of first yield.

To what degree is the calculated strength of stiffened panels influenced by this assumption? Until test results or an exact theoretical solution become available the question cannot be answered with finality. Fortunately, the computer program has made an investigation of the theoretical limits of

the influence possible. Such an investigation has been carried out here for the range of problems encompassed by the design nomographs of Ref. 12.

The investigation is separable into two parts:

1) The determination of the combinations of parameters for which the assumption has no effect on the ultimate panel strength. This determination was accomplished by a study of the data computed to construct the nomographs and is described in Chapter 6.

2) For problems for which the assumption does have an effect, the determination of the magnitude of the error introduced. For several different sets of parameters describing geometry and loading, the average stress - edge strain relationship representing the plate behavior was allowed to vary in the possible range between considered limits, and the results were compared to the ultimate strength which would result from the use of the design nomographs. This test simulation is described in Chapter 7.

6. A STUDY OF COMPUTED DATA

Let the edge strain which corresponds to the initial yielding in the plate be denoted by $(\bar{\epsilon}_p)_u$, where

$$\bar{\epsilon}_p = \frac{\epsilon_p}{\epsilon_{cr}} \tag{6.1}$$

If the assumption is to have any effect on the analysis of a stiffened panel subjected to ultimate loads, an edge strain greater than $(\bar{\epsilon}_p)_u$ must exist at some location along the panel. Positive moments produce positive plate strains (plate in compression); the largest positive moment in a stiffened panel subjected to both axial and lateral loads occurs at the panel mid-point when the loaded ends have identical boundary conditions. Since the computer program output includes the curvature at the panel mid-point $\bar{\emptyset}^o$, the value of the maximum moment $\bar{M}_{max}$ can be determined from the moment-curvature relationship

$$\bar{M}_{max} = f(\bar{\emptyset}^o, \bar{P}) \tag{6.2}$$

Consequently, the maximum plate stress $(\bar{\epsilon}_{p\ell})_{max}$ is known

$$(\bar{\epsilon}_{p\ell})_{max} = (\frac{\epsilon_{p\ell}}{\epsilon_{cr}})_{max} = f(\bar{M}_{max}) \tag{6.3}$$

It is evident now that if $(\bar{\epsilon}_{p\ell})_{max}$ is less than $(\bar{\epsilon}_p)_u$ when the panel is supporting ultimate loads, then the calculated

ultimate strength is not affected by the inelastic post-buckling behavior assumption.

It is desirable to be able to specify the combinations of parameters for the design nomograph of Ref. 12 for which $(\bar{\epsilon}_{p\ell})_{max}$ cannot be greater than $(\bar{\epsilon}_p)_u$. The nomograph is valid for the following ranges of parameters:

$$\frac{A_{st}}{A_p} = 0.20 \text{ to } 0.48$$

$$\frac{A_f}{A_{st}} = 0.35 \text{ to } 0.60$$

$$\frac{b}{t} = 60 \text{ to } 110$$

$$\frac{\sigma_{rc}}{\sigma_y} = 0.0 \text{ to } 0.15 \text{ (compressive residual stress)}$$

$$q\,\frac{d}{t} = 40 \text{ to } 480$$

In addition, the material of the plate and the stiffener is assumed to be described by the elastic-perfectly plastic stress-strain relationship, where

Yield stress for both the plate and stiffener = 47.0 ksi

Modulus of elasticity, E = 29,600 ksi

Poisson's ratio, ν = 0.30

When residual stresses exist in the plate

$$\frac{\sigma_{rt}}{\sigma_y} = -1.00 \text{ (tensile residual stress)}$$

To construct the design nomograph, each of the parameters listed above was allowed to take on specific values within the given range (holding all others constant). The design nomograph is essentially a series of plots of calculated results vs. input parameters. All of the data computed to construct the nomograph was studied to determine if some function F exists so that

$$(\bar{\epsilon}_{p\ell})_{max} = F\left(\frac{A_{st}}{A_p}, \frac{A_f}{Ast}, \frac{b}{t}, \frac{\sigma_{rc}}{\sigma_y}, \bar{P}, \bar{Q}\right) \qquad (6.4)$$

where

$$\bar{P} = \frac{P}{\sigma_{cr} A}$$

and

$$\bar{Q} = \frac{qbr}{\sigma_{cr} A} = \frac{q}{\sigma_{cr}}\left(\frac{1}{1+\frac{A_{st}}{A_p}}\right)\left(\frac{d}{t}\right)\left(\frac{r}{d}\right)$$

and if some simple criterion involving $(\bar{\epsilon}_p)_u$ could be determined so that the parameter combinations could be categorized as either influenced or not influenced by the assumption.

Some observations made are:

1) For any problem defined by a particular combination of parameters, the maximum strain $(\bar{\epsilon}_{p\ell})_{max}$ is larger for panels with pinned ends than for panels with fixed ends. Therefore, the limits of parameter combinations for which the ultimate strength is not

affected by the assumption can be determined from a study of pinned-end panels only; these limits will be conservative for fixed-end panels.

2) The strain $(\bar{\epsilon}_p)_u$ is dependent on b/t and σ_{rc}/σ_y, but principally on b/t. It is always given by the range

$$(\bar{\epsilon}_p)_u = 1.0\left(\frac{\sigma_y}{\sigma_{cr}}\right) \text{ to } 1.1\left(\frac{\sigma_y}{\sigma_{cr}}\right) \qquad (6.5)$$

3) The strain $(\bar{\epsilon}_{p\ell})_{max}$ is dependent principally on $\frac{A_{st}}{A_p}$, $\frac{A_f}{A_{st}}$, $\frac{b}{t}$, and $\bar{P}$. The dependence of $\bar{Q}$ is minor when $(\bar{\epsilon}_{p\ell})_{max}$ is less than $(\bar{\epsilon}_p)_u$ but significant otherwise. No dependence on σ_{rc}/σ_y was noticeable.

4) A plot of F* vs. $\frac{(\bar{\epsilon}_{p\ell})_{max}}{\sigma_y/\sigma_{cr}}$, where

$$F^* = (\bar{P})^{0.7}\ (\bar{Q})^{0.04}\ \left(\frac{A_{st}}{A_p}\right)^{0.6}\ \left(\frac{A_f}{A_{st}}\right)^{0.16} \qquad (6.6)$$

and $\bar{P}$ and $\bar{Q}$ are ultimate loads, is sufficient to isolate the combinations of parameters for which the design nomograph is not affected by the assumption.

The plot of F* vs. $\frac{(\bar{\epsilon}_{p\ell})_{max}}{\sigma_y/\sigma_{cr}}$ is shown in Fig. 29. Each of the points plotted represents a problem solved to compile data toward construction of the nomograph. The points shown

comprise approximately 40 per cent of the total problems solved for the pinned-end panel. The panel length $\bar{L}_{max}$ does not appear since each combination of parameters uniquely defines $\bar{L}_{max}$.

From Eq. 6.5, the minimum value of the strain $(\bar{\epsilon}_p)_u$ in Fig. 29 corresponds to

$$\frac{(\bar{\epsilon}_{p\ell})_{max}}{\sigma_y/\sigma_{cr}} = 1.0$$

This is illustrated by the vertical broken line. Therefore, any stiffened panel designed with the use of the nomograph for which the plot of the parameters would fall to the left of the broken line would not be influenced by the assumption. In other words, if

$$F^* \leq 0.33 \qquad (6.8)$$

then the assumption has no influence. This statement is valid for panels with fixed ends and pinned ends.

7. TEST SIMULATION

It is apparent from Fig. 29 that some stiffened panels designed with the use of the nomographs of Ref. 12 will be affected by the assumption. The extent should eventually be determined by tests. Until then, some feeling for possible errors can be developed by selecting a few parameters for which it is known that the plate is highly strained, varying the assumed portion of the average stress - edge strain relationship between considered limits of possible behavior, and examining the resulting effect on ultimate strength (Actually, the effect on the panel length is examined since the input parameters specify cross-sectional geometry, material properties, and ultimate loads.). Such a test simulation procedure will place limits of the possible error.

The problems selected for the test simulation are defined by the following parameters:

$$\frac{A_{st}}{A_p} = 0.48$$

$$\frac{A_f}{A_{st}} = 0.60$$

$$\bar{P} = 1.30$$

$$\frac{b}{t} = 110$$

$$\frac{\sigma_{rt}}{\sigma_y} = -1.0$$

$$\frac{\sigma_{rc}}{\sigma_y} = 0.075$$

$$\bar{Q} = 0.24,\ 0.50,\ 0.80,\ 1.07,\ \text{and}\ 1.90$$

The material properties remain as described in Chapter 6. The conspicuous points marked by crosses in Fig. 29 locate these parameter combinations for a panel with pinned ends. The five points correspond to the five different values of the lateral load $\bar{Q}$, with the increasing value leading to the increasing maximum plate strain. From the figure it is seen that the results of the test simulation for these parameters should be indicative of the greatest influence the assumption may have on the ultimate strength.

The solid line in Fig. 30 shows the average stress - edge strain curve for the plate, where the horizontal compression portion is the standard assumption. The solid line in Fig. 31 indicates the resulting moment-curvature relationship for $\bar{P}$ equal to 1.30. Denoted by "standard", the results of the analysis using these curves are listed in Tables 1 and 2. Table 1 is for panels with pinned ends and Table 2 is for panels with fixed ends.

The broken lines in Fig. 30 describe three different assumptions for the inelastic post-buckling behavior of the plate. It is believed that these modified average stress - edge strain curves represent realistic limits on the possible post-buckling behavior of the plate. In other words, it is expected that tests will establish that the true curve will be between curve 1 as an upper bound and curves 2 or 3, either of which may represent the lower bound. In Fig. 31 the moment-curvature relationship which is calculated for each of these modified curves is shown.

Tables 1 and 2 also contain the results of the analysis for which the behavior of the plate is described by curves 1, 2, and 3. The mid-point curvature $\overline{\emptyset}^{o}$, the panel length $\frac{L}{r}$, the mid-point deflection $\frac{y}{r}$, and either the end slope (for pinned ends) or the end moment (for fixed ends) were computed. The results are grouped for each value of $\overline{Q}$. Below each group the maximum deviation in results appears, where the plus quantity indicates the amount of the increase in strength or deformation resulting from the use of curve 1 and the negative quantity indicates the maximum per cent reduction caused by either curve 2 or 3. Of a special interest are the changes which occurred in the length of panel $\frac{L}{r}$ because this is the only parameter which appears in the nomograph.

The following observations can be noted:

1) For pinned-end panels, the maximum increase in length was 8.5 per cent. However, the maximum reduction resulting from the use of either curve 2 or 3 was only 1.4 per cent.

2) For fixed-end panels, the maximum change in length resulted from the use of curve 1 (4.0 per cent longer). The maximum reduction in length was 0.56 per cent.

3) Deformations such as $\overline{\emptyset}^{o}$, $\frac{y}{r}$, and θ_{s} may be very sensitive to changes in the average stress - edge strain relationship.

Results 1) and 2) indicate that good agreement in ultimate strength was found despite rather large variation in the plate behavior. The largest discrepancy occurred with the use of curve 1 indicating that the maximum error caused by the assumption may be on the conservative side. If the true plate behavior curve lies close to either curve 2 or 3, negligible differences in the ultimate strength should be expected.

8. SUMMARY AND CONCLUSIONS

In Part I of this report a method for the determination of the ultimate strength of longitudinally stiffened plate panels is presented in detail. Lateral interaction between stiffeners was assumed to be negligible so that the analysis of the stiffened panels could be reduced to the analysis of a beam-column with a representative cross section. The loads considered were the axial load applied to the column ends and uniformly distributed pressure acting on the plate surface. The effects of residual stresses in the plate were included. Numerical techniques developed specifically for computer application were used to solve equilibrium equations which include the non-linear effects of inelastic action and large deformations.

A computer program written to mass produce design data was briefly described (Ref. 14 is a detailed description of the program). This program was designed to determine the ultimate strength of longitudinally stiffened panels unrestricted by the dimensions of the plate component or by the stress-strain properties of the materials.

Of several simplifying assumptions made during the

development of the method of analysis, the assumption for the inelastic post-buckling behavior of the plate component was of primary concern because of the unknown influence on ultimate strength. A study of this assumption is the subject of Part II.

For the ranges of parameters for which the design nomographs of Ref. 12 are valid, an examination of computed data showed that the assumption can have an influence on ultimate strength, and a simple method to determine which parameter groups will be suspect was presented. To determine limits on the magnitudes of influence, the flexibility of the computer program was exploited by allowing the assumed post-buckling behavior of the plate to become a variable. The effect on ultimate strength caused by modifying the behavior curve between considered limits of behavior for various parameter combinations was studied. All of the evidence presented points to the conclusion that the dependence of ultimate strength on the plate behavior assumption is not significant and that the design nomographs may be used with confidence for all parameter combinations for which they were developed.

9. NOMENCLATURE

A	total area of the cross section
A_f	flange area of the stiffener
A_p	plate area, $A_p = bt$
A_{st}	area of the stiffener, $A_{st} = A_w + A_f$
A_w	web area of the stiffener, $A_w = dt_w$
b	width of the plate
c	width of the tensile residual stress zone
d	depth of the stiffener
E_t	tangent modulus of elasticity
H	horizontal stress resultant
$\overline{H}$	H/N_o
K	plate buckling coefficient
L	length of the panel
$\overline{L}$	L/r
$\overline{L}_{max}$	ultimate panel length
$\overline{L}_{FS}$	ultimate length of panel with fixed ends
$\overline{L}_{SS}$	ultimate length of panel with pinned ends
M	moment
$\overline{M}$	M/M_o
M_o	$N_o d$
$\overline{M}_F$	moment at the fixed ends
N	axial force
$\overline{N}$	N/N_o
N_o	$\sigma_o A$
N_p	number of points representing the plate stress-strain curve
$N_{M\phi}$	number of points representing the moment-curvature relationship

N_s	number of points representing the stiffener stress-strain curve
P	force applied at the panel ends
$\overline{P}$	P/P_o
P_o	$\sigma_o A$
q	uniformly distributed lateral loading
$\overline{Q}$	$\frac{qbr}{\sigma_o A}$
r	radius of gyration
s	distance along the centroidal axis
$\overline{s}$	s/r
t	plate thickness
t_w	stiffener web thickness
V	vertical stress resultant
$\overline{V}$	V/N_o
x	horizontal coordinate axis and distance
$\overline{x}$	x/r
y	vertical coordinate axis and distance or deflection
$\overline{y}$	y/r
$\overline{y}_F$	mid-point deflection for fixed-end panel
$\overline{y}_S$	mid-point deflection for pinned-end panel
α	nondimensional distance from the plate to the centroidal axis
Δs	segment length
$\Delta\overline{s}$	$\Delta s/r$
Δy	change in y in segment length Δs
$\Delta\overline{y}$	$\Delta y/r$
Δx	change in x in segment length Δs
$\Delta\overline{x}$	$\Delta x/r$
ϵ_{cr}	plate buckling strain
$\epsilon_{f\ell}$	strain in stiffener flange

$\bar{\epsilon}_{f\ell}$	ϵ_f/ϵ_o
$\epsilon_{p\ell}$	edge strain in plate
$\bar{\epsilon}_{p\ell}$	$\epsilon_{p\ell}/\epsilon_o$
ϵ_o	nondimensionalizing parameter, either ϵ_y or ϵ_{cr}
ϵ_y	yield strain for material of plate
θ	slope
θ_s	slope of panel at pinned ends
ν	Poisson's ratio
(σ,ϵ)	stress, strain in plate material
$(\bar{\sigma},\bar{\epsilon})$	$(\sigma/\sigma_o,\ \epsilon/\epsilon_o)$
σ_{cr}	plate buckling stress
(σ_f,ϵ_f)	stress, strain in stiffener material
$(\bar{\sigma}_f,\bar{\epsilon}_f)$	$(\sigma_f/\sigma_o,\ \epsilon_f/\epsilon_o)$
σ_o	nondimensionalizing parameter, either σ_y or σ_{cr}
(σ_p,ϵ_p)	average stress , edge strain in plate
$(\bar{\sigma}_p,\bar{\epsilon}_p)$	$(\sigma_p/\sigma_o,\ \epsilon_p/\epsilon_o)$
$\sigma_{p\ell}$	average stress in plate corresponding to $\epsilon_{p\ell}$
$\bar{\sigma}_{p\ell}$	$\sigma_{p\ell}/\sigma_o$
$\sigma_{f\ell}$	stress in stiffener flange
$\bar{\sigma}_{f\ell}$	$\sigma_{f\ell}/\sigma_o$
σ_{rc}	compressive residual stress in plate
σ_{rt}	tensile residual stress in plate
σ_y	yield stress for material of plate
γ	tolerance factor
ϕ	curvature
$\bar{\phi}$	ϕ/ϕ_o
ϕ^o	mid-point curvature
$\bar{\phi}^o$	ϕ^o/ϕ_o
ϕ_o	ϵ_o/d

10. TABLES AND FIGURES

Pinned Ends

$\bar{Q}$	Curve of Average Stress vs. Edge Strain		Mid-point Curvature $\bar{\phi}^o$	Panel Length $\frac{L}{r}$	Mid-point Deflection $\frac{y}{r}$	End Slope θ_s
0.24	Standard		10.25	85.20	0.87	0.033
	#1		12.62	89.59	1.17	0.042
	#2		11.13	84.01	0.90	0.034
	#3		10.09	86.83	0.90	0.034
% Deviation		max	+24	+5.1	+34	+27
		min	-1.6	-1.4	-0	-0
0.50	Standard		11.56	67.90	0.59	0.027
	#1		14.53	72.90	0.83	0.036
	#2		12.50	67.57	0.62	0.029
	#3		10.04	69.30	0.58	0.029
% Deviation		max	+26	+7.4	+40	+33
		min	-15	-0.48	-1.7	-0
0.80	Standard		13.60	57.61	0.46	0.025
	#1		14.95	62.31	0.61	0.031
	#2		12.47	57.37	0.45	0.025
	#3		10.05	58.56	0.42	0.023
% Deviation		max	+9.9	+8.1	+33	+24
		min	-26	-0.42	-2.2	-8
1.07	Standard		15.48	51.56	0.40	0.024
	#1		15.02	55.89	0.40	0.028
	#2		14.48	51.29	0.36	0.022
	#3		10.06	52.20	0.33	0.021
% Deviation		max	+0	+8.4	+22	+17
		min	-35	-0.52	-18	-13
1.90	Standard		18.79	40.66	0.28	0.020
	#1		15.17	44.12	0.31	0.022
	#2		12.55	40.26	0.22	0.016
	#3		10.07	40.79	0.20	0.017
% Deviation		max	+0	+8.5	+10	+10
		min	-46	-0.99	-29	-20

Table 1. Effect of Post-Buckling Plate Behavior For Pinned-End Panels

Fixed Ends

$\overline{Q}$	Curve of Average Stress vs. Edge Strain		Mid-point Curvature $\overline{\phi}^o$	Panel Length $\frac{L}{r}$	Mid-point Deflection $\frac{y}{r}$	End Moment $\overline{M}_F$
0.24	Standard		5.78	133.31	0.87	-1.06
	#1		6.41	133.33	1.02	-1.04
	#2		5.54	133.30	0.84	-1.04
	#3		5.42	133.31	0.92	-1.02
% Deviation		max	+11	+0.02	+17	+0
		min	-6.2	-0.01	-3.5	-4
0.50	Standard		9.82	102.41	0.94	-1.04
	#1		12.05	104.19	1.26	-1.04
	#2		10.32	101.83	0.98	-1.04
	#3		10.04	102.68	1.00	-1.02
% Deviation		max	+23	+1.7	+34	+0
		min	-0	-0.56	-0	-1.9
0.80	Standard		11.31	85.50	0.72	-1.04
	#1		13.34	87.87	0.96	-1.04
	#2		11.63	85.21	0.75	-1.04
	#3		10.06	85.81	0.71	-1.02
% Deviation		max	+18	+2.8	+33	+0
		min	-11	-0.34	-1.4	-1.9
1.07	Standard		11.74	75.81	0.58	-1.04
	#1		14.66	78.30	0.79	-1.04
	#2		12.38	75.62	0.61	-1.04
	#3		10.06	76.08	0.56	-1.02
% Deviation		max	+25	+3.3	+36	+0
		min	-14	-0.25	-3.4	-1.9
1.90	Standard		15.35	58.95	0.41	-1.04
	#1		15.12	61.28	0.49	-1.04
	#2		12.53	58.81	0.38	-1.04
	#3		10.09	60.00	0.34	-1.02
% Deviation		max	+0	+4.0	+19	+0
		min	-38	-0.24	-17	-1.9

Table 2. Effect of Post-Buckling Plate Behavior For Fixed-End Panels

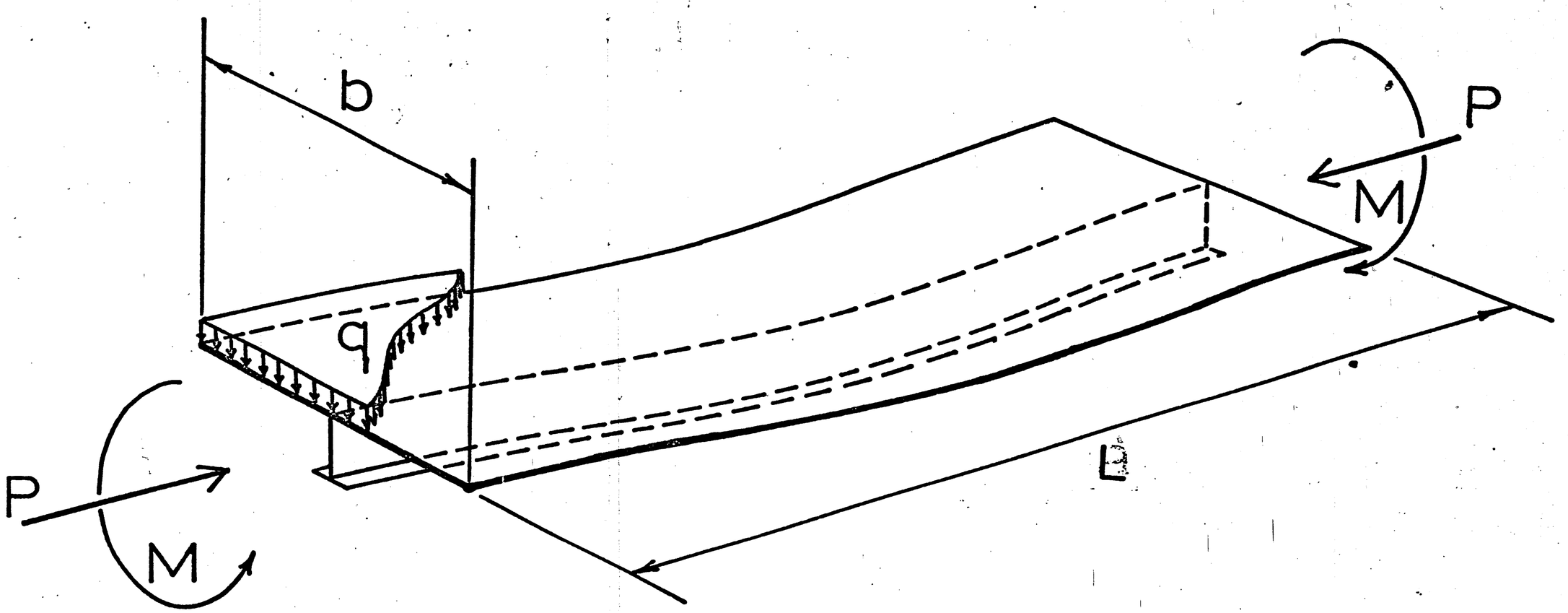

Fig. 1 Representative Plate Panel Under Combined Loading

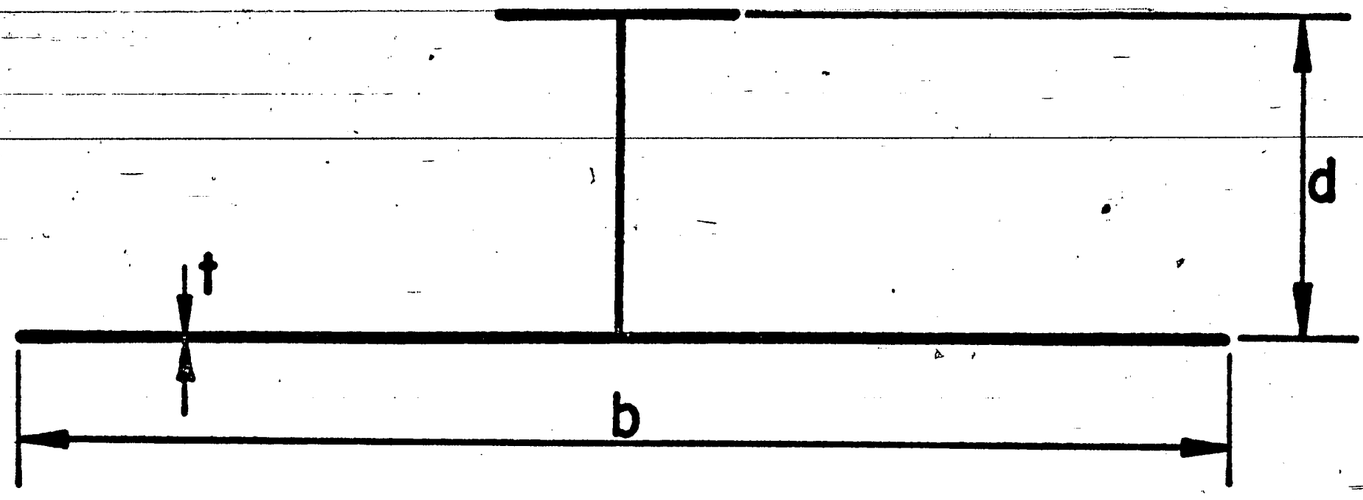

(a) Representative Section

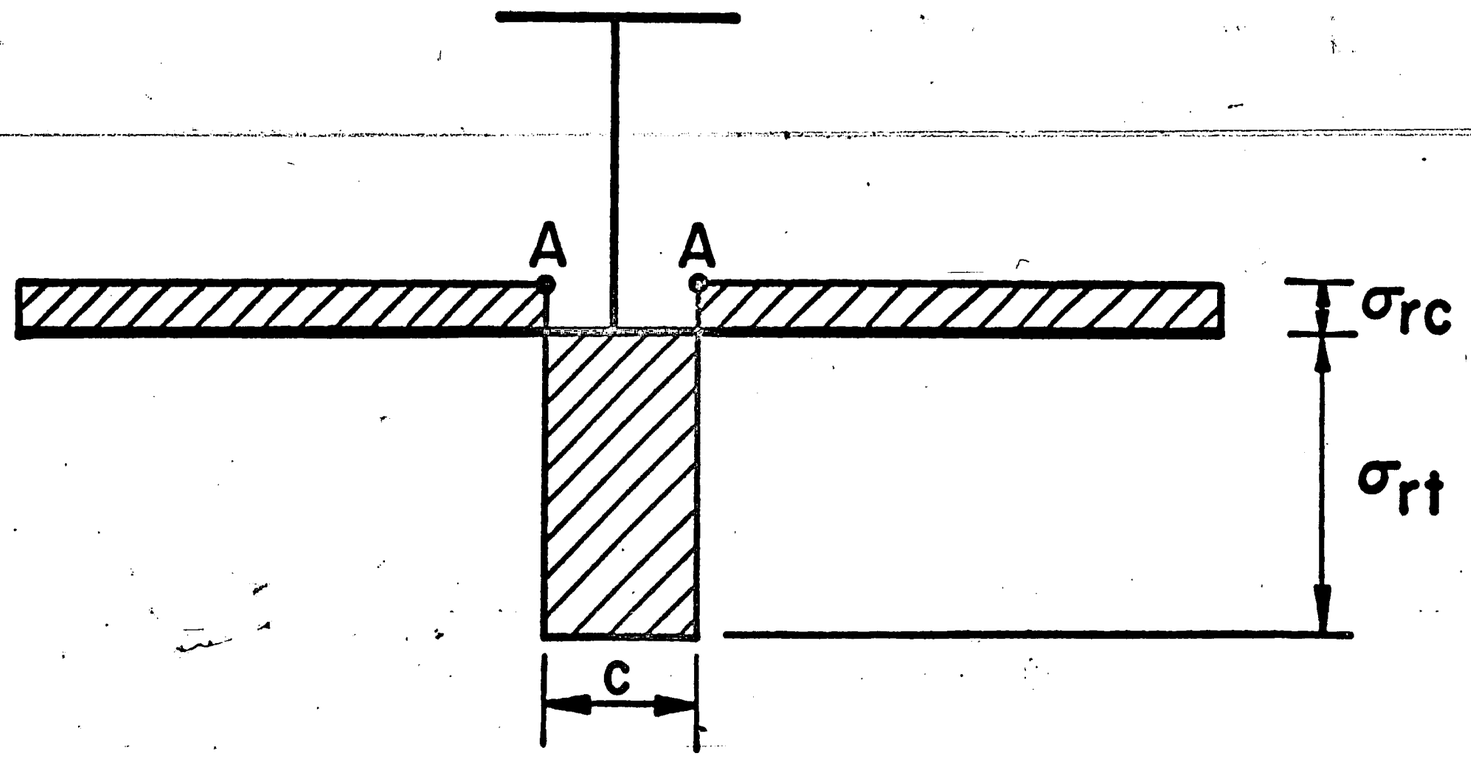

(b) Residual Stress Pattern

Fig. 2 Simplified Cross Section and Residual Stresses

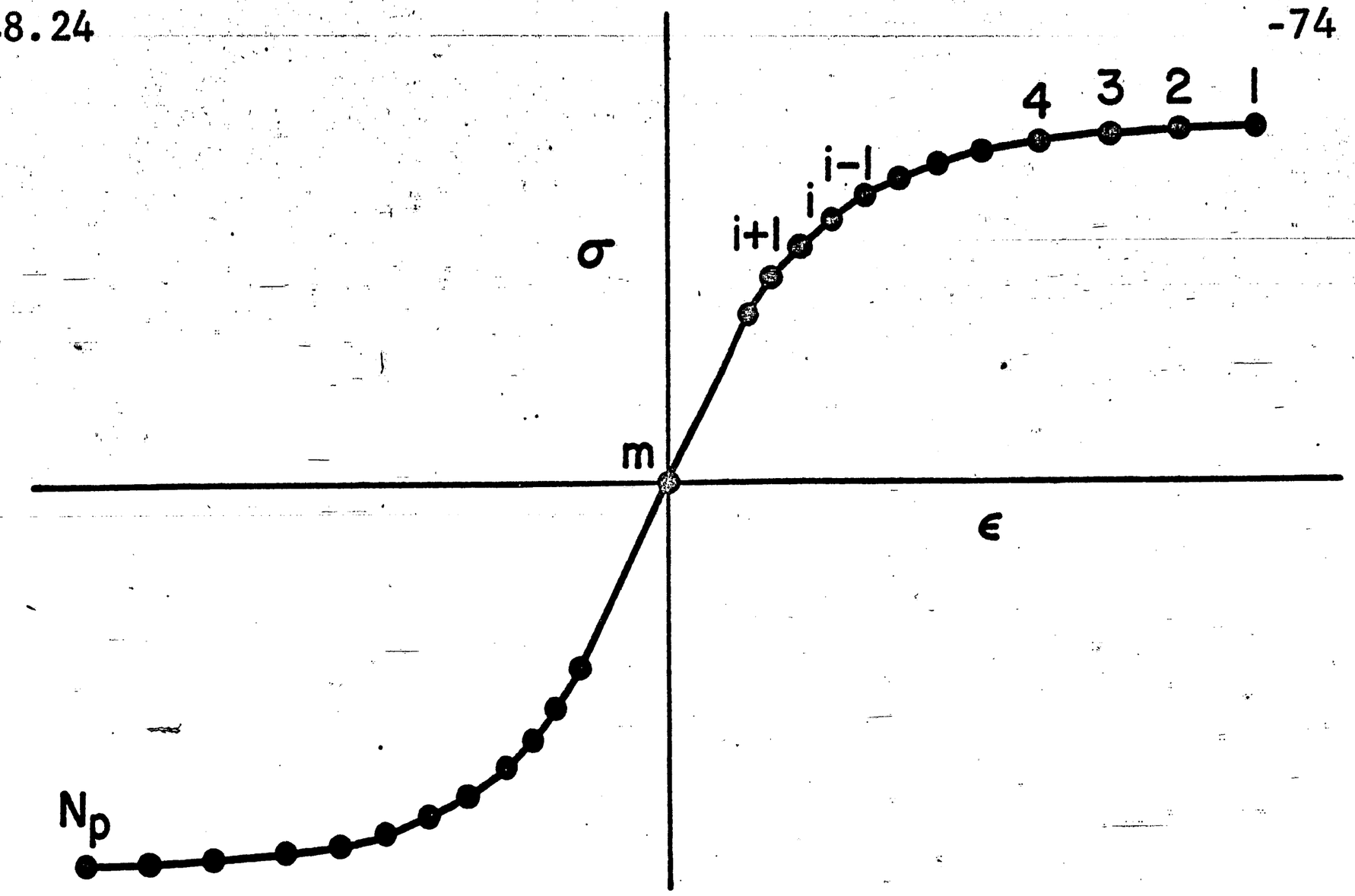

Fig. 3 A stress-Strain Curve Described by N_p Points

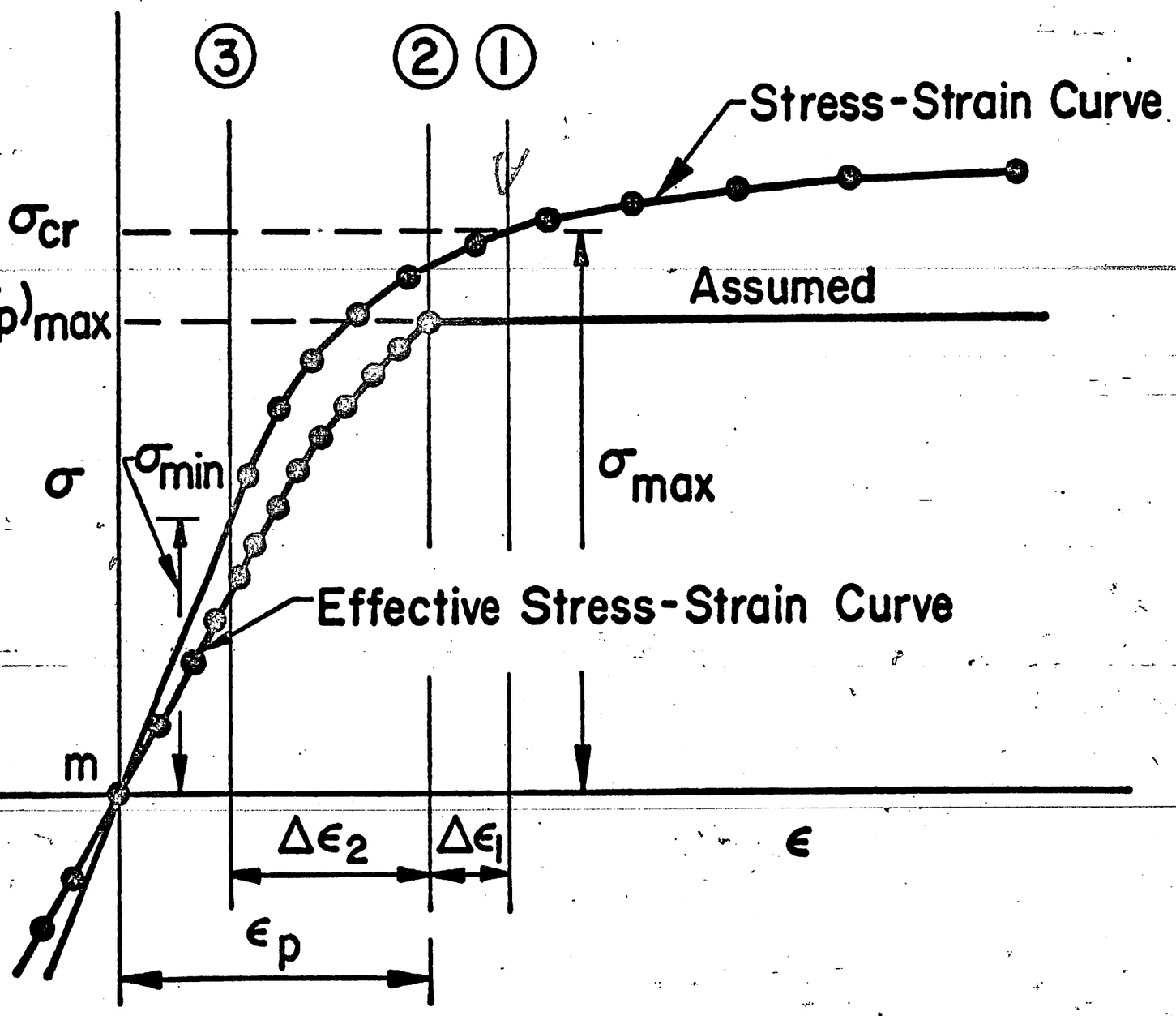

Fig. 4 Compression Branch of the Effective Stress-Strain Curve for Plate with Small b/t

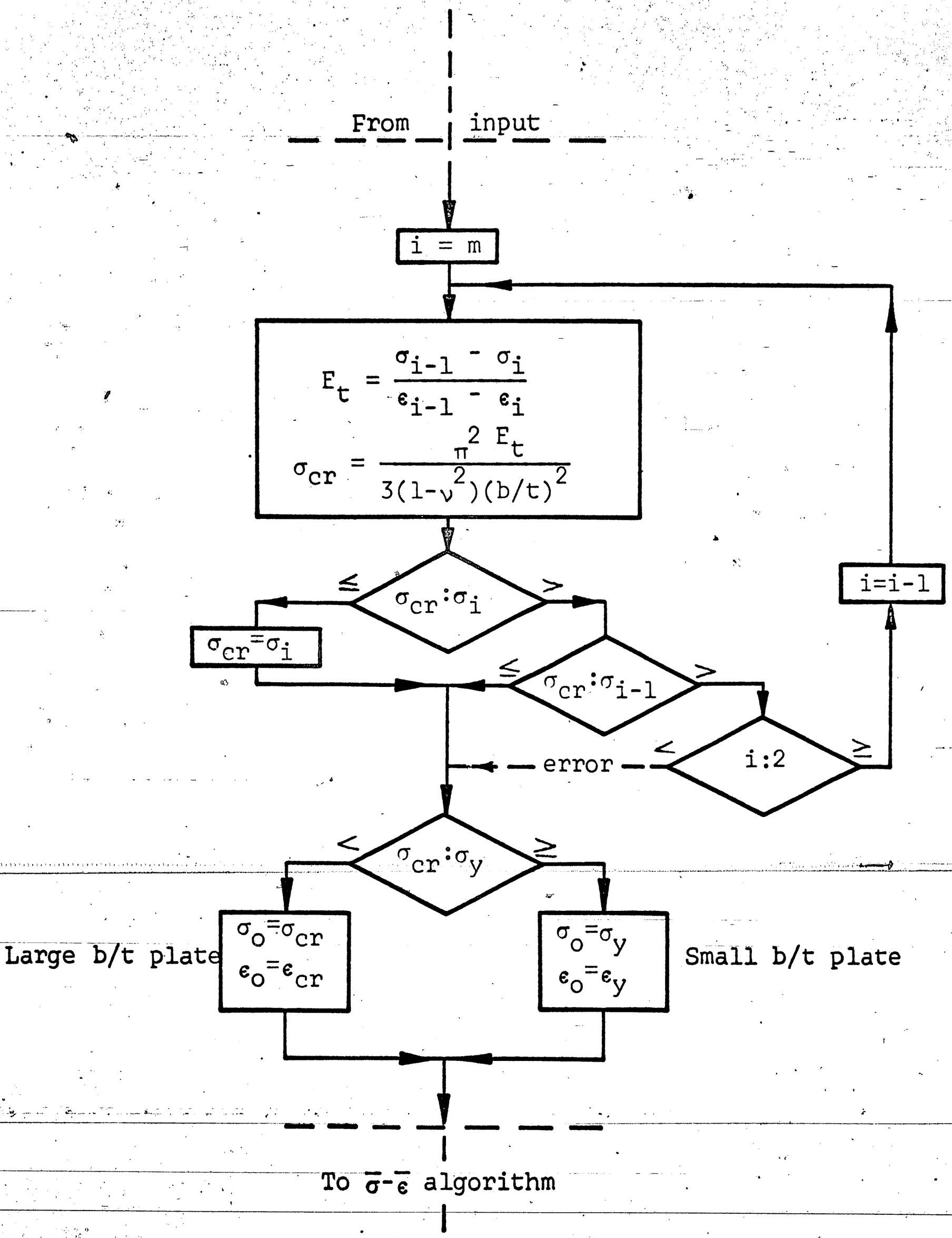

Fig. 5 Flow Diagram to Determine the Buckling Stress

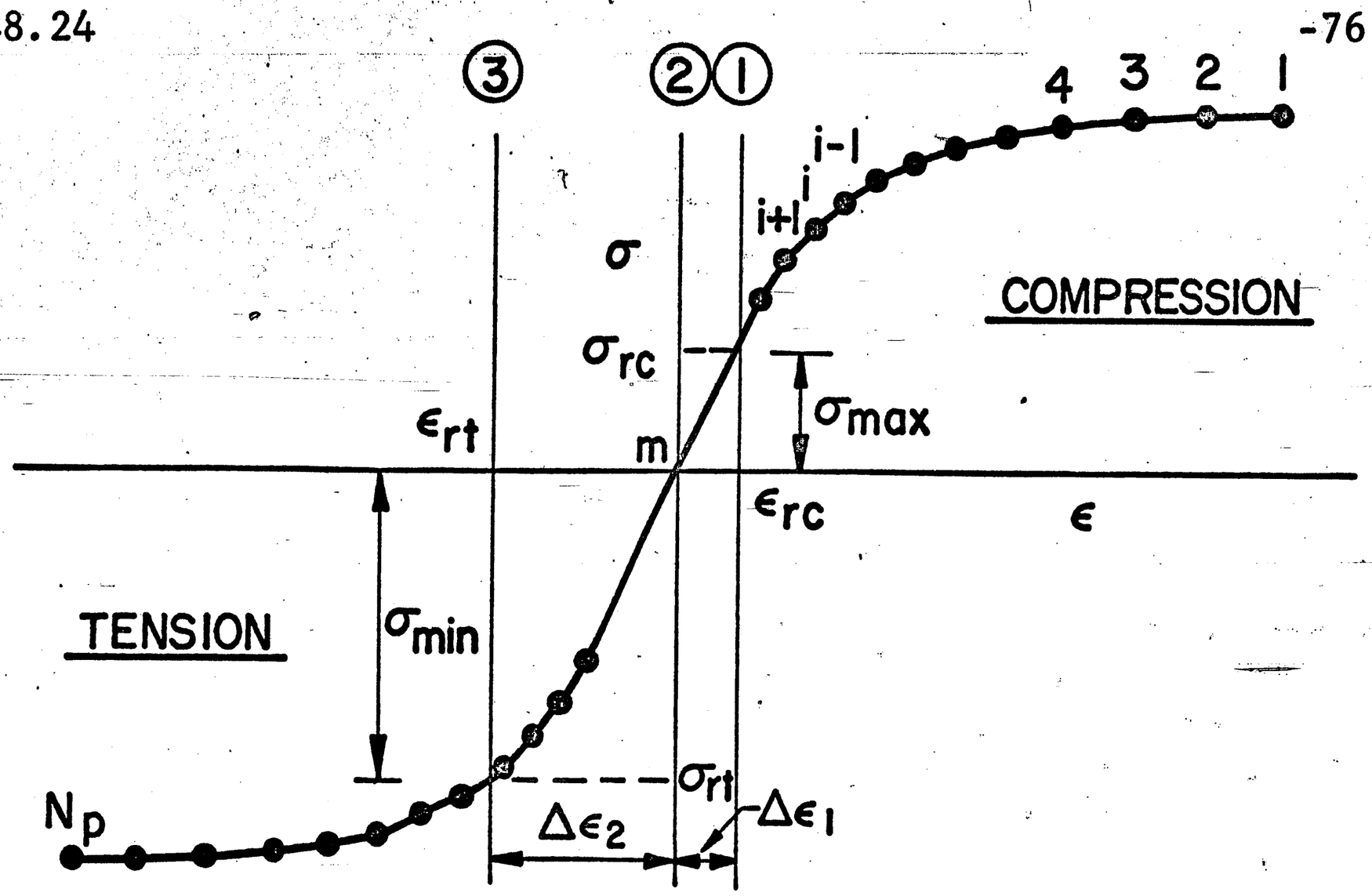

(a) Residual Stresses and Strains

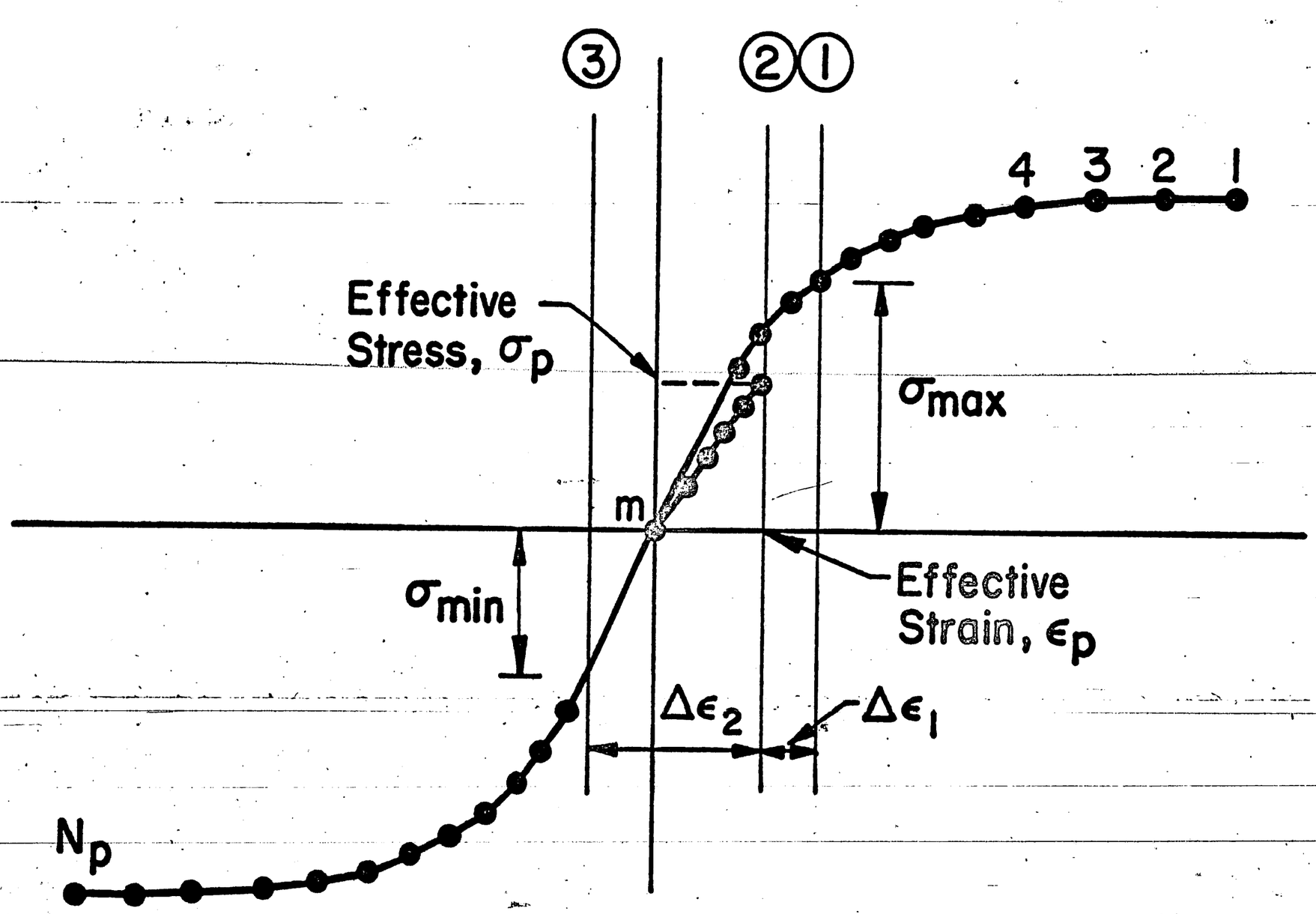

(b) Effective Stress and Strain

Fig. 6 Computation of the Effective Stress-Strain Curve

Known

Table of $(\sigma, \epsilon)_i$ for the plate,
where $i = 1,2,3,\cdots,N_p$
σ_y
σ_{cr}
σ_{rc}
σ_{rt}
$\frac{c}{b}$

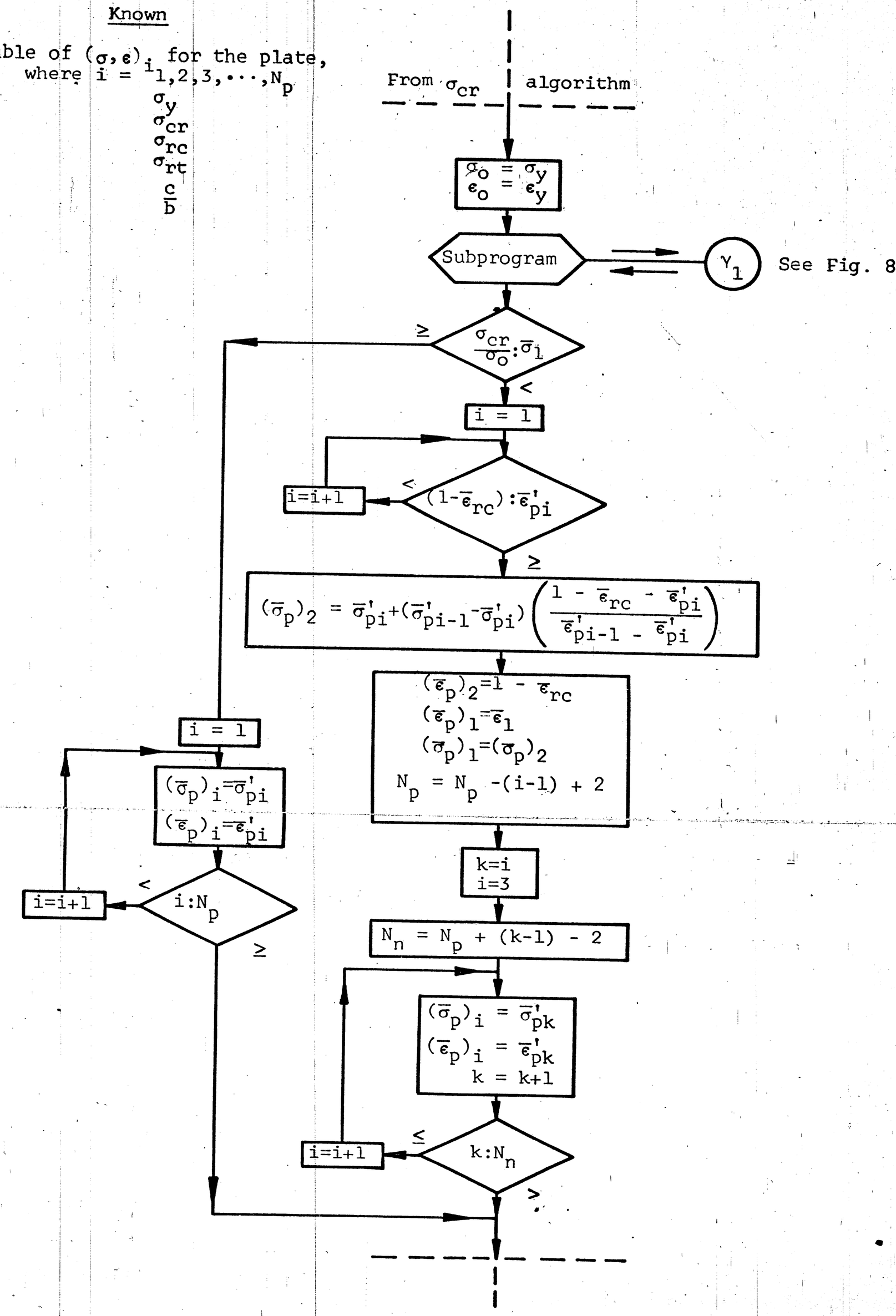

The nondimensional, effective stress-strain table is complete

Fig. 7 Flow Diagram for the Determination of the Effective Stress-Strain Relationship for Plates with Small b/t

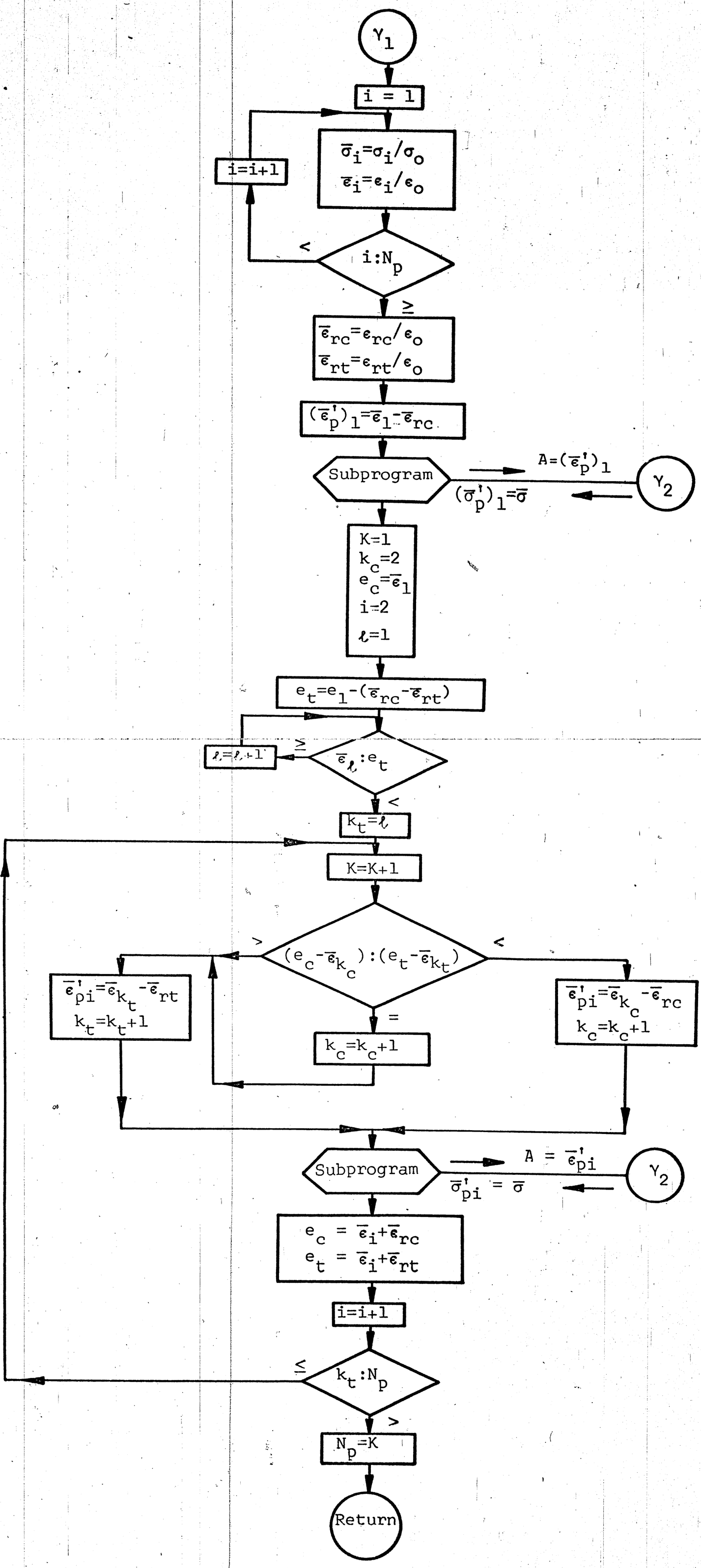

Fig. 8 Flow Diagram for Subprogram 1

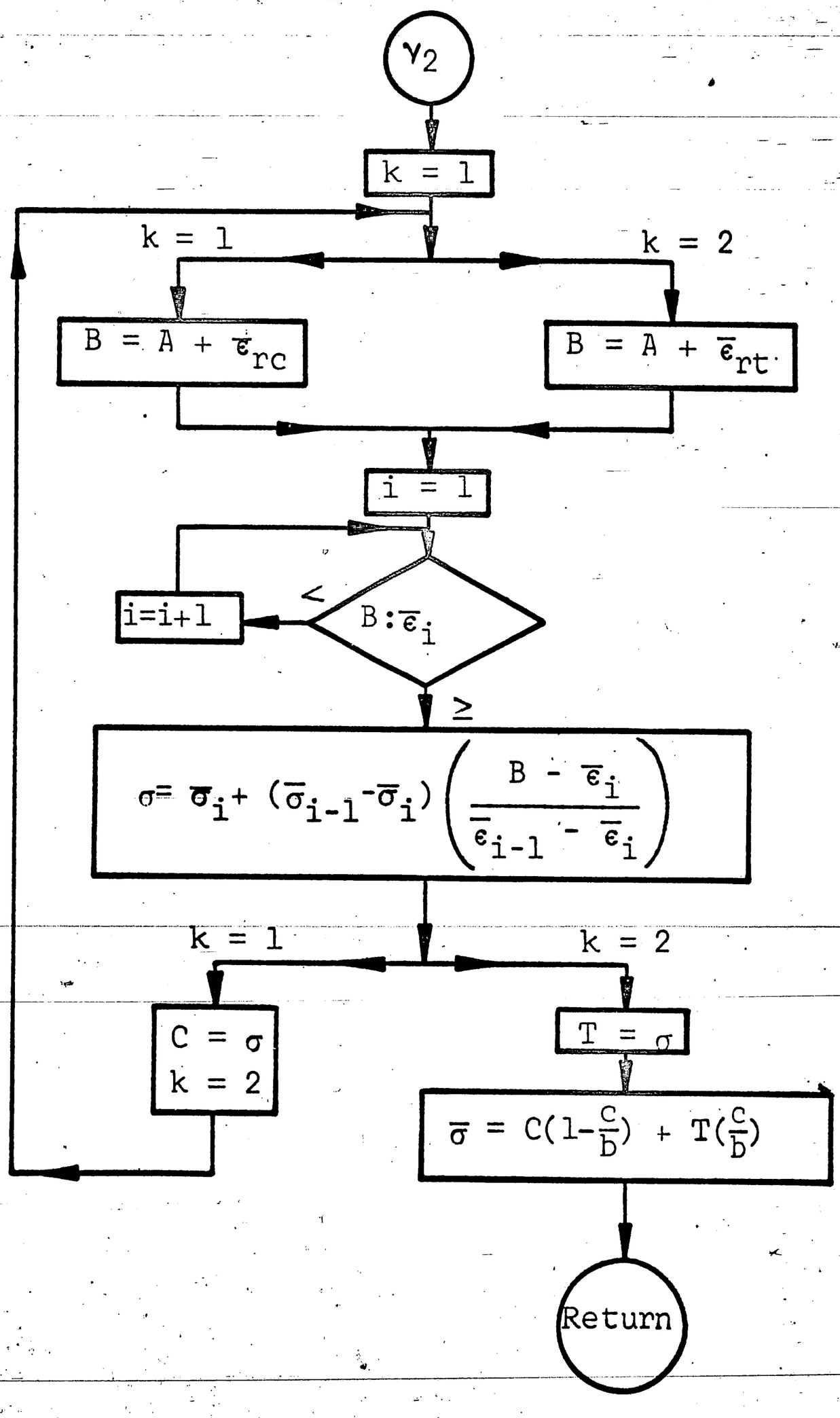

Fig. 9 Flow Diagram for Subprogram γ_2

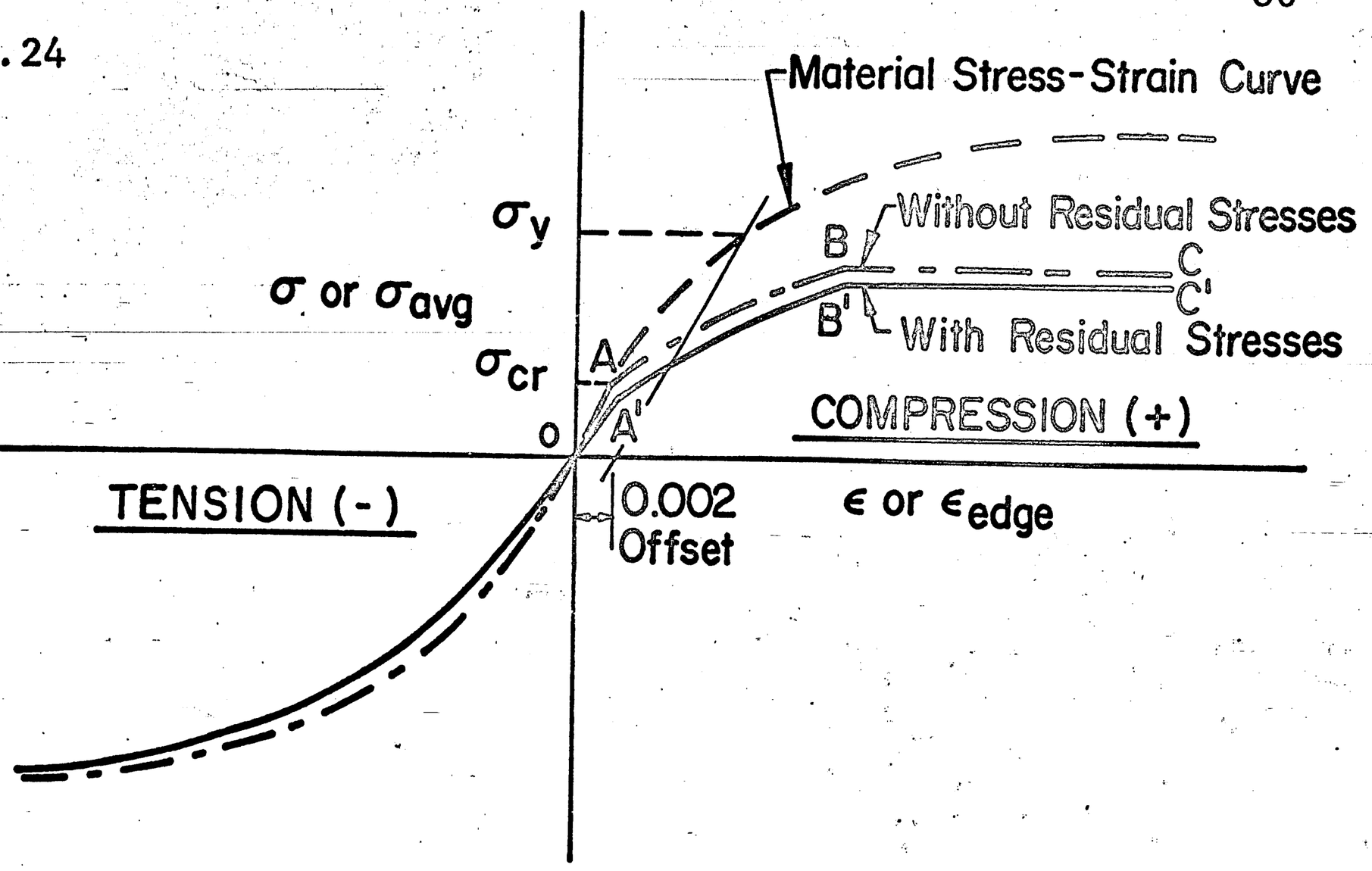

Fig. 10 Stress-Strain Curve for Plate with Large b/t

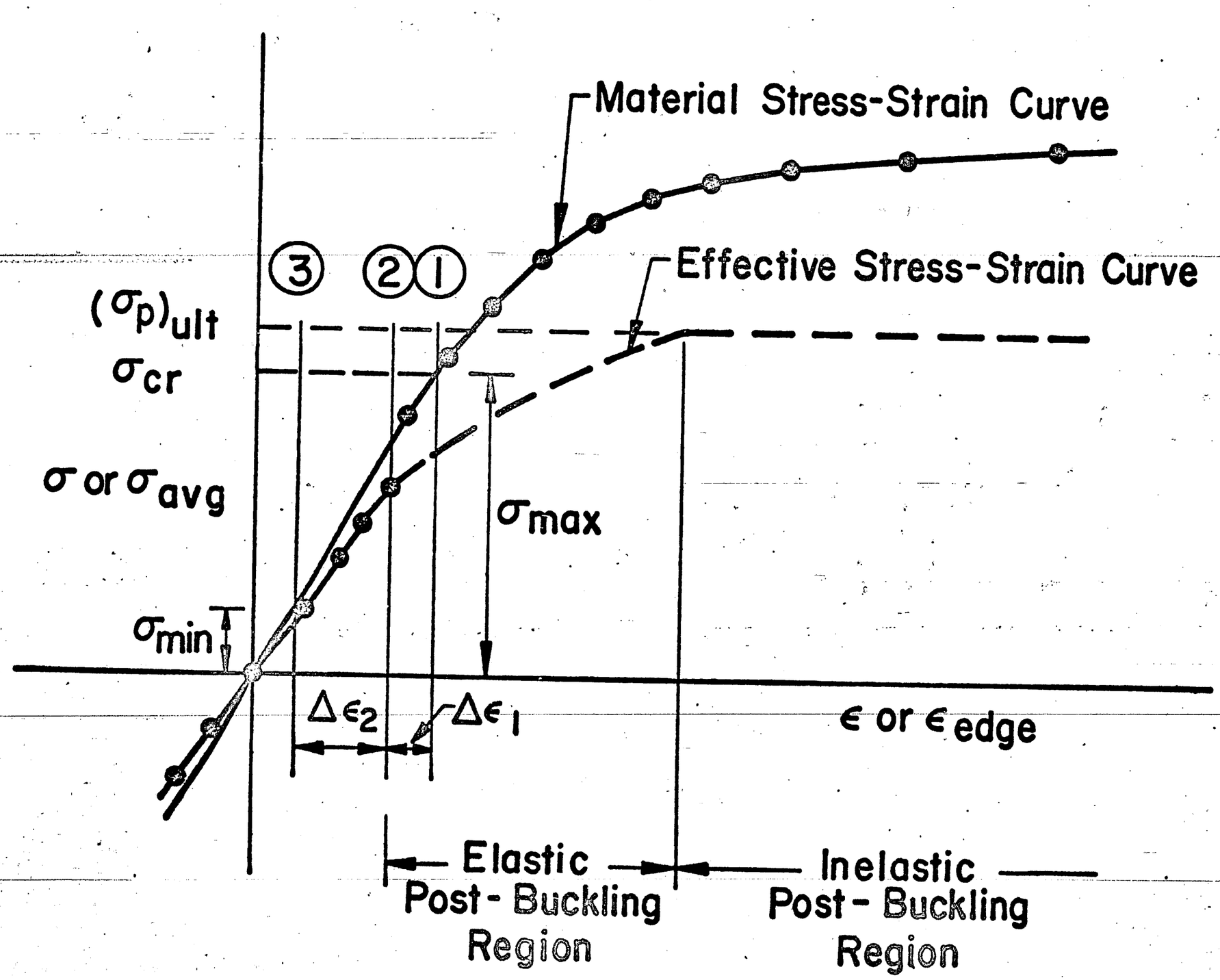

Fig. 11 Compression Branch of the Effective Stress-Strain Curve For Plate with Large b/t

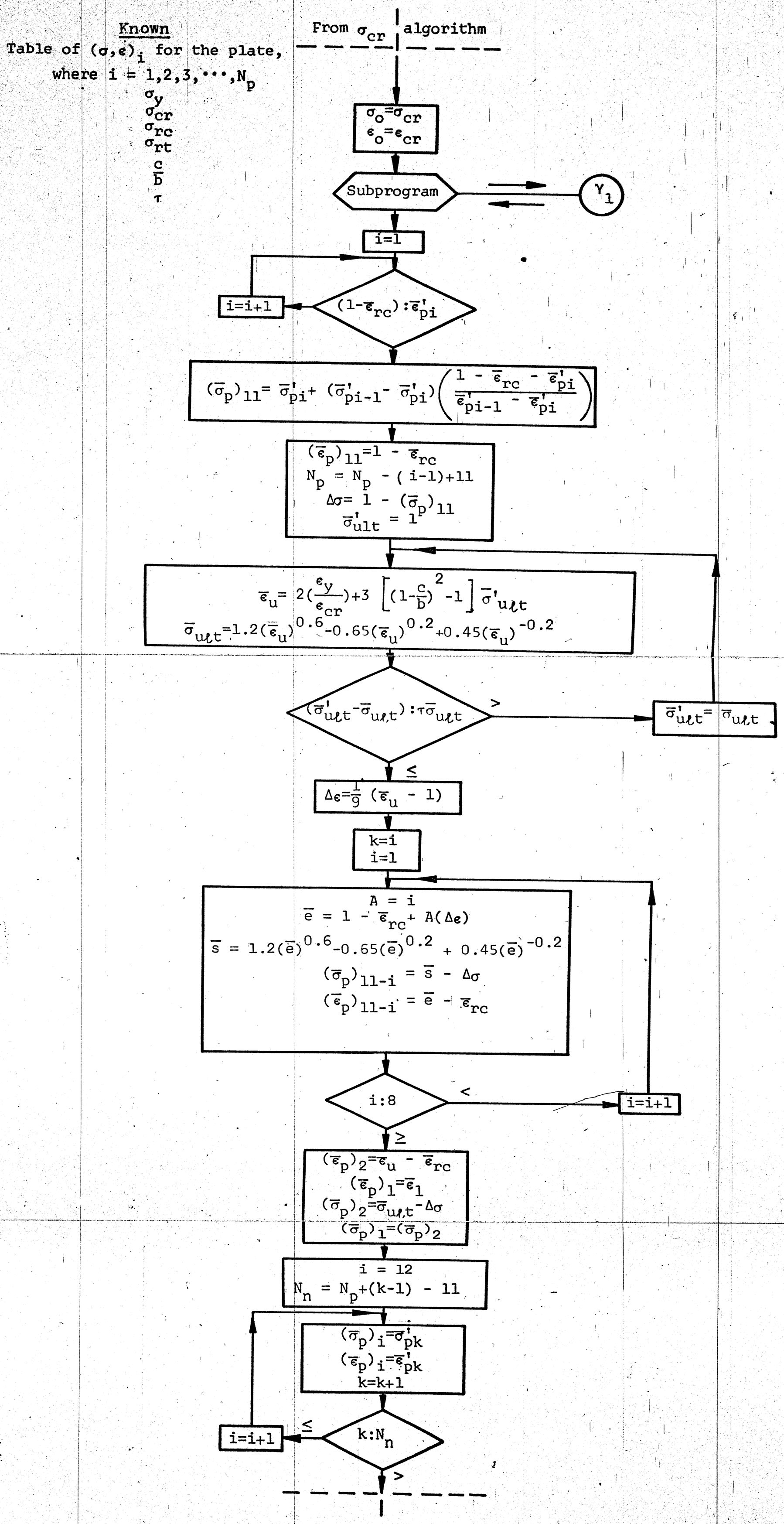

Fig. 12 Flow Diagram for the Determination of the Effective Stress-Strain Relationship for Plates with Large b/t

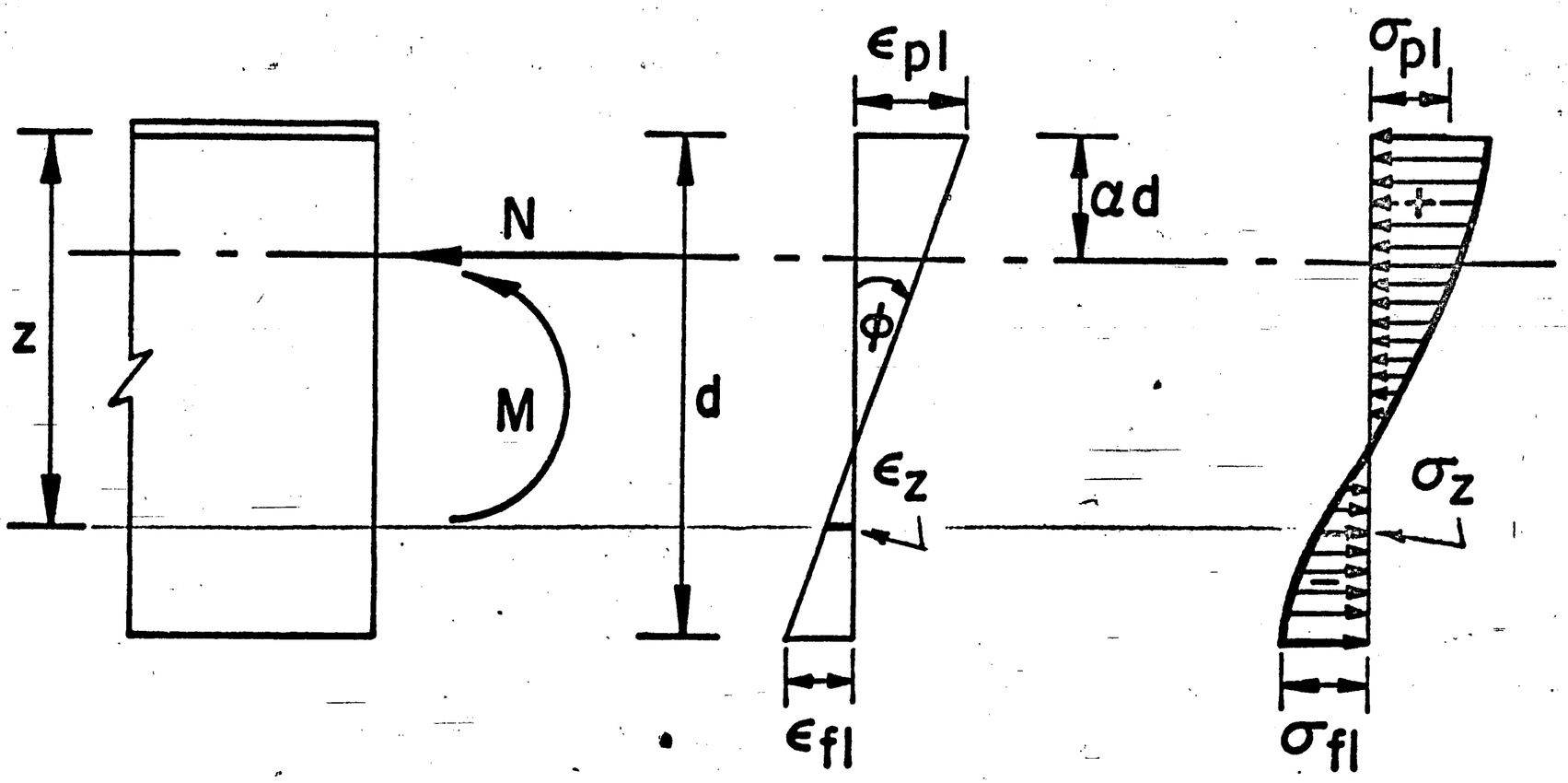

Fig. 13 Distribution of Stresses and Strains in the Cross Section Due to Loading

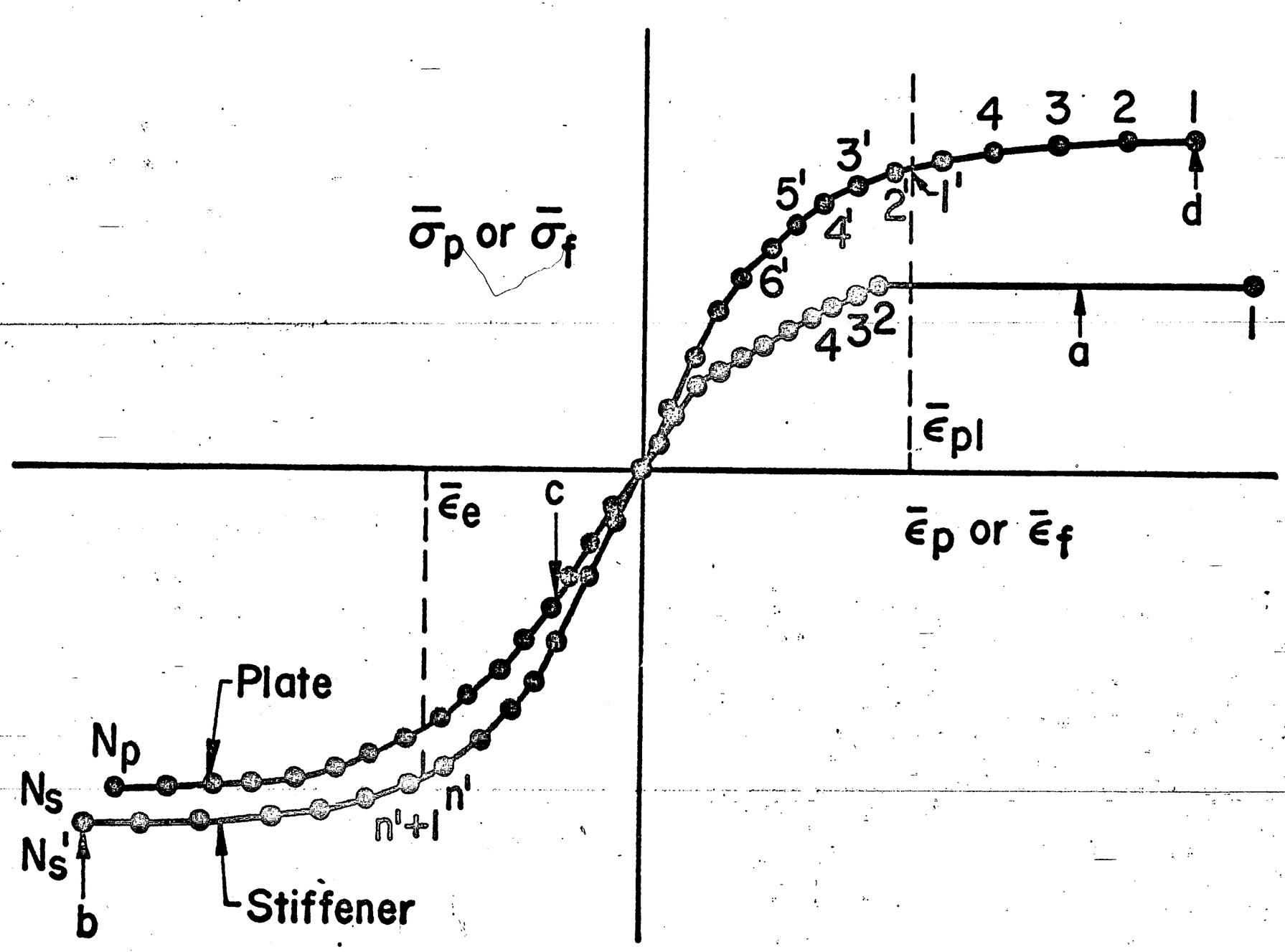

Fig. 14 Limits on Stress-Strain Curves

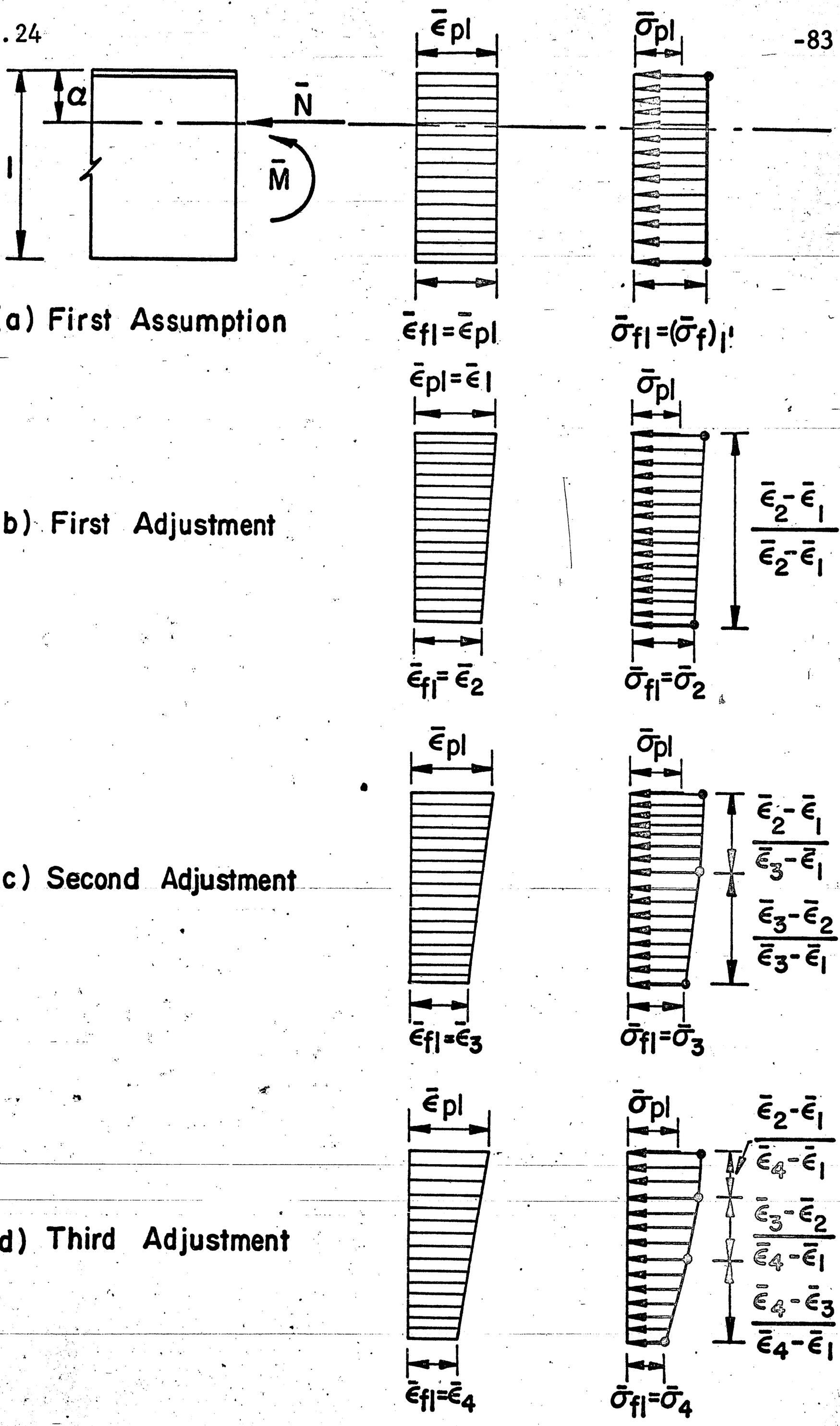

Fig. 15 Determination of $\bar{\epsilon}_{f\ell}$ for the Given N and $\bar{\epsilon}_{p\ell}$

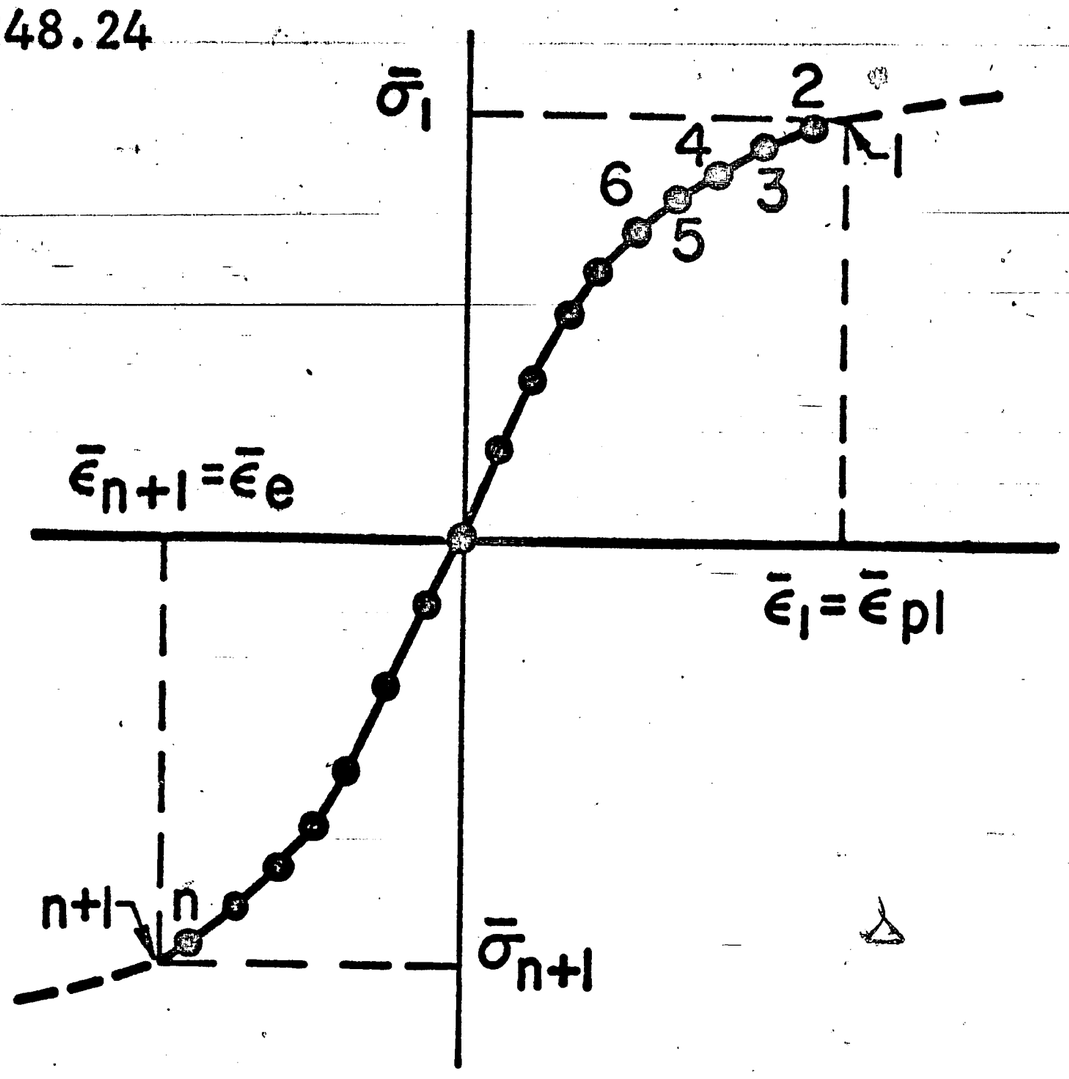

(a) Strain Range in the Stiffener

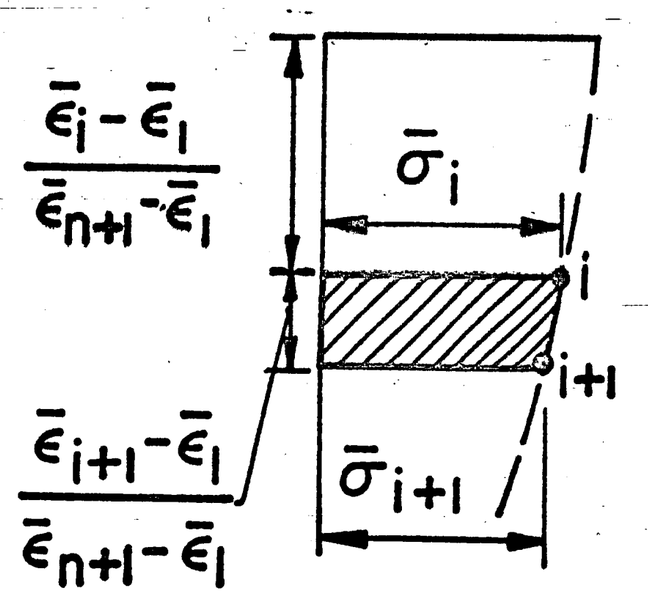

(b) Typical Stress Block

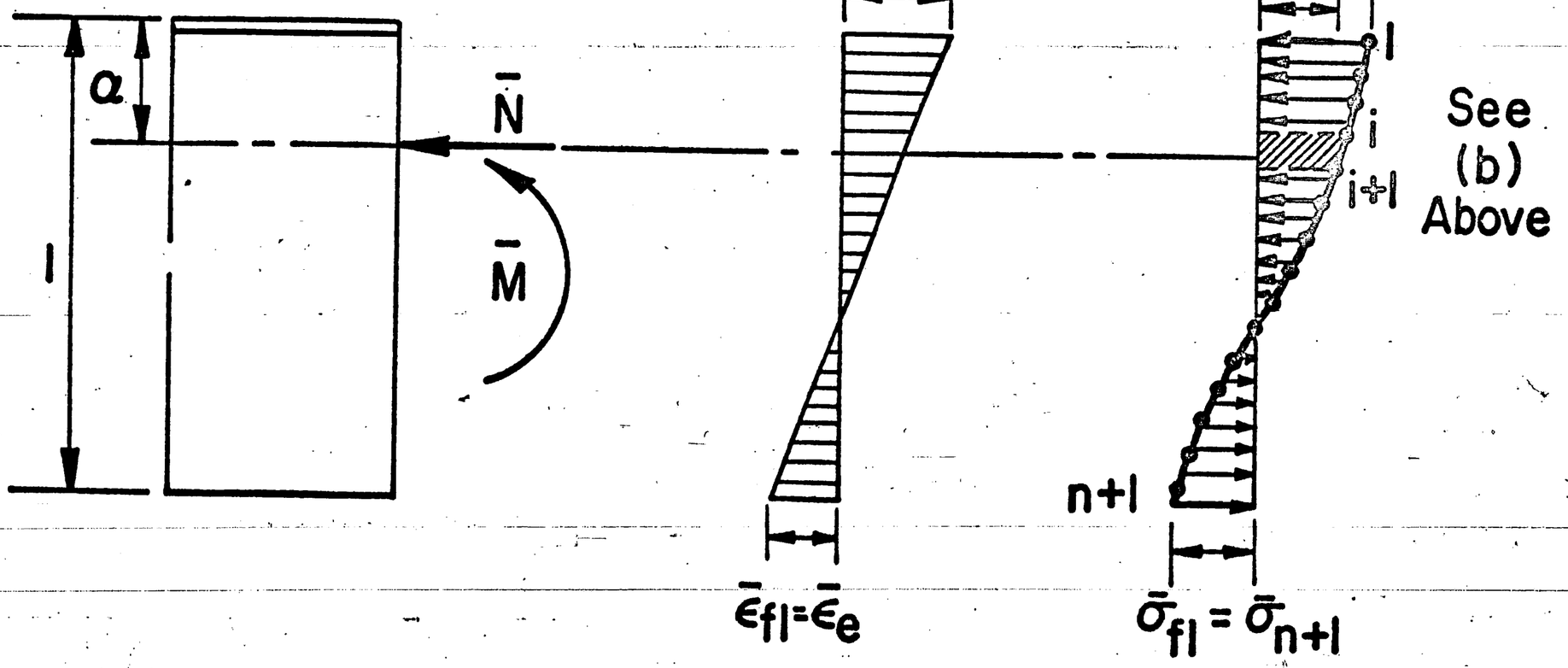

(c) Stresses and Strains in the Cross Section

Fig. 16 Determination of $\bar{M}$ for the Given $\bar{\epsilon}_{pl}$ and $\bar{\epsilon}_{fl}$

Known

$(\bar{\sigma}_p, \bar{\epsilon}_p)_i$ for $i=1,2,3\ldots,N_p$

$(\bar{\sigma}_f, \bar{\epsilon}_f)_i$ for $i=1,2,3\ldots,N_s$

$\bar{P}$

k_1

k_2

k_3

$N_{M\emptyset}$

τ

From $\bar{\sigma}$-$\bar{\epsilon}$ algorithm

$$B = \frac{(\bar{\epsilon}_p)_{N_p} - (\bar{\epsilon}_p)_1}{N_{M\emptyset}}$$

$$\emptyset_{max} = (\bar{\epsilon}_p)_1 - (\bar{\epsilon}_f)_{N_s}$$

$$\emptyset_{min} = (\bar{\epsilon}_p)_{N_p} - (\bar{\epsilon}_f)_1$$

$$\tau' = \frac{1}{5} \frac{\bar{\emptyset}_{max} - \bar{\emptyset}_{min}}{N_{M\emptyset}}$$

$K_t = 1$

$i_c = 1$

$$i_m = N_{M\emptyset} + 1 - i_c$$

$$x_c = i_c$$

$$x_c = \bar{\emptyset}_{max} + (x_c - 1)\left(\frac{\bar{\emptyset}_{max} - \bar{\emptyset}_{min}}{N_{M\emptyset}}\right)$$

Subprogram → $K = 1$ → γ_3 See Fig. 18

Subprogram → γ_4 See Fig. 19

$$E = \left|\bar{N} - \bar{P}\right| - \frac{1}{5}\tau\,\bar{P}$$

E:0

≤

$\bar{\emptyset}_{i_m} = 0$

$\bar{M}_{i_m} = \alpha\bar{N} - \frac{1}{2}(2k_2 + k_3)\,\bar{\sigma}_1'$

>

Subprogram → $n = i$ → γ_5 See Fig. 20

$\bar{\emptyset}_{i_m} = \bar{\epsilon}_i' - \bar{\epsilon}_{n+1}'$

i_c:2

<

≥

K_t:20

≥

<

$\left|\bar{\emptyset}_{i_m} - x_m\right|$:τ'

≤

>

Subprogram → $K = 2$ → γ_3

$\Sigma = 0$

$i = 1$

$$\Sigma = \Sigma + \bar{\sigma}_i'(\bar{\epsilon}_{i+1}' - \bar{\epsilon}_i')(\bar{\epsilon}_{i+1}' + \bar{\epsilon}_i' - 2\bar{\epsilon}_1) + \frac{1}{3}(\bar{\sigma}_{i+1}' - \bar{\sigma}_i')(\bar{\epsilon}_{i+1}' - \bar{\epsilon}_i')(2\bar{\epsilon}_{i+1}' + \bar{\epsilon}_i' - 3\bar{\epsilon}_1')$$

i:n

<

$i = i + 1$

≥

$$\bar{M}_{i_m} = \alpha\bar{N} - k_2\bar{\sigma}_{n+1}' - \frac{1}{2}\frac{k_3\Sigma}{(\bar{\epsilon}_{n+1}' - \bar{\epsilon}_1')^2}$$

i_c:$N_{M\emptyset}$

<

$i_c = i_c + 1$

≥

The $\bar{M}$-$\bar{\emptyset}$ table for $\bar{N}$-$\bar{P}$ is complete

To $\bar{L}$-$\bar{\emptyset}^o$ algorithm

Fig. 17 Flow Diagram for the Determination of the $\bar{M}$-$\bar{\emptyset}$-$\bar{N}$ Relationship

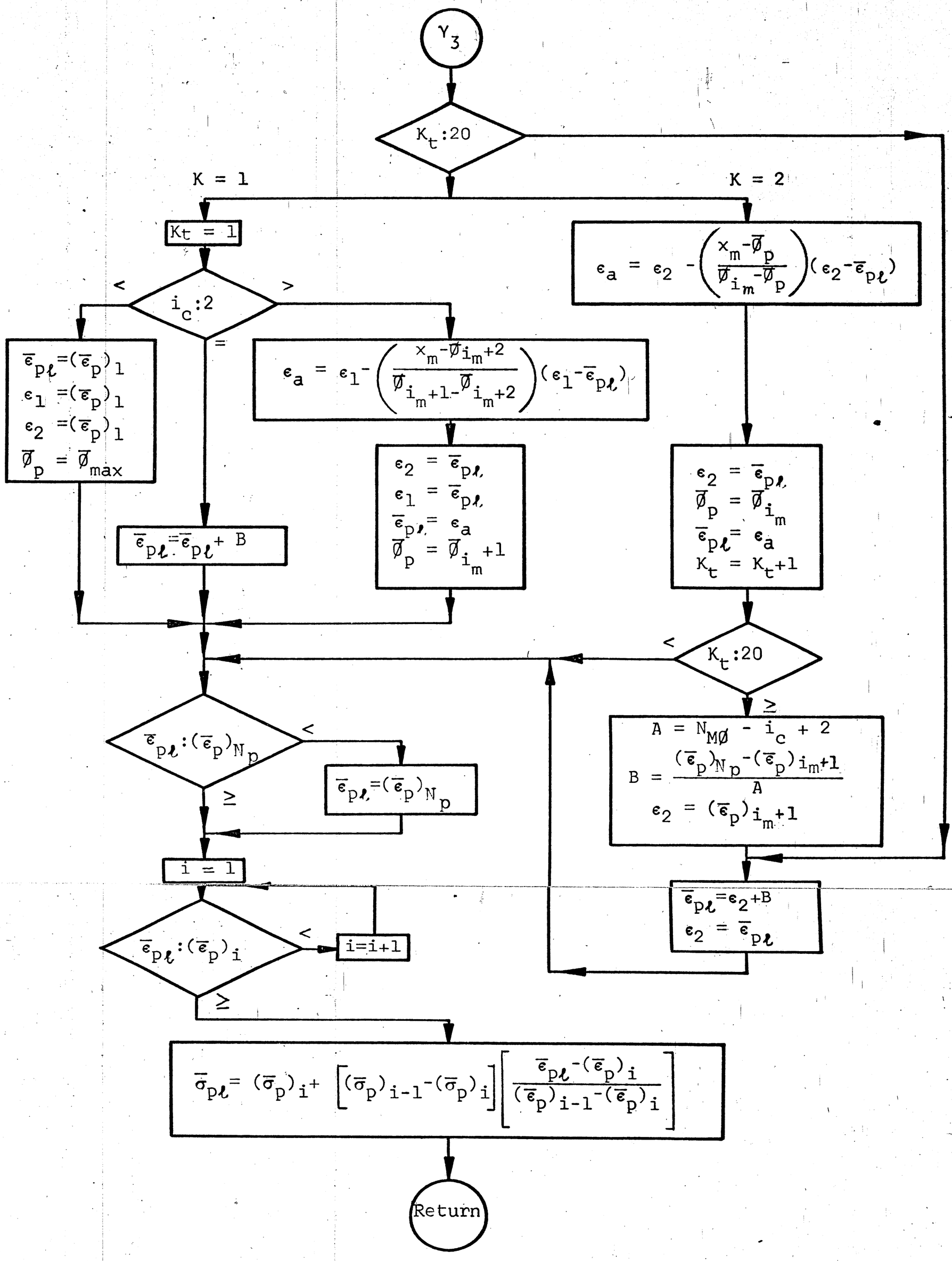

Fig. 18 Flow Diagram for Subprogram 3

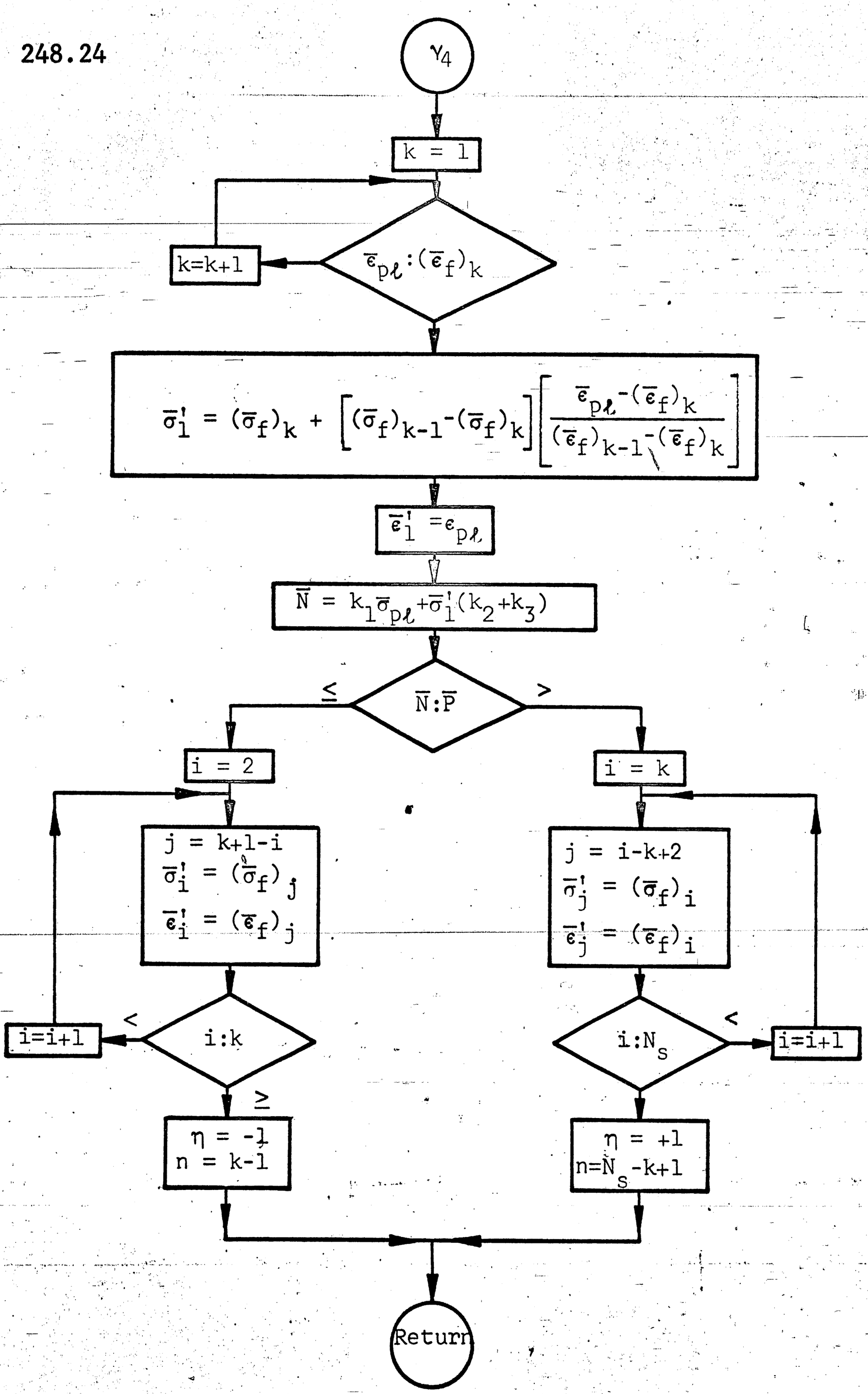

Fig. 19 Flow Diagram for Subprogram 4

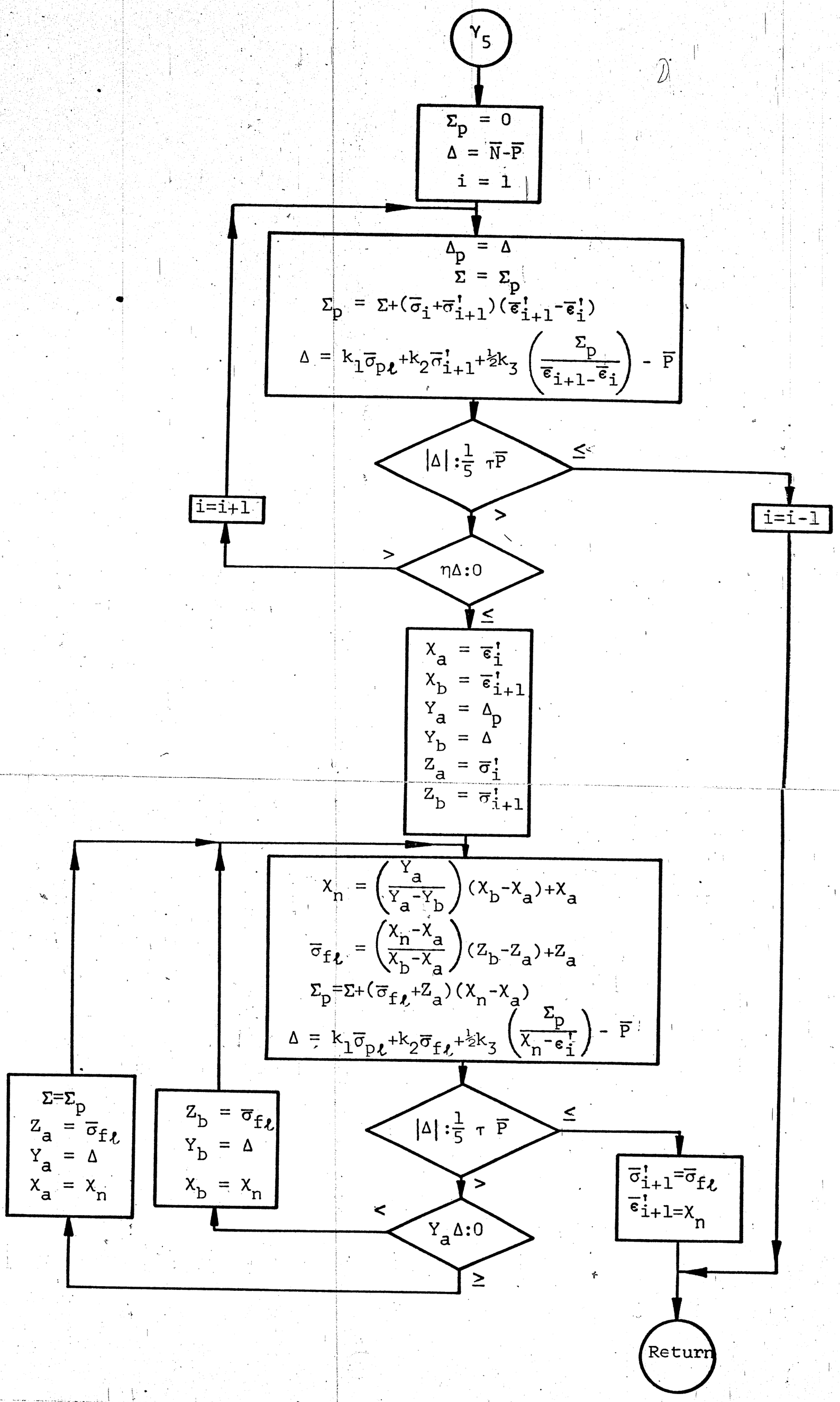

Fig. 20 Flow Diagram for Subprogram 5

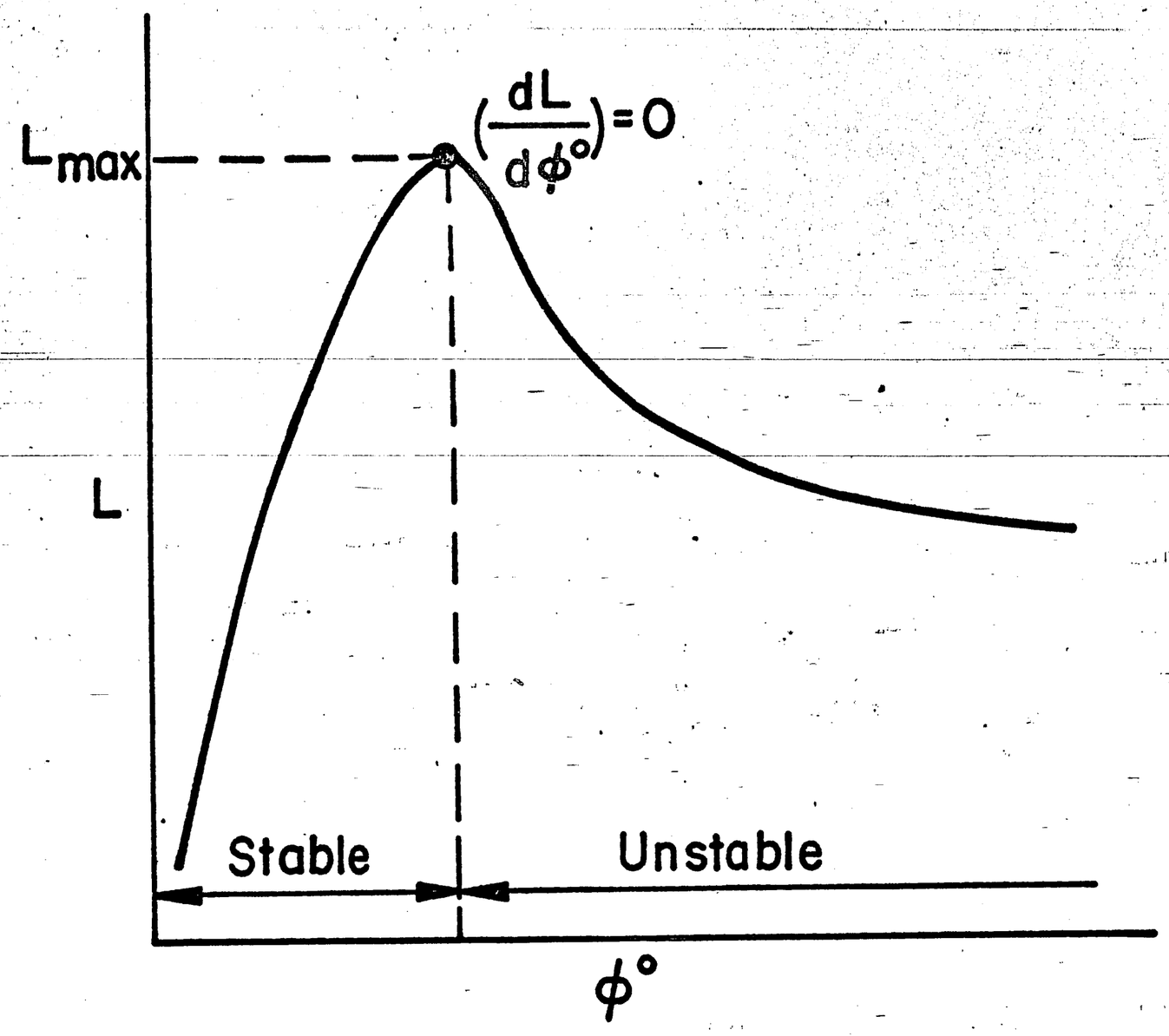

Fig. 21 A Column Length-Deformation Curve

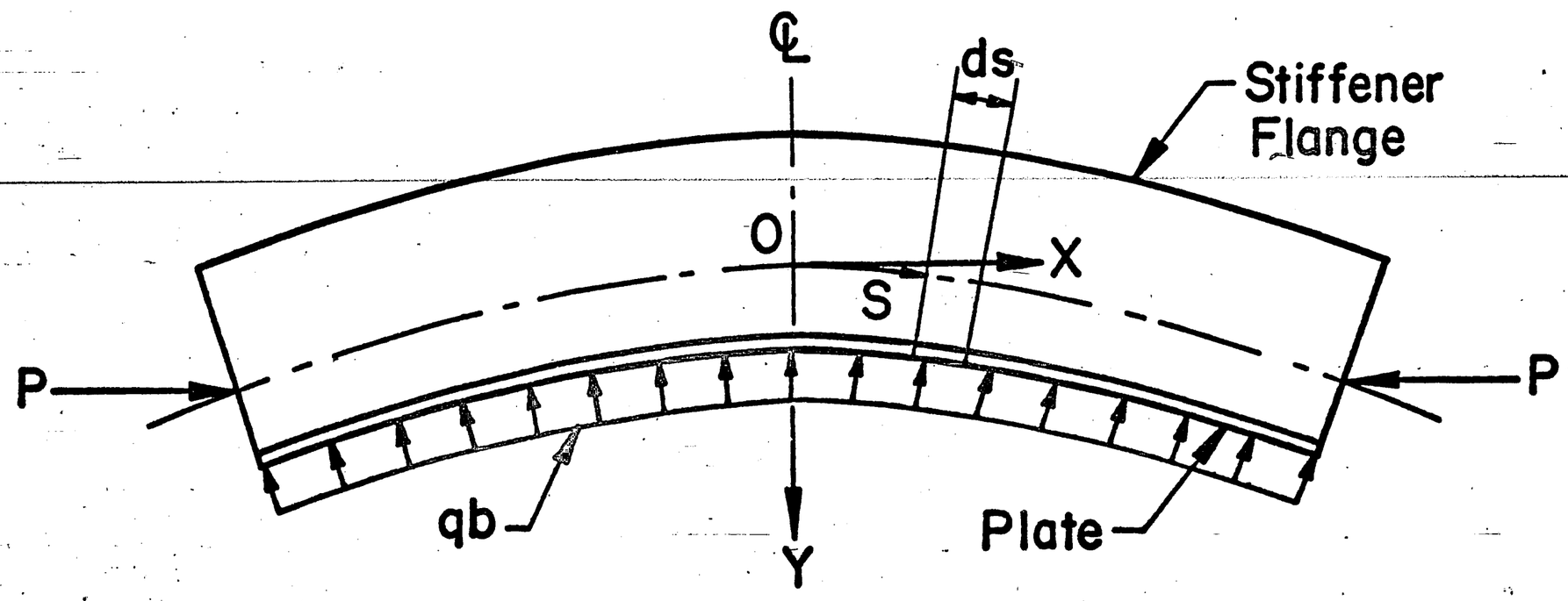

Fig. 22 A Longitudinally Stiffened Panel Under Combined Loading

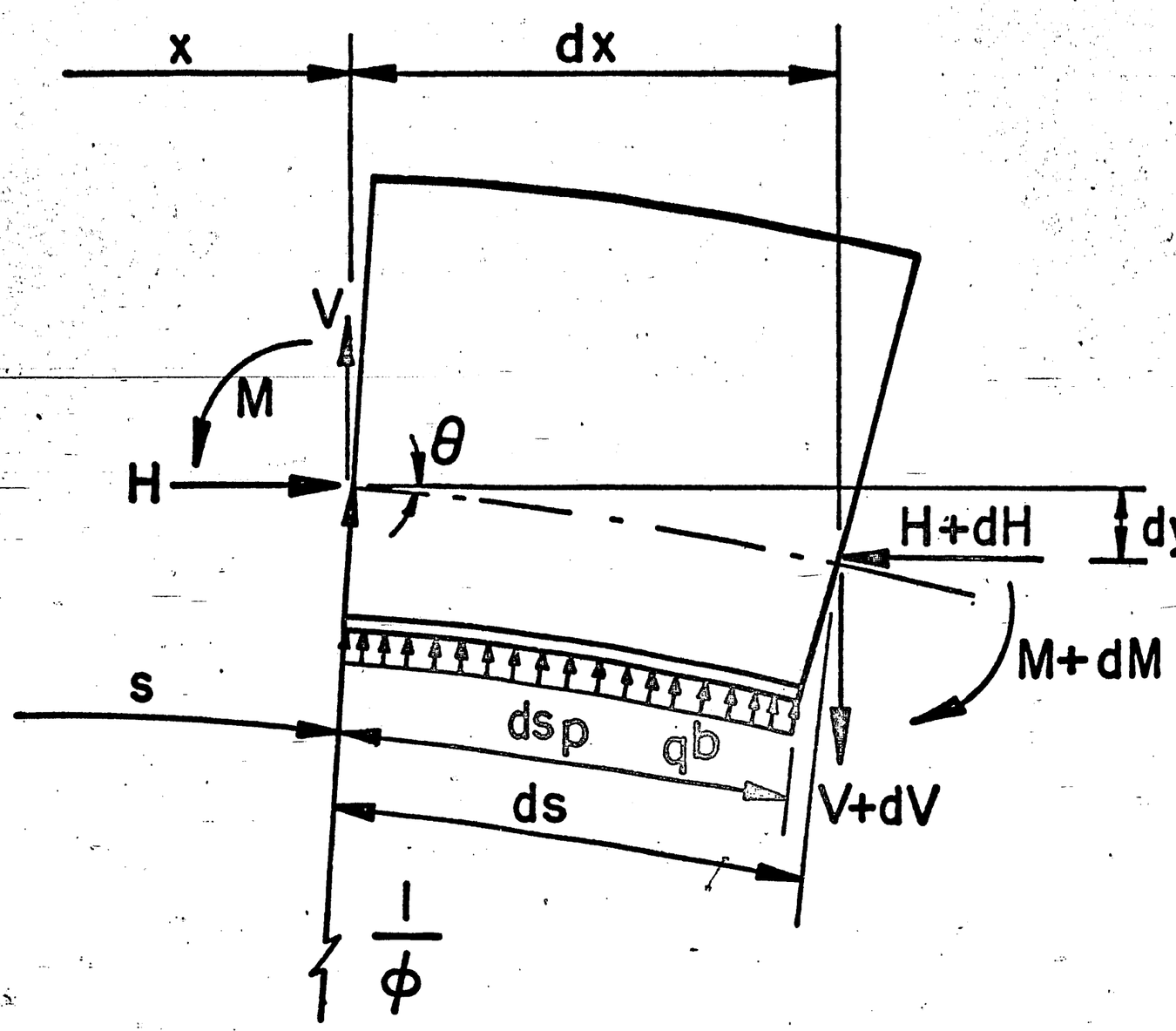

Fig. 23 Panel Segment of Length ds

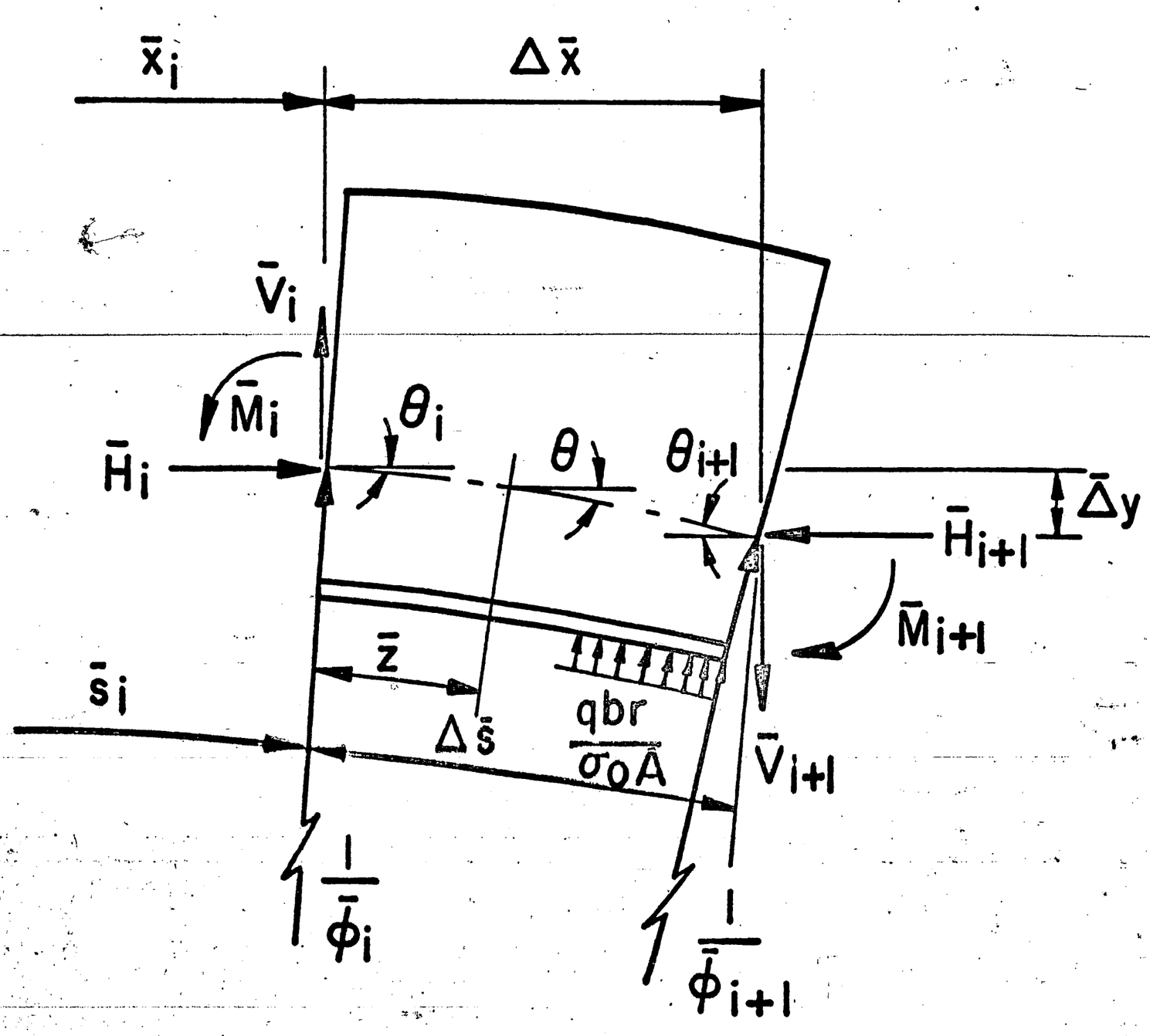

Fig. 24 Panel Segment of Length $\Delta\bar{s}$

Known

Table of $(\overline{M},\overline{\emptyset})_i$ for $\overline{N}=\overline{P}$,
where $i=1,2,3,\cdots,N_{M\emptyset}$

$$k_6 = \frac{qbr}{\sigma_o A}$$

$$k_5 = e_o \frac{r}{d}$$

$$k_7 = \alpha \frac{d}{r}$$

$$k_8 = -\frac{r}{d}$$

$\Delta\overline{s}_I$ = Input segment length

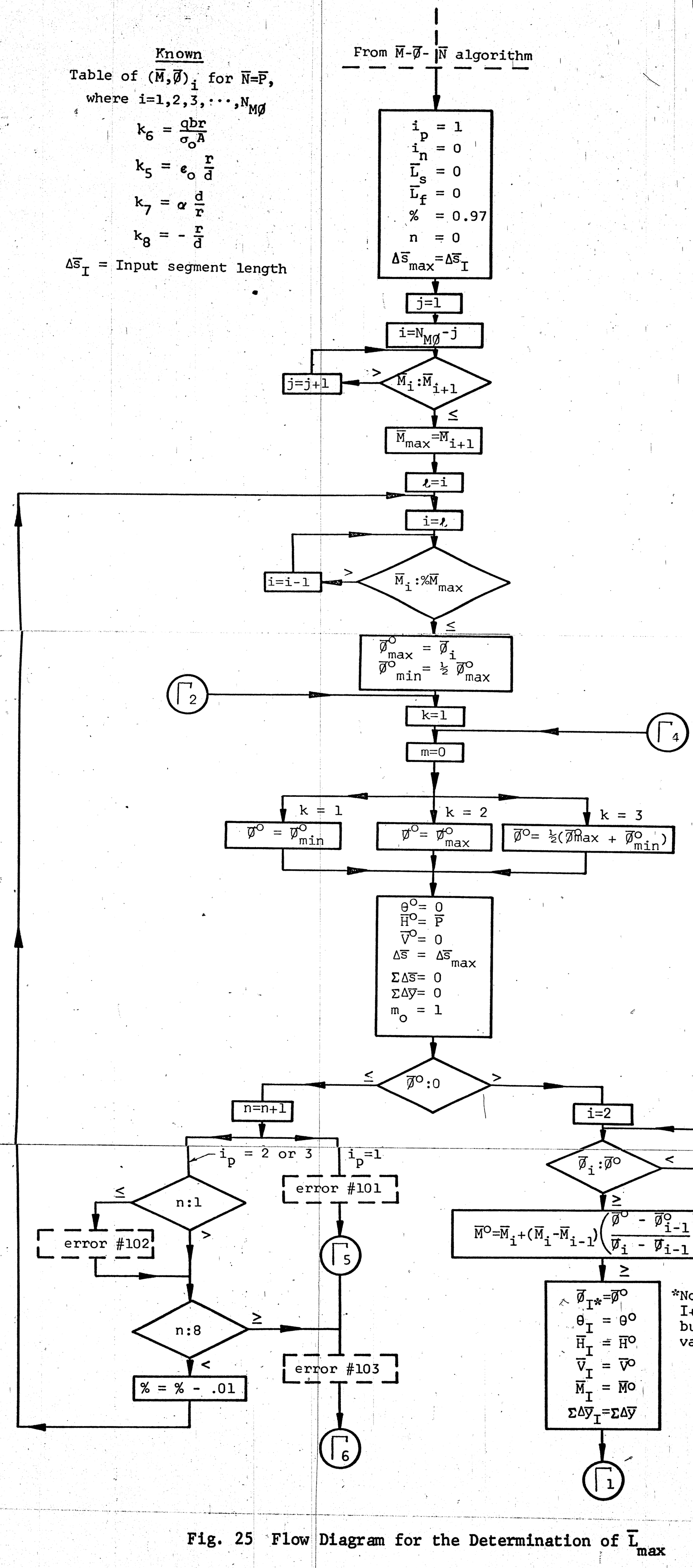

*Note: I, I-1, and I+1 are not indices, but part of the variable name.

Fig. 25 Flow Diagram for the Determination of $\overline{L}_{max}$

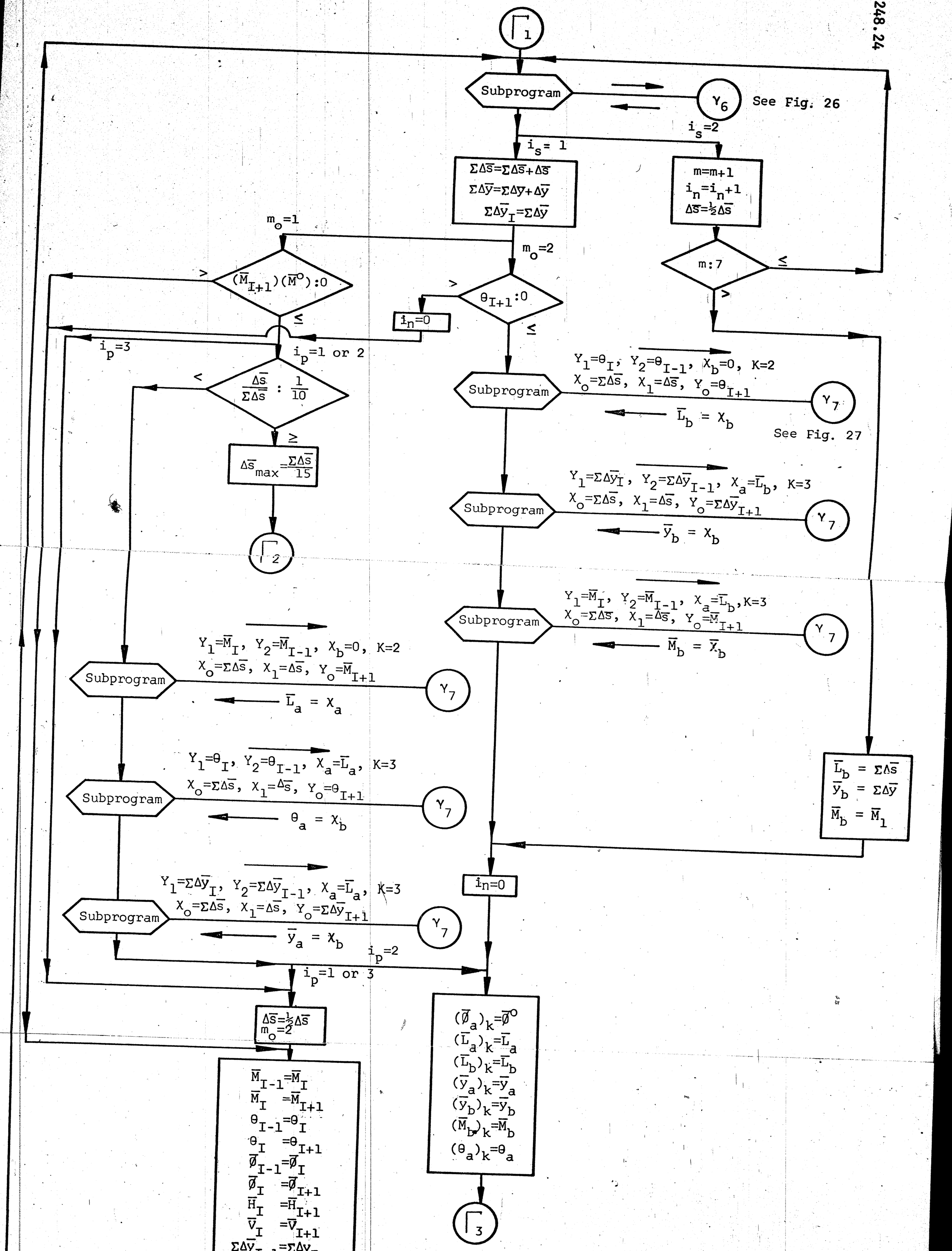

Fig. 25 (continued)

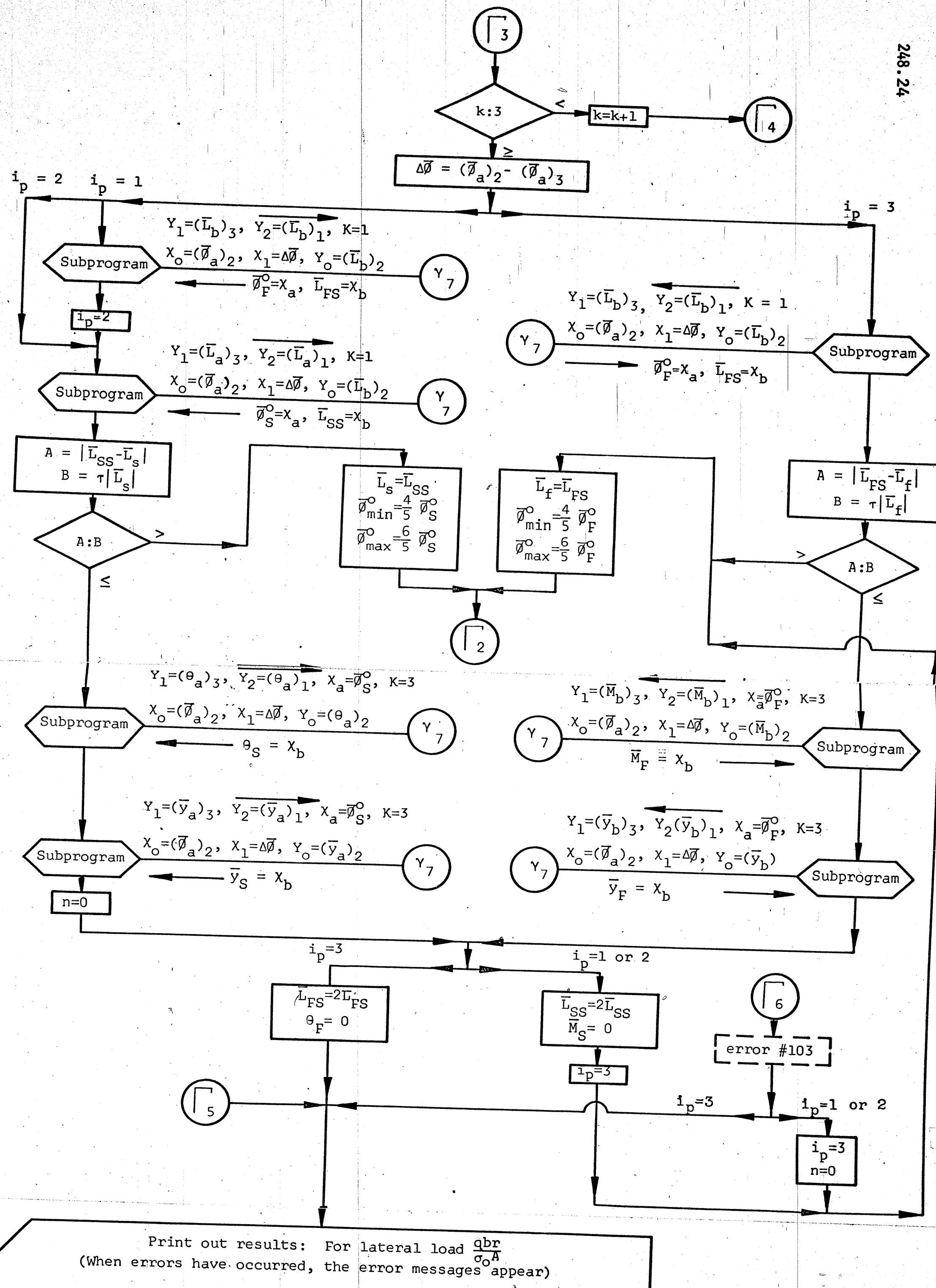

Print out results: For lateral load $\frac{qbr}{\sigma_o A}$
(When errors have occurred, the error messages appear)

Boundary Condition	$\bar{\phi}^o$ for $\bar{L}_{max}$	$\bar{L}_{max}$	Mid-point deflection	End moment	End slope
Simple support	$\bar{\phi}^o_S$	$\bar{L}_{SS}$	$\bar{y}_S$	$\bar{M}_S$	θ_S
Fixed support	$\bar{\phi}^o_F$	$\bar{L}_{FS}$	$\bar{y}_F$	$\bar{M}_F$	θ_F

Fig. 25 (continued)

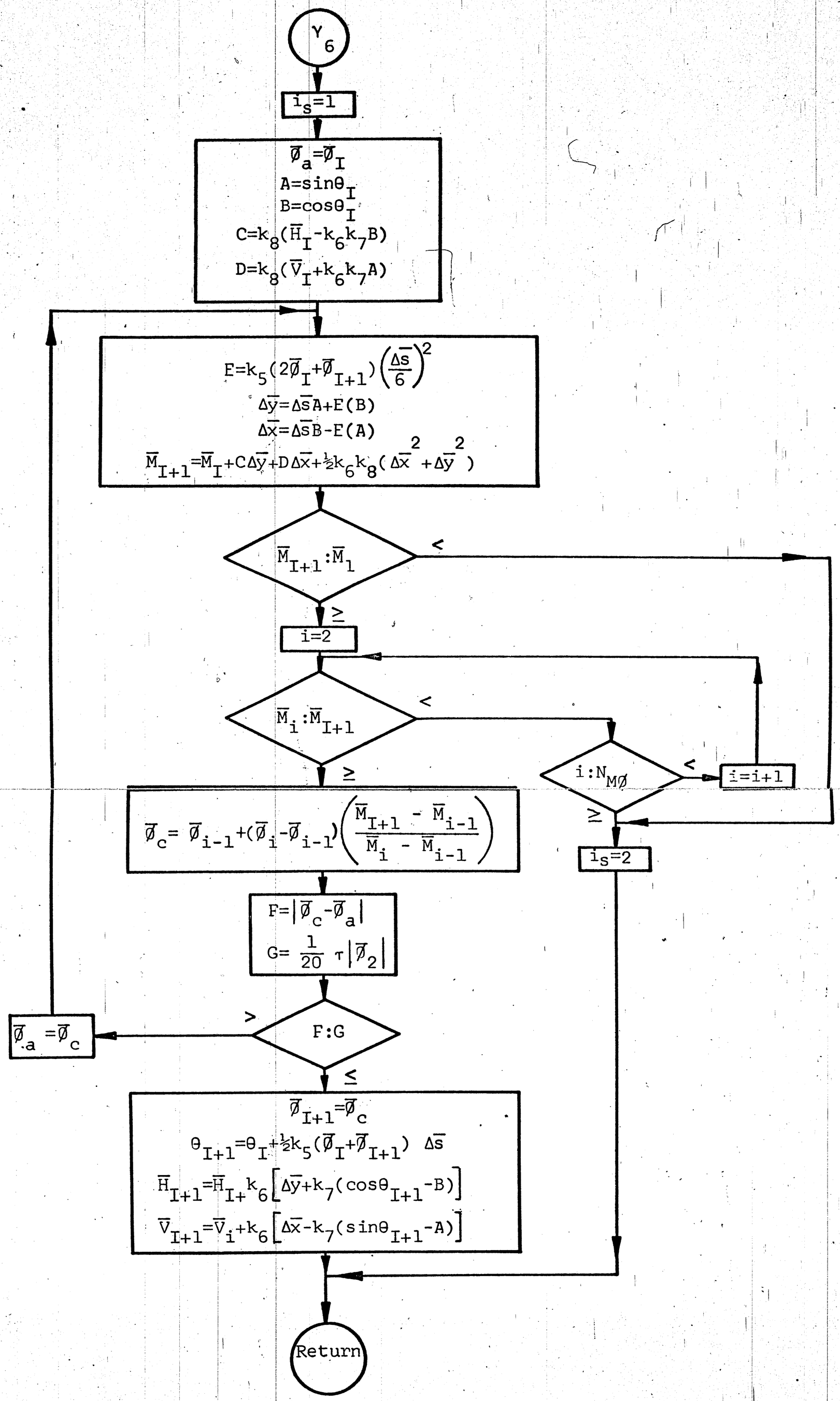

Fig. 26 Flow Diagram for Subprogram 6

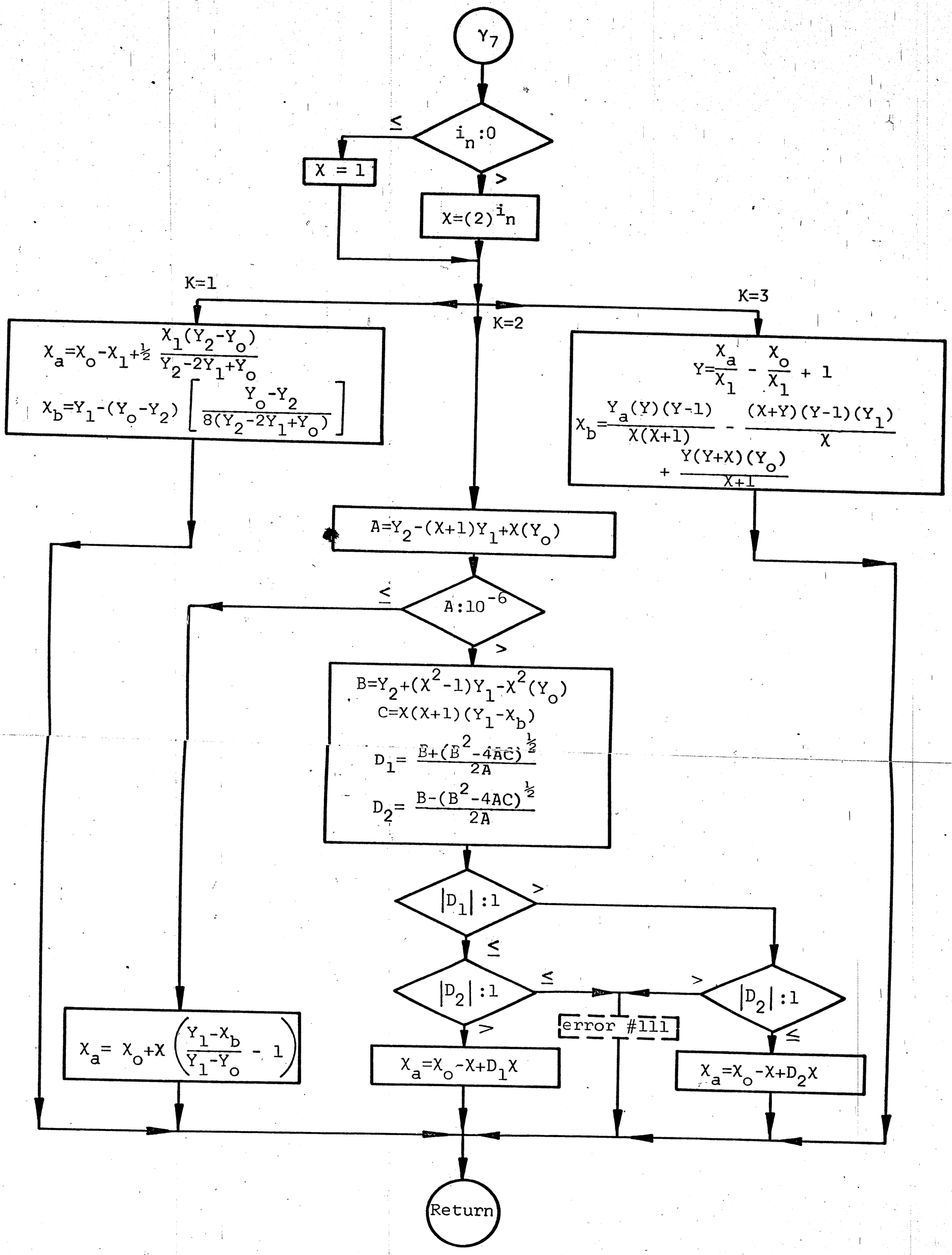

Fig. 27 Flow Diagram for Subprogram 7

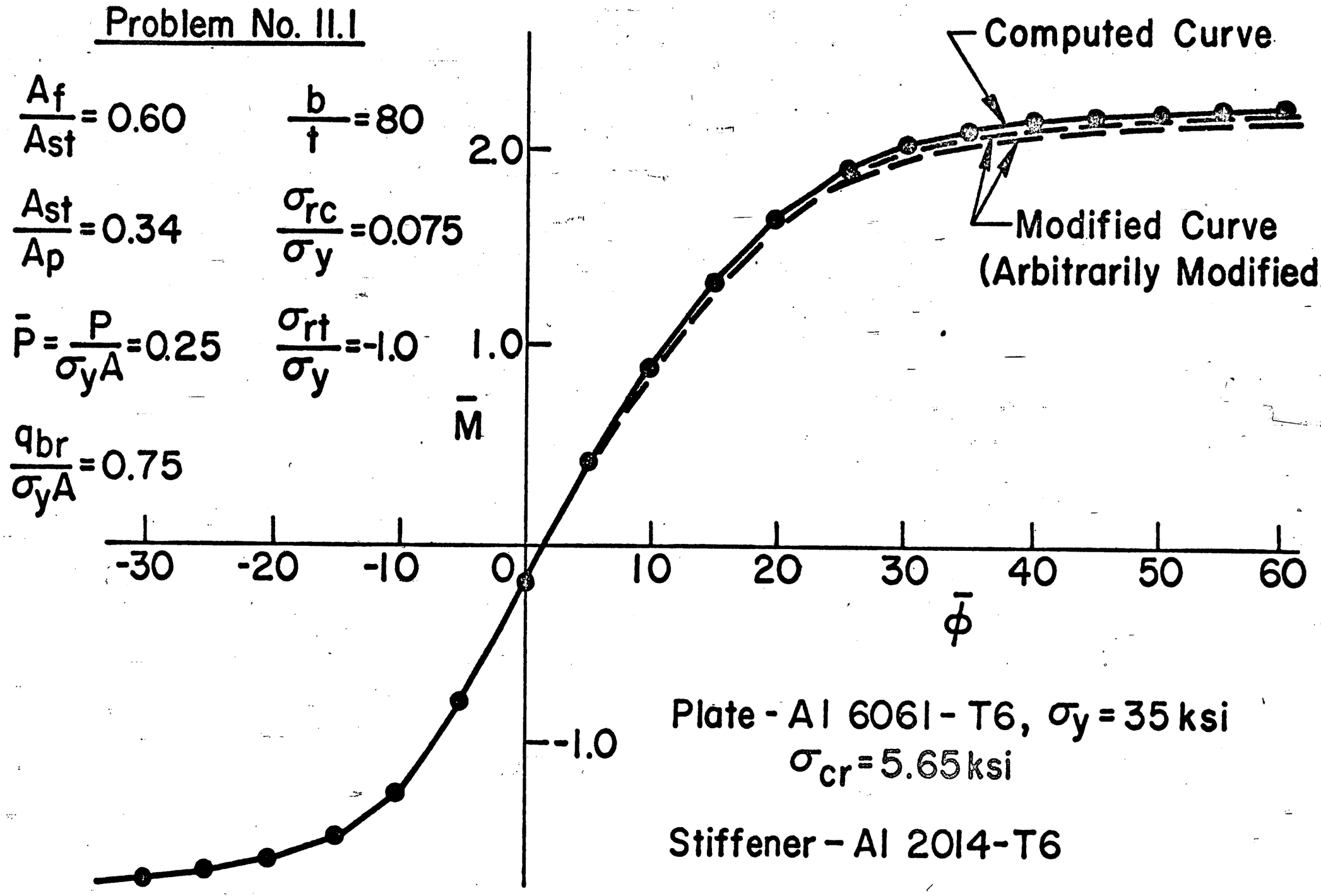

(a) Example Moment-Curvature Relationships

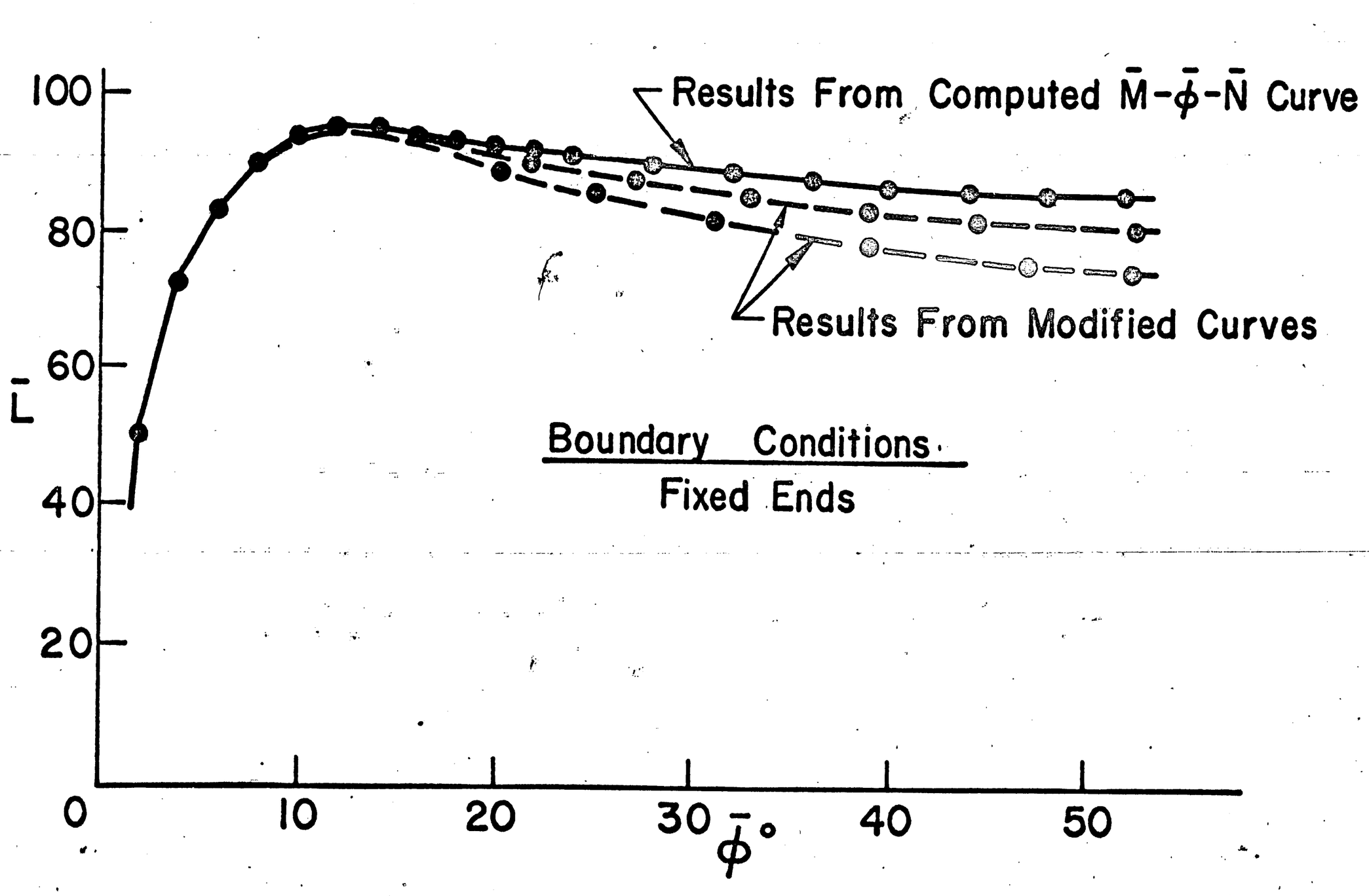

(b) Example Length - Deformation Relationships

Fig. 28 Error Source in Stepwise Integration

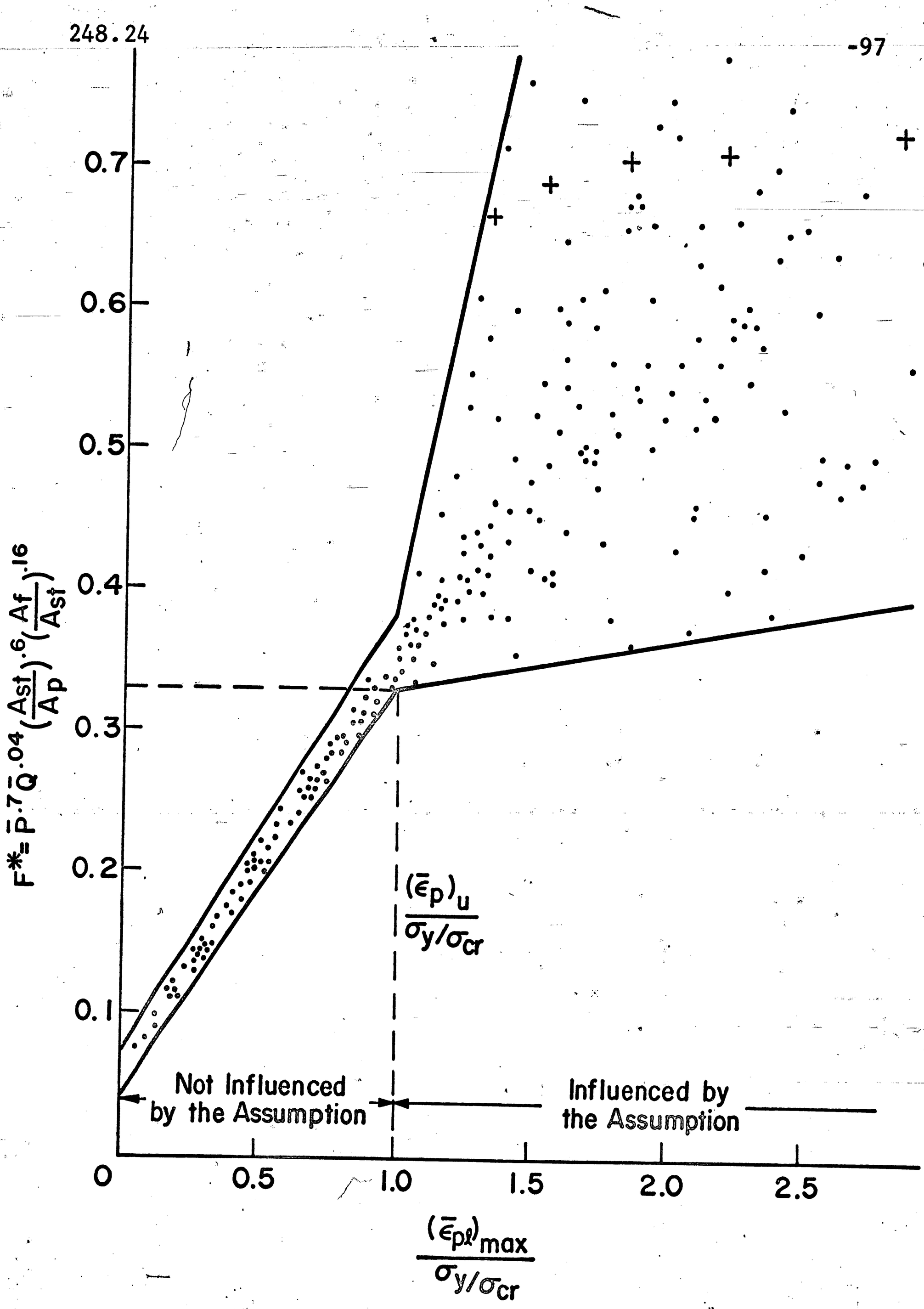

Fig. 29 Pinned-End Panels Designed by the Nomograph of Ref. 12

248.24

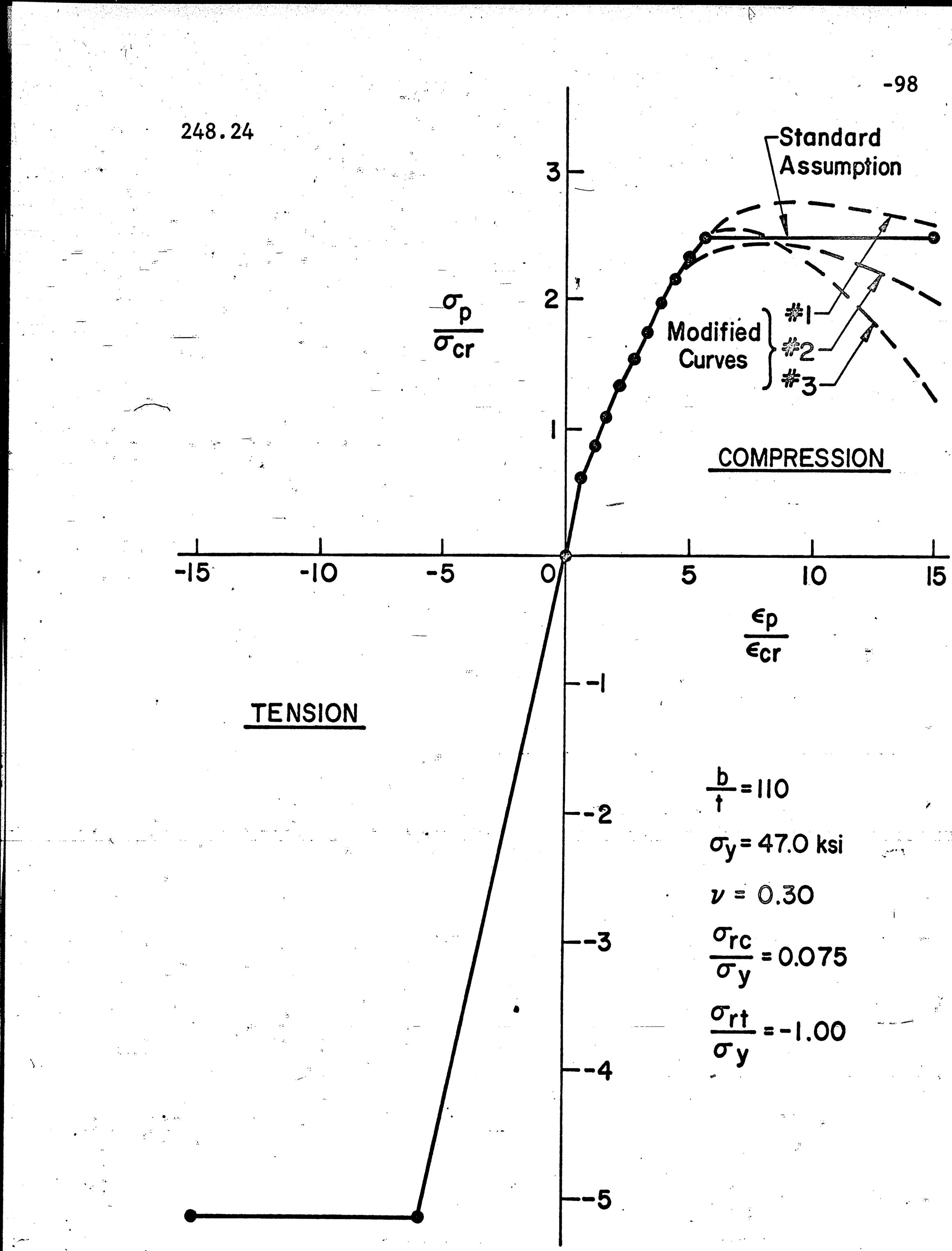

Fig. 30 Average Stress-Edge Strain Curve with Modifications

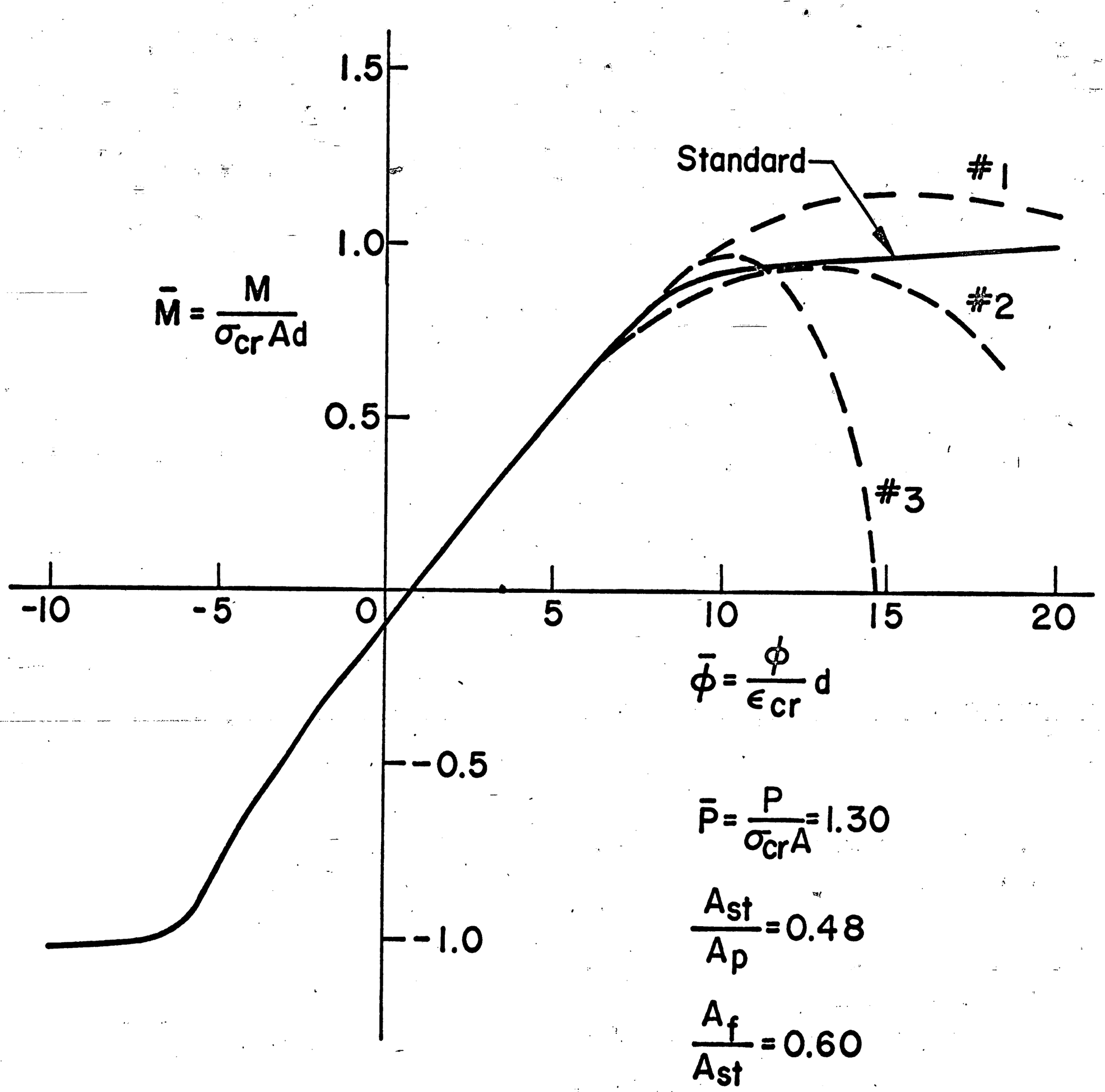

Fig. 31 Moment-Curvature Relationship with the Effects of Modifications

11. REFERENCES

1. Koiter, W.T.
THE EFFECTIVE WIDTH OF FLAT PLATES FOR VARIOUS LONGITUDINAL EDGE CONDITIONS AT LOADS FAR BEYOND BUCKLING LOAD, Nationaal Luchtvaartlaboratorium (Netherlands), Rep. S287, 1943, (In Dutch)

2. Besseling, J.F.
THE EXPERIMENTAL DETERMINATION OF THE EFFECTIVE WIDTH OF FLAT PLATES IN THE ELASTIC AND PLASTIC RANGE, Nationaal Luchtvaartlaboratorium (Netherlands), Rep. S414, 1953, (In Dutch)

3. Botman, M.
THE EXPERIMENTAL DETERMINATION OF THE EFFECTIVE WIDTH OF FLAT PLATES IN THE ELASTIC AND PLASTIC RANGE (PART II), Nationaal Luchvaartlaboratorium (Netherlands), Rep. S438, 1954, (In Dutch)

4. Ojalvo, M., and Hull, F.H.
EFFECTIVE WIDTH OF THIN RECTANGULAR PLATES, Proc. ASCE, 84(EM-3) Paper 1718, July 1958

5. Stein, M.
LOADS AND DEFORMATIONS OF BUCKLED RECTANGULAR PLATES, NASA TR R-40, 1959

6. Ostapenko, A., and Lee, Ti-ta
TESTS ON LONGITUDINALLY STIFFENED PLATE PANELS SUBJECTED TO LATERAL AND AXIAL LOADING, Fritz Laboratory Report No. 248.4, Lehigh University, August 1960

7. Rampetsreiter, R.H., Lee, Ti-ta, and Ostapenko, A.
TESTS ON LONGITUDINALLY STIFFENED PLATE PANELS, Fritz Laboratory Report No. 248.5, Lehigh University, July 1962

8. Kondo, J., and Ostapenko, A.
TESTS ON LONGITUDINALLY STIFFENED PLATE PANELS WITH FIXED ENDS, Fritz Laboratory Report No. 248.12, Lehigh University, July 1964

9. Kondo, J.
ULTIMATE STRENGTH OF LONGITUDINALLY STIFFENED PLATE PANELS SUBJECTED TO COMBINED AXIAL AND LATERAL LOADING, Fritz Laboratory Report No. 248.13, Lehigh University, August 1965

10. Davidson, H.L.
POST-BUCKLING BEHAVIOR OF LONG RECTANGULAR PLATES, Fritz Laboratory Report No. 248.15, Lehigh University, June 1965

11. Tsuiji, T.
STRENGTH OF LONGITUDINALLY STIFFENED PLATE PANELS WITH LARGE b/t, Fritz Laboratory Report No. 248.14, Lehigh University, June 1965

12. Vojta, J.F., and Ostapenko, A.
ULTIMATE STRENGTH DESIGN OF LONGITUDINALLY STIFFENED PLATE PANELS WITH LARGE b/t, Fritz Laboratory Report No. 248.18, Lehigh University, August 1967

13. Vojta, J.F., and Ostapenko, A.
ULTIMATE STRENGTH DESIGN CURVES FOR LONGITUDINALLY STIFFENED PLATE PANELS WITH LARGE b/t, Fritz Laboratory Report No. 248.19, Lehigh University, August 1967

14. Rutledge, D.R.
COMPUTER PROGRAM FOR ULTIMATE STRENGTH OF LONGITUDINALLY STIFFENED PANELS (LARGE AND SMALL b/t, GENERAL MATERIAL PROPERTIES), Fritz Laboratory Report No. 248.23, Lehigh University, July 1968

12. VITA

Donald R. Rutledge was born on February 19, 1939, in Brownwood, Texas, the second child of Marion and Katherine Rutledge. He attended schools in Brownwood and Waco, graduating as valedictorian from Midway High School in Waco in 1957.

He served in the U.S. Navy from 1959 to 1963 as a destroyer radarman. An honorable discharge was received in 1964.

His undergraduate studies were conducted principally at Texas Technological College in Lubbock, Texas. He was active in the student chapter of ASCE, serving as Secretary during his senior year. Recognitions included regular inclusion on the Dean's Honor Roll and election to Tau Beta Pi. He was awarded the General Contractor's Scholarship during his junior and senior years and the NSF Undergraduate Research Scholarship for study at Duke University during 1965. In June 1966, he received his Bachelor of Science degree in Civil Engineering from Texas Technological College.

He worked briefly as a junior research engineer for Pan American Petroleum Corporation, Marine Structures Division,

and then accepted a NDEA Graduate Fellowship for study at Illinois Institute of Technology in Chicago. He joined the Civil Engineering Department of Lehigh University as a research assistant in February 1967. Since then he has been actively engaged in research on the plastic design of built-up members.